BRUNA RAGE BALDONE LARA

BIOCOMPOSITES OF WHEY PROTEIN ISOLATE/POLYVINYL ALCOHOL/NANO-SILICA FOR FOOD FLEXIBLE PACKAGING – CONVENTIONAL AND BILAYER CORONA DISCHARGE-TREATED FILMS

LAVRAS – MG
2022

BRUNA RAGE BALDONE LARA

BIOCOMPOSITES OF WHEY PROTEIN ISOLATE/POLYVINYL ALCOHOL/NANO-SILICA FOR FOOD FLEXIBLE PACKAGING – CONVENTIONAL AND BILAYER CORONA DISCHARGE-TREATED FILMS

Tese apresentada à Universidade Federal de Lavras, como parte das exigências do Programa de Pós-Graduação em Engenharia de Biomateriais, área de concentração em Produtos e Nanoprodutos Alimentícios, para a obtenção do título de Doutor.

Orientadora
Profa. Dra. Marali Vilela Dias

Coorientador
Prof. Dr. Mario Guimarães Junior

LAVRAS – MG
2022

Ficha catalográfica elaborada pelo Sistema de Geração de Ficha Catalográfica da Biblioteca Universitária da UFLA, com dados informados pelo(a) próprio(a) autor(a).

Lara, Bruna Rage Baldone.
Biocomposites of Whey Protein isolate/Polyvinyl alcohol/Nano-silica for food flexible packaging - Conventional and bilayer corona discharge-treated films / Bruna Rage Baldone Lara. - 2022.
118 p. : il.

Orientador(a): Marali Vilela Dias.
Coorientador(a): Mario Guimarães Júnior.
Tese (doutorado) - Universidade Federal de Lavras, 2022.
Bibliografia.

1. Isolado proteico de soro do leite. 2. Poli (álcool vinílico). 3. Biocompósitos para embalagens. I. Dias, Marali Vilela. II. Guimarães Júnior, Mario. III. Título.

BRUNA RAGE BALDONE LARA

BIOCOMPOSITES OF WHEY PROTEIN ISOLATE/POLYVINYL ALCOHOL/NANO-SILICA FOR FOOD FLEXIBLE PACKAGING – CONVENTIONAL AND BILAYER CORONA DISCHARGE-TREATED FILMS

Tese apresentada à Universidade Federal de Lavras, como parte das exigências do Programa de Pós-Graduação em Engenharia de Biomateriais, área de concentração em Produtos e Nanoprodutos Alimentícios, para a obtenção do título de Doutor.

APROVADA em 20 de janeiro de 2022.

Dr. Allan Robledo Fialho e Moraes	UFV
Dr. Gustavo Henrique Denzin Tonoli	UFLA
Dra. Lizzy Ayra Alcântara Veríssimo	UFLA

Orientadora
Dra. Marali Vilela Dias

Coorientador
Dr. Mario Guimarães Junior

LAVRAS – MG
2022

AGRADECIMENTOS

Agradeço a Deus, a Nossa Senhora Aparecida e a São Geraldo, pela oportunidade de realizar esta pesquisa e pela saúde e capacidade a mim concedida para concluí-la.

À minha orientadora, professora Marali Vilela Dias, pela confiança constante e por agir para comigo sempre com paciência, compreensão e empatia. Obrigada por ser uma grande incentivadora de todos os meus planos e anseios, sejam eles acadêmicos, profissionais ou pessoais!

Ao professor Mario Guimarães Júnior, pelo interesse constante no desenvolvimento deste trabalho, pelo auxílio em cada passo desta jornada. Obrigada por me orientar sempre com tanta competência e disposição!

Ao meu colega, que no período da realização dos experimentos desta tese era o mais brilhante aluno de iniciação científica com quem convivi, Paulo Sérgio de Andrade, o meu muitíssimo obrigada! Você contribuiu de forma significativa para que esse trabalho pudesse ser concluído com qualidade. Agradeço sua amizade, sua gentileza e bondade, sua paciência e sua constante disponibilidade. Agradeço, principalmente, a Deus, por ter me permitido contar com você como meu braço direito.

Aos meus queridos pais, Weber e Sandra, pelo amor infinito e confiança constate. Vocês são os maiores e melhores exemplos que eu poderia ter em todos os aspectos: familiar, social e profissional. Foi graças a todas as oportunidades que Deus e vocês me permitiram ter e agarrar que estou sendo agora titulada como "doutora". Apesar de isso não significar nada perante aos ensinamentos de vida que vocês me dão a cada dia, gostaria de dizer o quão grata eu sou a vocês por me incentivarem a realizar mais essa conquista. Eu os amo com todas as forças!

Ao meu amado marido, Marcos, por ser minha fonte incessável de calmaria, sensatez e de muito apoio. Comecei essa jornada ainda como sua namorada, e a finalizo, muito feliz e grata, como sua esposa.

A minha irmã, Laura, por ser minha grande e melhor amiga e sempre incentivar meus planos e desejos. Obrigada por ter me escutado sempre que precisei dos seus sensíveis ouvidos e das suas sábias palavras.

A minha avó Marília e a todos os meus familiares: tios, tias, primos e primas, pelas energias e orações a mim enviadas e dedicadas.

A todos os amigos e colegas da UFLA, em especial à Ana Cristina Moreira Andrade Araújo, por ser minha fiel confidente e companheira e por me abrigar em sua casa sempre com tanto carinho.

À Coordenação de Aperfeiçoamento de Pessoal de Nível Superior (Capes) pela concessão da bolsa de estudos (Código de Financiamento 001).

À Universidade Federal de Lavras, ao Programa de Pós-graduação de Engenharia de Biomateriais, ao Departamento de Ciência dos Alimentos, e aos professores e funcionários

pelos auxílios técnicos, ensinamentos e pela oportunidade concedida para a realização deste doutorado.

A todos os meus amigos e demais pessoas que cruzaram comigo ao longo desta caminhada, que torcem e rezam por mim, e que desejam a minha felicidade.

Muito obrigada.

RESUMO

O presente trabalho propõe a inédita adição de nano-sílica coloidal (NS) à matriz de isolado proteico de soro de leite (IPS) e poli (álcool vinílico) (PVOH), formando um novo biocompósito com elevada resistência à tração e flexibilidade para aplicação como embalagem flexível para alimentos. Além disso, propõe a utilização do método de laminação com descarga corona em filmes de IPS e PVOH, para modificação de propriedades mecânicas de tração. Para tal, foram desenvolvidas blendas com 70% de IPS e 30% de PVOH acrescidas com 0%, 1%, 2%, 3% e 4% de NS pelo método de *casting*. Os biocompósitos produzidos foram caracterizadas quanto às propriedades: mecânicas (teste de tração), morfológicas (Microscopia Eletrônica de Varredura – MEV), de interação (Espectroscopia na Região do Infravermelho – FTIR), temperatura de transição vítrea (Calorimetria Diferencial Exploratória), de permeabilidade, difusividade e solubilidade ao vapor de água, e de interação com umidade sob atividades de água e temperaturas variadas (isotermas de sorção). A adição de 4% de NS levou à obtenção de um biocompósito com resistência à tração de 10.2 MPa (43% mais elevado que o do filme sem NS), e com módulo de elasticidade de 78.2 MPa, sendo estes ótimos resultados para aplicação como embalagens flexíveis. A 4% de NS também se obteve uma redução de 17% na sorção, de 58% na difusividade, e de 40% na permeabilidade ao vapor de água, e uma menor espontaneidade do processo de sorção comparando-se ao filme com 0% de NS, mostrando uma maior capacidade de manter a integridade do alimento e da própria embalagem durante a aplicação. Numa segunda fase do trabalho, foram produzidos novos biocompósitos laminados via *casting*, com uma primeira camada de PVOH/NS e uma segunda de IPS/NS, fixando-se a quantidade de NS (4% m/m polímero) e aplicando-se diferentes tempos de descarga corona (0s, 30s, 60s, 90s) como melhorador de adesão entre as camadas. As análises de FTIR, ângulo de contato com água e energia superficial da primeira camada mostraram que, quanto maior o tempo de descarga corona, maiores foram a molhabilidade e energia de superfície obtidas, levando a uma maior adesão entre as camadas. Os biocompósitos laminados finais foram avaliados quanto às propriedades: morfológica da região de união entre as camadas (MEV), mecânicas (teste de tração), e de permeabilidade, difusividade e solubilidade ao vapor de água. Biocompósitos laminados e tratados com 90s de descarga corona mostraram uma região de transição entre as camadas mais homogênea (comparado aos demais tempos de tratamento) e uma resistência à tração de 12.6 MPa, sendo 72% e 23% mais resistentes, respectivamente, que o filme laminado não tratado com corona e que o filme não-laminado (camada única). Além disso, a laminação com 90s de corona, proporcionou uma flexibilidade 7,4 vezes maior comparando-se ao filme não-laminado. Apesar do aumento na resistência à tração e na flexibilidade, a laminação juntamente à descarga corona aumentou a permeabilidade e a afinidade do filme com água.

Palavras-chave: Isolado proteico de soro de leite. Poli (álcool vinílico). Nano-sílica coloidal. Biocompósito. Descarga corona. Filmes laminados. Embalagens alimentícias.

ABSTRACT

The present work proposes the unprecedented addition of colloidal nano-silica (NS) to the matrix of whey protein isolate (WPI) and poly (vinyl alcohol) (PVOH), forming a new biocomposite with high tensile strength and flexibility for application as flexible packaging for food. Furthermore, it proposes the use of the lamination method with corona discharge in WPI and PVOH films, to modify tensile mechanical properties and moisture barrier. For this purpose, blends with 70% WPI and 30% PVOH plus 0%, 1%, 2%, 3%, and 4% NS were developed using the casting method. The biocomposites produced were characterized according to the properties: mechanical (tensile test), morphological (Scanning Electron Microscopy - SEM), interaction (Infrared Region Spectroscopy - FTIR), glass transition temperature (Differential Scanning Calorimetry), permeability, diffusivity, and solubility to water vapor, and interaction with moisture under different water activities and temperatures (sorption isotherms). The addition of 4% NS led to a biocomposite with a tensile strength of 10.2 MPa (43% higher than that of the film without NS), and with a tensile modulus of 78.2 MPa, which are excellent results for application as flexible packaging. At 4% of NS there was also a reduction of 17% in sorption, 58% in diffusivity, and 40% in water vapor permeability, and a lower spontaneity of the sorption process compared to film with 0% of NS, showing a greater ability to maintain the integrity of the food and the packaging itself during application. In a second phase of the work, new bi-layered biocomposites were produced via casting, with a first layer of WPI/NS and a second layer of PVOH/NS, fixing the amount of NS (4% m/m polymer) and applying different corona discharge periods (0s, 30s, 60s, 90s) to improve adhesion between layers. The analysis of FTIR, water contact angle, and surface energy of the first layer showed that the longer the corona discharge time, the greater the wettability and surface energy obtained, leading to greater adhesion between the layers. The final laminated biocomposites were evaluated under the properties: morphological of the joining region between the layers (MEV), mechanical (tensile test), and permeability, diffusivity, and solubility to water vapor. Laminated biocomposites treated with 90s corona discharge showed a more homogeneous joining region between the layers (compared to the other treatment periods), and a tensile strength of 12.6 MPa, being 72% and 23% more resistant, respectively, than the laminated film not treated with corona and that the non-laminated film (single layer). Furthermore, lamination with 90s of corona provided a 7.4 times greater flexibility compared to non-laminated film. Despite the increase in tensile strength and flexibility, lamination together with corona discharge increased the permeability and affinity of the film with water.

Keywords: Whey protein isolate. Poly (vinyl alcohol). Colloidal nano-silica. Biocomposite. Corona discharge. Bi-layer films. Food packaging.

SUMÁRIO

PRIMEIRA PARTE

1 INTRODUÇÃO

A utilização de polímeros renováveis e biodegradáveis como potenciais substituintes para os polímeros de origem fóssil, muitas vezes é limitada pelas propriedades que os primeiros apresentam. Ao serem testados mecânica, térmica e fisicamente, em geral, biopolímeros tendem a apresentar propriedades pobres de resistência e barreira quando comparados aos polímeros convencionais. Na tentativa de tornar esses materiais mais atrativos e aplicáveis no âmbito das embalagens para alimentos, muitos pesquisadores e empresas buscam desenvolver blendas, compósitos, ou mesmo novos métodos de processamento, para que biopolímeros apresentem propriedades adequadas na contenção e proteção de alimentos.

Antes mesmo da adequação das propriedades, deve-se priorizar o fato de que biopolímeros para embalagens precisam ser abundantes e ter origem renovável. Aqueles oriundos de resíduos industriais, em geral, se adequam a essas requisições. O isolado proteico de soro de leite (IPS) é um biopolímero comestível e biodegradável, o qual é obtido como subproduto da indústria de queijos, e pode ser utilizado como matriz na produção de filmes para embalagens. Não fugindo da problemática citada, apesar de suas desejáveis propriedades de transparência e boa barreira ao oxigênio, filmes de IPS são comumente frágeis e quebradiços devido às interações entre diferentes grupos funcionais das cadeias proteicas. Por esse motivo, na busca pela obtenção de propriedades mecânicas e de barreira aplicáveis à embalagem, diversas pesquisas relacionadas à produção de blendas de IPS com outros polímeros são desenvolvidas, principalmente, com amido e quitosana. O desenvolvimento de blendas de IPS com poli (álcool vinílico) (PVOH), por sua vez, se mostra bastante efetivo na redução da rigidez e fragilidade proporcionada pelo IPS.

O PVOH é um polímero sintético, biodegradável, solúvel em água e, seus filmes, usualmente, apresentam boa capacidade de estiramento. Este é obtido através do acetato de vinila proveniente da oxidação do etileno, que por sua vez, pode vir da cana-de-açúcar, uma origem renovável. Apesar da desejável modificação nas propriedades mecânicas do IPS quando acrescido de PVOH, a blenda formada por esses dois polímeros tende a apresentar uma reduzida barreira à umidade. Esse fato é explicado pela forte interação com água, dada a presença de grupos polares nas proteínas do soro do leite, bem como a vasta quantidade de grupos hidroxila apresentados pelo PVOH, principalmente aquele com alto grau de hidrólise. Nano-materiais,

neste contexto, podem ser utilizados como melhoradores de barreira, quando bem dispersos nos espaços entre as cadeias poliméricas.

A nano-sílica constitui-se em um material com elevada área de superfície específica, e alta energia de superfície dada a presença de ligações químicas insaturadas e oxigênio. Tais características usualmente permitem uma boa dispersão deste nano-material em matrizes poliméricas, principalmente aquelas de polímeros com nitrogênio e oxigênio em suas estruturas, como o IPS e o PVOH. Além disso, a nano-sílica apresenta propriedades como biocompatibilidade, atoxicidade, estabilidade térmica, tornando-as adequadas para o processamento e utilização em embalagens alimentícias. A adição de nano-sílica coloidal à blenda IPS/PVOH, portanto, tem potencial para apresentar uma boa dispersão e, consequentemente, contribuir para o aumento da barreira à umidade. Até o momento, não foi estudada a adição de nano-sílica à matriz IPS/PVOH, o que, juntamente com a possibilidade de um aumento de barreira à umidade da blenda em questão, torna o estudo deste novo biocompósito tão importante. Além disso, ainda não foi estudada a utilização do método de laminação com descarga corona em filmes de IPS e PVOH, e consequentemente em compósitos IPS/PVOH/nano-sílica, o qual tem potencial para intensa modificação de propriedades em geral.

No que se refere à produção de filmes para embalagens, o método de *casting* é o mais utilizado em pesquisas preliminares de novos materiais dada a simplicidade do processo, o baixo custo para a escala laboratorial, requisição de quantidades menores de material e a não submissão do polímero a tensões, como ocorre na extrusão, por exemplo. Através do processamento do compósito IPS/PVOH/nano-sílica em sua forma convencional pelo método de *casting*, é provável a obtenção de um material com propriedades mecânicas e de barreira à umidade adequadas à aplicação como embalagem para alimentos na forma de filmes flexíveis. Entretanto, um compósito diferente, com mais fases, pode ser formado por esses materiais através da laminação de camadas, o que possivelmente traria mudanças as suas propriedades em geral. A formação de uma primeira camada de PVOH/nano-sílica e seguinte adição de uma segunda camada de IPS/nano-sílica, constitui-se em exemplo de um novo compósito formado por esses mesmos materiais.

Ao produzir um material único formado por duas camadas poliméricas diferentes, é importante garantir que suas camadas tenham uma boa aderência, para que as mesmas não se separem durante as solicitações mecânicas. Para isso, pode-se, por exemplo, fazer uso da

descarga corona, a qual vem sendo usada industrialmente em poliolefinas para modificação de suas propriedades adesivas. O efeito corona é um processo ambientalmente amigável, sem geração de resíduos, que não requer uso de água ou mesmo de solventes. Através do mesmo, pode-se conferir diferentes propriedades adesivas, de molhabilidade e de energia superficial à polímeros, a depender da natureza química do próprio polímero, e das condições de aplicação, como potência, tempo e distância entre a descarga e o material. O efeito corona apresenta-se como potencial agente adesivo entre as camadas de PVOH e IPS, principalmente devido à forte presença de grupos oxigenados nesses materiais.

Buscando aumentar a resistência mecânica e a barreira à umidade, mantendo-se a ductilidade de blendas de IPS/PVOH, o presente trabalho propõe o desenvolvimento de compósitos convencionais (monocamada) de IPS/PVOH e nano-sílica coloidal (na forma de uma dispersão estável) nas concentrações de 0 a 4%. Além disso, verificada a concentração mais efetiva de nano-sílica, propõe-se a produção de um compósito laminado, com uma primeira camada de PVOH/nano-sílica e uma segunda de IPS/nano-sílica. Declarada a intenção de se aplicar os materiais desenvolvidos como embalagens flexíveis na área de alimentos, os mesmos foram caracterizados quanto às propriedades: mecânicas de tração, morfológicas, físicas, de permeabilidade ao vapor de água, de solubilidade e de interação com umidade sob determinadas atividades de água e temperatura.

2 REFERENCIAL TEÓRICO

2.1 Embalagens plásticas alimentícias

Embalagens desempenham um papel fundamental na manutenção das características proporcionadas pelo processamento dos alimentos, ou mesmo das propriedades desejáveis de produtos *in natura*. Essas permitem que alimentos possam ser transportados com segurança, por curtas ou longas distâncias, de forma que estes se mantenham em condições adequadas até chegarem ao consumidor. Materiais plásticos, por sua vez, têm dominado cada vez mais o mercado de embalagens, sendo utilizados junto aos alimentos desde a produção até o transporte e distribuição. Segundo a Associação Brasileira de Embalagens (ABRE), em 2019 o valor estimado do faturamento da indústria de embalagens no Brasil foi de R$ 75,9 bilhões, dos quais os materiais plásticos representam a maior parcela frente aos demais (39,6%) (ABRE, 2020).

Em 2019, a produção mundial de plásticos excedeu 368 milhões de toneladas, comprovando assim, o uso extremamente difundido desse material (EPRO, 2020). Vale ressaltar que, antes da expansão do uso de materiais poliméricos, o vidro era o material mais utilizado no acondicionamento de produtos alimentícios líquidos e sólidos. A introdução dos polímeros no mercado propiciou uma redução no consumo global de energia, principalmente pelo fato de que a produção e reciclagem do vidro consomem montantes de energia usualmente superiores aos necessários para a produção de embalagens plásticas (RABELLO; DE PAOLI, 2013).

Espera-se, a cada ano, um crescimento da utilização de embalagens plásticas, dadas as vantagens oferecidas pelos polímeros com relação aos demais materiais, a necessidade diária pelo consumo de alimentos e a exigência crescente dos consumidores por produtos práticos, prontos para o consumo, de alta qualidade e segurança. Apesar de ter crescido a destinação desses materiais, após o uso, à reciclagem ou à recuperação energética, ainda é alta a quantidade de plásticos destinadas à aterros ou descartados de forma imprópria no ambiente pelos consumidores. Segundo a EPRO, em 2019, das 29,1 milhões de toneladas de plástico descartados na Europa, 24,9% ainda foram destinados a aterros (EPRO, 2020). O alto consumo, associado ao descarte inadequado e a resistência da maioria dos plásticos à degradação, têm ocasionado um grande acúmulo de resíduos desse material no meio ambiente. Vale ressaltar que tal impacto ambiental ocorre porque, ainda, falta por parte da população, a consciência de

que o descarte inadequado dos materiais poliméricos, ou mesmo a destinação a aterros, provocam a perda da energia gasta no processo de produção dos mesmos (MAGRINI *et al*., 2012). Além disso, é preciso exigir das empresas que fazem uso de embalagens plásticas para contenção de seus produtos, a responsabilidade pela destinação correta das embalagens que distribuem no mercado, bem como exigir dos governos políticas e leis de incentivo à reciclagem. É importante o entendimento de que a resistência à degradação desses materiais é fator fundamental para a sua capacidade de serem reciclados, possibilitando um ciclo de vida com eficiência energética maior do que todos os seus concorrentes.

Segundo Magrini *et al*. (2012), as principais motivações para o desenvolvimento de plásticos oriundos de biopolímeros têm sido a substituição de matérias-primas de origem fóssil e o referido problema do acúmulo desses materiais no ambiente dado seu descarte inadequado. Entretanto, entende-se que o descarte de biopolímeros também não pode ser realizado de forma aleatória e deliberada. Além disso, cerca de apenas 4% do petróleo extraído é destinado para a produção de plásticos, e o acúmulo desses resíduos é passível de ser resolvido com destinação correta dos mesmos à reciclagem ou recuperação energética. Por outro lado, de fato, em qualquer setor, é desejável a existência de fontes alternativas de matéria-prima. No setor de embalagens para alimentos, principalmente, o qual consome montantes de materiais poliméricos diariamente, anseia-se por novas fontes de matéria-prima as quais sejam renováveis ou obtidas através de resíduos com reduzido valor agregado. Desta forma, justifica-se a busca por biopolímeros visando a aplicação no setor de embalagens alimentícias.

2.2 Biopolímeros

Biopolímeros são definidos como macromoléculas formadas por organismos vivos, incluindo proteínas, ácidos nucleicos e polissacarídeos (IUPAC, 1996). Esses materiais também podem ser enquadrados como polímeros extraídos de materiais renováveis e, além de possibilitar a redução do volume de resíduos acumulados no meio ambiente, também podem, ao invés de descartados, ser utilizados na compostagem de plantas (BERTOLINI, 2007). A biodegradabilidade apresentada por grande parte desses materiais, bem como sua abundância, já que são oriundos de fonte renovável ou de resíduos industriais, são os mais fortes fatores de competição desses materiais na tentativa de substituir os polímeros de baixo custo com origem no petróleo.

Apesar de a busca por materiais biodegradáveis ter sido um dos combustíveis para o desenvolvimento das pesquisas relacionadas a biopolímeros, nem todos esses materiais irão apresentar essa propriedade. A biodegradabilidade vai depender de fatores morfológicos, como a forma e o tamanho da cadeia, fatores químicos, incluindo a estrutura química e composição, fatores físicos, como as condições de processamento, além da presença do microorganismo adequado no ambiente de degradação. Além disso, vale ressaltar que nem sempre a biodegradabilidade é fator desejável, já que muitos materiais precisam ser armazenados ou transportados por longas distâncias e por maiores períodos de tempo, sendo essencial a manutenção das funções das embalagens durante esse processo. Tal propriedade é desejável, por sua vez, em ambientes naturais nos quais a coleta de lixo é dificultada, como praias, por exemplo, ou mesmo em situações em que o produto armazenado tem vida útil curta ou é embalado na forma de revestimento comestível.

De acordo com a fonte e com o tipo de síntese, polímeros caracterizados como biodegradáveis são usualmente divididos em quatro classes:

a) Polímeros originados de biomassa, de fontes agrícolas vegetais ou animais, como polissacarídeos (amidos de milho, batata, etc.), produtos lignocelulósicos, e outros como quitosana, quitina, pectinas e proteínas do leite;
b) Polímeros obtidos por microorganismos (polihidroxialcanoato – PHA, polihidroxibutirato-PHB, entre outros);
c) Polímeros sintetizados quimicamente através de monômeros de fontes agrícolas, como por exemplo o poli (ácido lático) ou o poli (álcool vinílico) (PVA) obtido pela desidratação do álcool etílico da cana-de-açúcar;
d) E polímeros em que seus monômeros e a própria molécula polimérica final são obtidos pela síntese química de fontes fósseis, como as policaprolactonas (PCL), os poliesteramidos (PEA), o PVOH, entre outros (VIEIRA *et al*., 2011).

Biopolímeros podem ser amplamente aplicados na indústria alimentícia como materiais para embalagens, desde que apresentem propriedades adequadas de resistência mecânica e barreira, principalmente. Desta forma, alguns atributos são responsáveis pela determinação da aplicação desses materiais a alimentos, como a possibilidade de eles serem comestíveis, as propriedades mecânicas de tração e punctura, a capacidade de barreira a gases e à água, a estabilidade sob diferentes condições de temperatura e umidade, entre outras.

Dentre os biopolímeros com origem renovável e potencial aplicação na área embalagens, pode-se citar o Isolado proteico de soro de leite, o qual vem sendo amplamente estudado na tentativa de tornar suas propriedades mais atrativas a esse grande setor do mercado.

2.3 Soro de leite e isolado proteico de soro de leite (IPS)

Segundo o Regulamento Técnico de Identidade e Qualidade do Soro de Leite, o soro de leite é definido como "o líquido obtido a partir da coagulação do leite destinado à fabricação de queijo, caseína e produtos lácteos similares", o qual possui 5g de proteína láctea a cada litro (BRASIL, 2013). Os teores de proteína do soro de leite são inferiores quando comparados aos leites integral e desnatado, entretanto, o grande volume de soro oriundo da indústria de queijos, permite que seja vantajosa a extração da proteína deste subproduto.

O mercado atual mostra uma tendência de crescimento na produção mundial de leite de 9% em países desenvolvidos até 2027, dos quais 37% irão para a produção de queijos (FAO; OECD, 2018). Essa tendência de crescimento, associada ao fato de que a produção de queijos gera, em média, até 9kg de soro de leite para cada quilo de queijo produzido, torna o aproveitamento do soro bastante atrativo (GONZÁLEZ-SISO *et al*., 2015). Esse subproduto já foi, inclusive, considerado como poluente, considerando-se o fato de que era comum o seu descarte em cursos d'água, aumentando a demanda bioquímica de oxigênio. Entretanto, com o passar dos anos, a o crescimento da consciência ambiental por parte da população e das indústrias, bem como a necessidade destas últimas em gerar lucros até mesmo sobre os subprodutos, uma vasta gama de produtos lácteos passou a ser produzida a partir do soro de leite, como o leite em pó, bebidas lácteas e o isolado proteico de soro de leite (CHAVAN *et al*., 2015).

Fernandes (2010) cita que o soro líquido contém cerca de 20% das proteínas do leite original, sendo essas, em sua maioria, β-lactoglobulina, α-lactoglobulina, albumina sérica e proteose-peptona. A Figura 1 mostra um segmento de cadeia da estrutura primária, com sete resíduos de aminoácidos, da β-lactoglobulina, a proteína majoritária em soro de leite de ruminantes. Em relação à separação das proteínas do soro, podem ser produzidos dois tipos de produto: o concentrado proteico de soro de leite (CPS) e o isolado proteico de soro de leite (IPS) (CHAVAN *et al*., 2015). Ao remover os componentes não-proteicos do soro de leite pasteurizado, geralmente pelo método de membranas por ultrafiltração, obtém-se o CPS, com

composição de 30 a 90% de proteínas e o restante de lactose, lipídeos e cinzas. As etapas de preparação do CPS por esse método envolvem a clarificação do soro (50 °C), a ultrafiltração e, por último a secagem por spray drying. Os concentrados com menor porcentagem de proteínas são utilizados em produtos de panificação, doces, laticínios, entre outros, enquanto os CPS mais concentrados em proteínas são utilizados também em confeitaria, carnes, suplementos proteicos e para o desenvolvimento de filmes biopoliméricos (FERNANDES, 2010).

Figura 1 – Estrutura de um segmento de cadeia da β-lactoglobulina com sete resíduos de aminoácidos (H-Ala-Leu-Pro-Met-His-Ile-Arg-OH, 142–148)

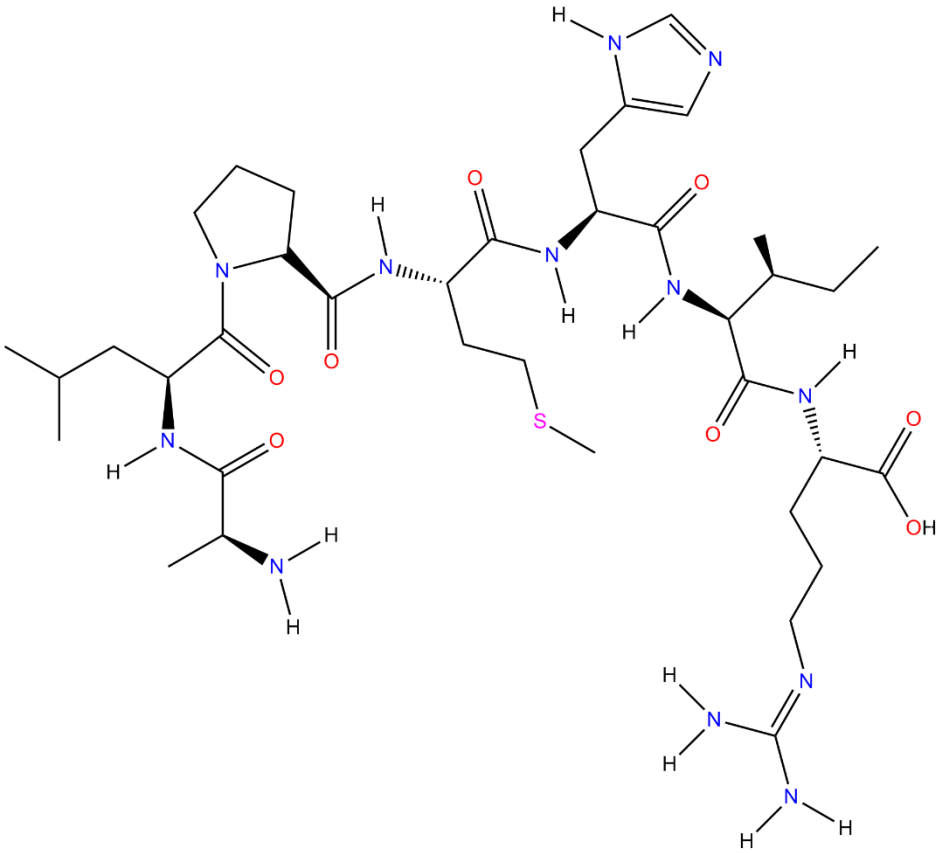

Fonte: Adaptado de NCBI (2017).

O IPS, por sua vez, é obtido de maneira semelhante ao CPS, porém com a adição de mais uma etapa ao processo, que é a cromatografia de troca iônica. Essa etapa tem a função de remover os minerais da mistura, obtendo-se, assim, isolados com teores de proteína que podem ser maiores que 90%, e contendo, portanto, uma porcentagem de proteínas mais elevada e menor quantidade de lactose e lipídeos que o CPS. Segundo o U.S. Dairy Export Council, a

composição usual do isolado é de 90-92% de proteína, 0,5-1% de lactose, 0,5-1% de lipídeos e 2-3% de cinzas (FERNANDES, 2010).

O IPS é utilizado em laticínios, panificações, carnes, doces e como fonte proteica em suplementos. Pelo fato de poder ser produzido utilizando-se um subproduto gerado em grande volume pela indústria de queijos, a qual apresenta-se em cenário de crescimento, o isolado proteico de soro de leite, recentemente, desperta interesse de pesquisas, não somente no âmbito alimentício ou nutricional. O IPS também vem sendo alvo de estudos para sua utilização como matriz polimérica na produção de filmes biodegradáveis.

2.4 Filmes de IPS

Recentemente, o IPS vem sendo bastante explorado em pesquisas visando sua aplicação como matriz polimérica para produção de filmes biodegradáveis para embalagem de alimentos (AZEVEDO *et al*., 2017; LARA *et al*., 2019; SAMADANI; BEHZAD; SAEID ENAYATI, 2019; SILVA *et al*., 2018). Em geral, tais filmes apresentam propriedades como boa barreira a oxigênio e versatilidade de propriedades mecânicas, quando combinados com compostos e nanomateriais específicos, além de apresentarem boa transparência e possibilidade de serem incorporados a agentes ativos diversos.

Apesar das desejáveis características citadas, filmes de IPS usualmente se apresentam frágeis e quebradiços, dadas as várias interações que se formam entre os diferentes grupos funcionais das proteínas (SCHMID, 2013). O aquecimento é essencial na produção dos filmes de IPS por induzir a desnaturação das proteínas. Entretanto, com a desnaturação ocorre a exposição de grupos sulfidril internos da cisteína (Cys), que promove a formação de ligações dissulfídicas entre as cadeias, como mostra a Figura 2 (SCHMID *et al*., 2017). Tais ligações estão diretamente associadas ao comportamento frágil e rígido dos filmes de IPS, os quais apresentam baixa capacidade de estiramento.

Figura 2 – Segmentos da cadeia da β-lactoglobulina constituídos por resíduos de aminoácido cisteína formando ligação dissulfídica

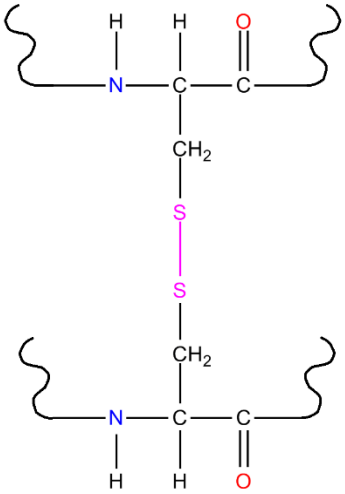

Fonte: (LARA *et al*., 2019).

Além da fragilidade, a capacidade de interação com a umidade faz com que a aplicação de filmes de IPS em embalagens para alimentos seja, ainda, limitada. Filmes de IPS costumam apresentar permeabilidade ao vapor de água (4.92 $g.mm.m^{-2}.dia^{-1}.kPa^{-1}$ a 25°C) aproximadamente dez vezes maior que aquela referente ao polietileno de baixa densidade (PEBD, 0.21 - 0.84 $g.mm.m^{-2}.dia^{-1}.kPa^{-1}$ a 25°C), amplamente utilizado na área de embalagens flexíveis alimentícias (LANGE; WYSER, 2003; LARA *et al*., 2019). Na tentativa de reverter esse fato, utilizam-se modificações como a adição de outros polímeros para formação de blendas, a inserção de outros materiais para formação de compósitos, ou mesmo mudanças nas variáveis de produção dos filmes, como temperatura e pH. Samadani, Behzad e Enayati (2019) produziram filmes de IPS com óleo de nozes e nanofibras de celulose modificadas, obtendo um aumento expressivo na hidrofobicidade com relação ao filme de IPS puro. Alizadeh Sani, Ehsani e Hashemi (2017) adicionaram nanopartículas de titânio e óleo essencial de alecrim em filmes de IPS/nanofibra de celulose e obtiveram um compósito com aumento significativo da resistência à umidade. Silva *et al*. (2016) produziram uma blenda de IPS com goma de alfarroba (*locust bean gum*) e conseguiram maiores flexibilidade, resistência à tração e barreira ao vapor de água quando comparado ao filme de IPS. Oymaci e Altinkaya (2016), por sua vez, obtiveram uma redução da hidrofilicidade dos filmes de IPS através da adição de nanopartículas de zeína.

A adição de PVOH ao IPS, formando uma blenda, por sua vez, foi estudada por Lara *et al*. (2019), mostrando uma provável compatibilidade entre os polímeros e produzindo um material mais dúctil, com flexibilidade nove vezes maior comparado ao filme de IPS puro. As

propriedades mecânicas de tração da blenda formada por 70% de IPS e 30% de PVOH se mostraram semelhantes àquelas pertencentes ao polietileno de baixa densidade (PEBD), o qual é amplamente utilizado no setor de embalagens alimentícias. Apesar de a adição de PVOH não ter alterado a baixa barreira à umidade de filmes de IPS, a redução na rigidez e na fragilidade são justificativas para que se amplie o estudo dessa blenda, pensando, por exemplo, em alternativas para melhoria da barreira através da adição de outros materiais.

2.5 Poli (álcool vinílico) (PVOH)

Segundo Halima (2016), o PVOH é um polímero sintético, solúvel em água, composto por uma cadeia principal de carbono e biodegradável sob condições aeróbicas e anaeróbicas. Este foi sintetizado pela primeira vez em 1924, por Herrman e Haehnel, através da hidrólise do poli (acetato de vinila), metodologia essa utilizada até hoje para sua obtenção. Desde então, diferentes tipos de PVOH vêm sendo produzido em grande escala mundialmente, sob diferentes condições, por apresentar propriedades subordinadas ao grau de polimerização e de hidrólise. As estruturas do PVOH 100% hidrolisado (a) e com grau de hidrólise menor que 100% (b) são mostradas na Figura 3.

Figura 3 – Estrutura do (a) PVA 100% hidrolisado, sem grupos acetato; e (b) PVA com grau de hidrólise menor que 100%, com a presença de grupos acetato na cadeia.

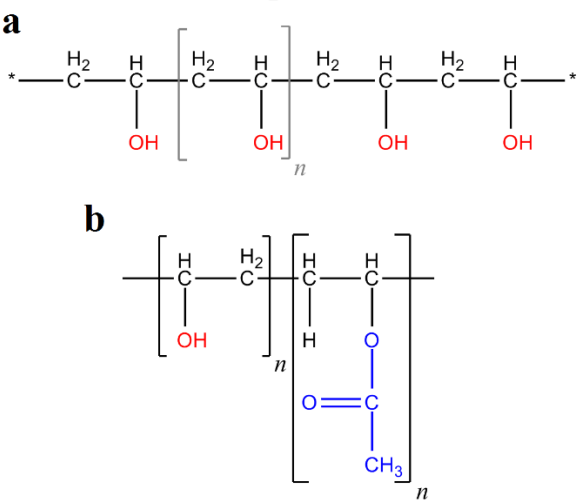

Fonte: Adaptado de Halima (2016).

O PVOH é obtido através da polimerização do acetato de vinila, gerando o poli (acetato de vinila) (PVAc), seguida pela reação de hidrólise alcalina do PVAc, a partir da qual se obtém

o PVOH como produto final (FIGURA 4). A sintetização ocorre nessas duas etapas uma vez que o álcool vinílico é um composto instável que se converte em acetaldeído espontaneamente e, portanto, não pode ser obtido de forma direta. O acetato de vinila, que é a matéria prima para sua produção, é produzido pela oxidação de etileno na presença de paládio (MESQUITA, 2002). O etileno, por sua vez, pode ser obtido através dos processos de transformação do petróleo, ou através da desidratação do álcool etílico. Produzindo-se acetato de vinila e, portanto, PVOH, do álcool etílico proveniente da cana-de-açúcar, pode-se afirmar que esse último é proveniente de fonte renovável.

Figura 4 – Representação esquemática da sequência de reação utilizada na produção industrial de PVOH.

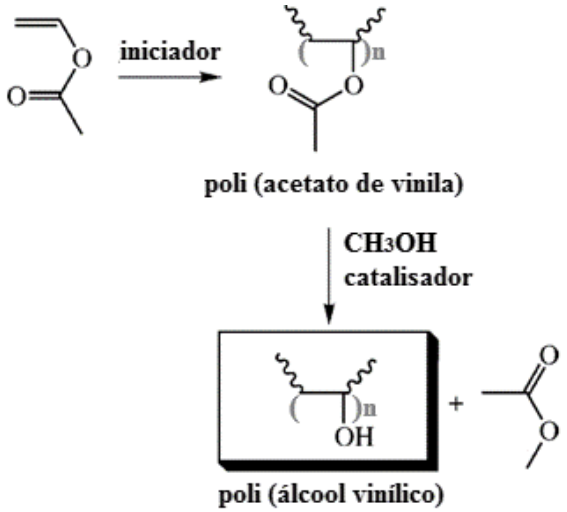

Fonte: Adaptado de Chiellini *et al*. (2003).

Por ser um polímero biodegradável em condições aeróbia e anaeróbia, o PVOH é alvo recorrente de pesquisas na área dos biomateriais. Silvério (2013) destaca a capacidade do PVOH em formar ligações de hidrogênio intra e intermolecular, sua alta capacidade de estiramento, além de suas propriedades térmicas, de barreira e de resistência a solventes orgânicos, as quais variam com o grau de cristalinidade do polímero. A cristalinidade, por sua vez, vai estar diretamente conectada ao grau de hidrólise e massa molecular média do polímero, demonstrando, portanto, a possibilidade de se obter uma grande variedade nas propriedades do PVOH e adequá-lo a diferentes aplicações.

Segundo Ozaki (2004) existe uma gradativa redução nos custos de produção do PVOH, o que tem contribuído para a expansão de sua aplicação. Além disso, por suas propriedades ajustáveis e adequadas à aplicação em embalagens e sua biodegradabilidade, o PVOH é,

portanto, um material com grande potencial na modificação de propriedades de outros polímeros biodegradáveis, como o IPS, para torná-los mais adequados ao acondicionamento de alimentos.

2.6 Filmes de PVOH

O PVOH apresenta excelente capacidade de formação de filmes por *casting*, além de propriedades emulsificantes e adesivas, e de ser considerado completamente seguro para utilização na área de embalagens para alimentos. Quanto às propriedades, filmes de PVOH apresentam resistência à óleos e solventes, alta resistência à tração, ótima barreira a oxigênio e aroma, além de ser inodoro e atóxico. A resistência à tração de filmes de PVOH, em torno de 10 MPa, pode ser considerada semelhante à do PEBD, o que aumenta o interesse da utilização do primeiro como embalagem (LARA *et al*., 2019; SHEBANI *et al*., 2018). Entretanto, as propriedades desse material podem variar de acordo com a umidade. Com teores mais elevados de água, e consequente maior adsorção de umidade por parte da matriz, maior o efeito plastificante provocado pela água e, assim, menor a resistência à tração e maior o potencial de elongação do filme (TANG; ALAVI, 2011).

Na grande maioria das pesquisas de aplicação do PVOH em embalagens, faz-se a junção desse material com outros polímeros de origem renovável e mais baratos através de blendas poliméricas, para assim, obter materiais mais resistentes, com boa biodegradabilidade e custos mais baixos. Cazón, Velazquez e Vázquez (2019) produziram filmes de celulose bacteriana (CB) acrescidos de PVOH e glicerol, obtendo um material com maior resistência à ruptura e maior flexibilidade que o filme de CB puro. Guimarães Jr. *et al*. (2015) relataram que a blenda formada entre amido e PVOH, apresenta, quanto maior a concentração de PVOH, maior flexibilidade, ductilidade e transparência. Foi constatado também, que a adição de PVOH à quitosana, formando uma blenda antimicrobiana, aumentou a flexibilidade e a barreira ao oxigênio e à água; enquanto a adição de nanoargila a essa blenda quitosana/PVOH produziu um compósito com barreira ainda maior à umidade (GIANNAKAS *et al*., 2016). A adição de nano-sílica coloidal em blendas de IPS e PVOH, por sua vez, ainda não foi reportada.

2.7 Blendas poliméricas

As blendas são misturas físicas de dois ou mais polímeros, os quais se mantêm unidos por interações secundárias, podendo resultar em uma mistura miscível ou imiscível. A produção de blendas constitui-se em uma estratégia em crescimento na tentativa de tornar polímeros biodegradáveis com propriedades adequadas a determinadas aplicações, como por exemplo, no setor de embalagens. Ao produzir uma blenda entre dois polímeros é possível obter um material com propriedades inéditas, o que, usualmente, é mais economicamente viável do que o desenvolvimento de um novo produto. Por outro lado, nem sempre a miscibilidade é alcançada ao se misturar dois polímeros diferentes.

A miscibilidade de uma blenda obedece a segunda lei da termodinâmica, a qual leva em consideração e entalpia (ΔH^M), a entropia (ΔS^M) e a temperatura (T) da mistura, como mostrado na Equação 1. Os componentes da blenda só irão se misturar perfeitamente, formando uma única fase, se a energia livre de Gibbs de mistura (ΔG^M) for negativa. A maioria das blendas de polímeros com monômeros de alto peso molecular são imiscíveis devido às fracas interações secundárias entre as fronteiras de fases dos materiais, o que usualmente produz blendas com pobres propriedades termomecânicas. Como estratégia para o melhoramento da compatibilidade dos materiais na blenda, comumente, se faz o uso de compatibilizantes diversos, os quais são capazes de interagir com ambas as fases, formando uma rede de ligações covalentes (THOMAS; MISHRA; KALARIKKAL, 2017).

$$\Delta G^M = \Delta H^M - T\Delta S^M \quad (1)$$

A verificação da miscibilidade de dois polímeros em uma blenda pode ser feita também através da análise da temperatura de transição vítrea (Tg) da blenda produzida. A temperatura de transição vítrea é a temperatura a partir da qual ocorre o início do movimento das cadeias poliméricas, passando de um estado vítreo, com moléculas mais ordenadas, para um estado borrachoso, onde as mesmas adquirem maior flexibilidade e menor ordenação (CANEVAROLO JUNIOR, 2006). Usualmente, ao se misturar dois polímeros com diferentes valores de Tg, a observação de uma única Tg para a blenda remete à miscibilidade dos materiais. Enquanto isso, para polímeros imiscíveis, a blenda demonstra claramente dois valores de Tg para os respectivos componentes puros, independentemente da composição da mesma. As

blendas parcialmente miscíveis, portanto, apresentam valores de Tg intermediários às Tg's dos polímeros isolados (KALOGERAS; BROSTOW, 2008).

Blendas de IPS/PVOH mostraram possível miscibilidade quando até 30% de PVOH é adicionado ao IPS, visto que, somente um valor de Tg foi encontrado para as mesmas (LARA *et al*., 2020). Além disso, a compatibilidade desses polímeros é corroborada pelo aumento da flexibilidade dos filmes de IPS acrescidos de PVOH (ductilidade aumentada em 10 vezes), além da não observação de separação de fases em microscopias eletrônicas de varredura (LARA *et al*., 2019). Apesar da maior flexibilidade, blendas de IPS com até 30% de PVOH demonstraram uma não alteração da barreira à umidade ou da resistência à tração com relação ao filme de IPS puro. Portanto, considerando as características positivas desses polímeros, como a origem renovável e biodegradabilidade, bem como a provável miscibilidade entre eles, justifica-se avançar no estudo de materiais para embalagens envolvendo os mesmos. Nesse sentido, a adição de nanopartículas à blenda IPS/PVOH, formando um compósito, pode representar este avanço.

2.8 Compósitos

Materiais compósitos podem ser definidos como aqueles constituídos por dois ou mais materiais com propriedades físicas ou químicas significativamente diferentes, os quais, quando combinados, produzem um material que possui características únicas diferentes daquelas pertencentes aos constituintes isolados (RAJAK *et al*., 2019). A classificação de compósitos pode variar de acordo com a escala ou o tipo do reforço, bem como quanto ao material da matriz e quanto à origem da matriz e do reforço, conforme mostrado na Figura 5. Compósitos poliméricos geralmente possuem uma fase polimérica principal (matriz), com o material em maior quantidade, assim como uma segunda fase formada por outro material disperso nessa matriz, usualmente chamado de reforço ou *filler*.

Figura 5 – Esquema dos tipos de classificação de materiais compósitos

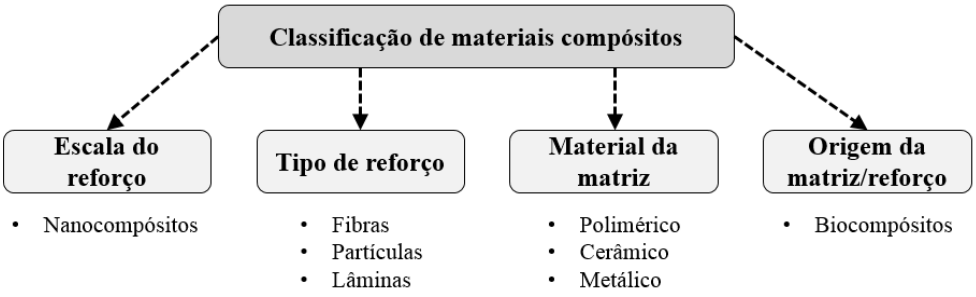

Fonte: Adaptado de Rajak *et al*. (2019).

No âmbito das pesquisas relacionadas a embalagens flexíveis para alimentos, muitos compósitos de matriz polimérica vêm sendo desenvolvidos, principalmente utilizando-se matrizes com origem renovável ou que sejam biodegradáveis (biocompósitos). Diferentes biocompósitos de matriz de IPS já foram desenvolvidos com o objetivo de modificar propriedades mecânicas e de barreira, alterando-se o tipo da fase dispersa: adição de emulsão de óleo de girassol (GÖKKAYA ERDEM; DIBLAN; KAYA, 2019), lâminas (*sheets*) de argila montmorilonita (AZEVEDO *et al*., 2015), nanopartículas de zeína (OYMACI; ALTINKAYA, 2016), nanopartículas de dióxido de titânio (ZOLFI *et al*., 2014); nanofibras de celulose (QAZANFARZADEH; KADIVAR, 2016), entre outros. Até o momento, entretanto, nenhuma pesquisa foi publicada avaliado o efeito da adição de nano-sílica coloidal em matriz de IPS/PVOH aplicáveis como filmes para embalagem.

O compósito formado pela dispersão da nano-sílica coloidal em matriz de IPS/PVOH pode ser classificado como um biocompósito, dadas as origens renováveis do IPS e do PVOH (quando o PVAc, sua matéria-prima, tem origem no álcool etílico da cana-de-açúcar) e sua biodegradabilidade. Além disso, caso a nano-sílica se mantenha bem dispersa na matriz (não formando aglomerados de escala maior que 100 nm), esse novo material também pode ser classificado como um nanocompósito, ou nanobiocompósito. A adição da nano-sílica tem potencial para reduzir o volume livre entre as cadeias poliméricas da matriz de IPS/PVOH, possivelmente proporcionando maior barreira à umidade, bem como maior resistência à tração por dificultar o deslocamento das cadeias umas sobre as outras durante a solicitação mecânica.

2.9 Nano-sílica

O dióxido de silício, mais comumente conhecido como sílica, é composto pelos dois elementos mais abundantes na crosta terrestre e é caracterizado por sua forma cristalina ou amorfa, sendo usualmente encontrado na natureza na forma de areia ou quartzo. Esse material possui um campo muito vasto de aplicação, sendo utilizado como matéria prima na produção de vidro e outras cerâmicas, em tecnologias diversas como fibras óticas e instrumentos analíticos, na área da medicina em produtos farmacêuticos, além de ser também um aditivo alimentício com função nutricional e/ou anti-aglomerante.

Ao reduzir a sílica à escalas nanométricas, obtêm-se materiais com elevada área de superfície específica e com alta receptividade à introdução de grupos funcionais à sua superfície Além disso, propriedades como biocompatibilidade, atoxicidade, estabilidade térmica, associadas à possibilidade de imobilização de materiais diversos à sua superfície, fizeram das nanopartículas de sílica um material com bastantes aplicações na área da farmacologia e biomedicina (VIVERO-ESCOTO, 2012).

Segundo Hassannia-Kolaee *et al*. (2016), a grande área superficial específica, a alta energia de superfície, as ligações químicas insaturadas, bem como a presença do oxigênio permitem uma boa dispersão da nano-sílica em matrizes poliméricas. Vale ressaltar também que, foi publicado no *European Food Safety Authority (EFSA) Journal* a não observação de efeito adverso com a nano-sílica nos estudos de toxicidade oral disponíveis in vivo, até o momento da publicação, em março de 2018, não impedindo sua utilização como aditivo alimentício (YOUNES *et al*., 2018). Apesar disso, poucos são os estudos relacionados à adição dessas em materiais para embalagens.

No âmbito das embalagens para alimentos, foi estudada a influência das nanopartículas de sílica coloidal em filmes de polipropileno bi-orientado revestido com pululano, observando-se uma melhoria nas propriedades de barreira do filme, manutenção das propriedades óticas e aumento da molhabilidade com a adição da nano-sílica (GHAANI *et al*., 2016). Apesar desse aumento na molhabilidade ocasionado pela presença da nano-sílica nessa pesquisa em específico, essas nanopartículas são amplamente estudadas em áreas diversas do conhecimento, justamente pelo fato de provocar hidrofobicidade na matriz em que são adicionadas. Já foi relatado que a adição de nanopartículas de sílica em filmes de poliuretano utilizando etanol como não-solvente provocou a formação de uma camada superior superhidrofóbica (SEYFI *et*

al., 2016). Yao *et al*. (2011), por sua vez, avaliou a estrutura e as propriedades de filmes híbridos de amido/PVOH/nano-sílica, e observou que a presença das nanopartículas de sílica possibilitou a obtenção de uma estrutura com um maior número de cristais, além de retardar o envelhecimento do filme (YAO *et al*., 2011).

Dadas as características apresentadas sobre a nano-sílica, espera-se uma boa dispersão das mesmas em matrizes poliméricas de IPS e PVOH e, consequentemente, que essas atuem no sentido de aumentar a resistência mecânica e a barreira à umidade da blenda.

2.10 Aditivos usados em filmes e compósitos flexíveis para embalagem

A elaboração de filmes comuns ou compósitos flexíveis para embalagens de alimentos usualmente envolve a adição de plastificantes como aditivo. Plastificantes são moléculas orgânicas de baixa massa molecular utilizadas para aumentar a flexibilidade e a processabilidade de materiais poliméricos através da redução da Tg. O pequeno tamanho das moléculas permite com que plastificantes ocupem espaços intermoleculares entre as cadeias poliméricas, reduzindo as forças secundárias entre elas e reduzindo o volume livre, garantindo maior mobilidade molecular (VIEIRA *et al*., 2011).

Em filmes de IPS, é essencial a utilização de plastificantes dada a sua natureza rígida e frágil. Os plastificantes mais utilizados para esses filmes são glicerol e sorbitol, mas também já foi avaliada a adição de outros como xilitol, polietilenoglicol (PEG) e ácido cítrico (GÖKKAYA ERDEM; DIBLAN; KAYA, 2019; HUNTRAKUL; HARNKARNSUJARIT, 2020; MACHADO AZEVEDO *et al*., 2018; OSÉS *et al*., 2009; RAMOS *et al*., 2012, 2013). Em sua pesquisa comparando a estabilidade de filmes de IPS acrescidos de glicerol e sorbitol, Osés *et al*. (2009) comprovou que o glicerol se mostrou um plastificante mais estável, já que após o envelhecimento, somente o filme de IPS/glicerol manteve a mesma aparência e as mesmas propriedades mecânicas.

No presente trabalho, glicerol e ácido cítrico são adicionados aos compósitos de IPS/PVOH/nano-sílica. O glicerol ou propanotriol é um álcool líquido e viscoso à temperatura ambiente, o qual é capaz de interagir facilmente por ligação de hidrogênio com os grupos polares das proteínas do IPS e com as hidroxilas do PVOH altamente hidrolisado. Essa interação ocorre dada a presença de três grupos OH na sua molécula, conforme mostrado na Figura 6 – a, permitindo boa dispersão e ação plastificante na matriz IPS/PVOH.

Figura 6 – a) molécula de glicerol, com três grupos OH e b) molécula de ácido cítrico, com um grupo OH e três carboxilas.

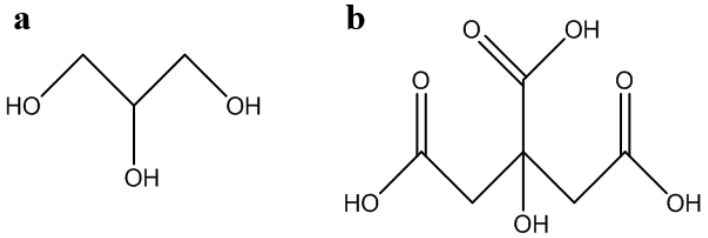

Fonte: Do autor (2022).

O ácido cítrico, por sua vez, é um ácido orgânico fraco, que também possui átomos de oxigênio em grupos de hidroxila e carboxila (FIGURA 6 – b), entretanto, que pode assumir outras funções além da de plastificante quando adicionado em filmes para embalagem. Este pode ser usado em filmes de IPS para fornecer efeito ativo antioxidante e/ou antimicrobiano, produzir reticulação entre cadeias de proteínas (efeito oposto ao de plastificante) ou até para melhorar a dispersão de nanomateriais na matriz (AZEVEDO *et al*., 2015; LI et al., 2018; MACHADO AZEVEDO *et al*., 2018; RAMOS *et al*., 2012). Neste trabalho, justifica-se a adição do ácido cítrico: (i) para melhorar as interações entre as cadeias poliméricas, uma vez que o grupo hidroxila e os 3 grupos carboxila da molécula deste ácido podem interagir através de ligações de hidrogênio com os átomos de nitrogênio (N) e oxigênio (O) de proteínas de soro de leite e com os grupos hidroxila do PVOH (FIGURA 7); (ii) para garantir uma boa distribuição da nano-sílica coloidal na matriz de IPS/PVOH; e (iii) para acrescentar uma característica funcional de conservante de alimentos aos biocompósitos IPS/PVOH/nano-sílica, a qual pode ser explorada em um estudo futuro com estes aplicados a frutas frescas.

Figura 7 – Esquema de representação de algumas das possíveis interações por ligação de hidrogênio entre o ácido cítrico e: o IPS (trecho de uma molécula de β-lactoglobulina) e o PVOH altamente hidrolisado.

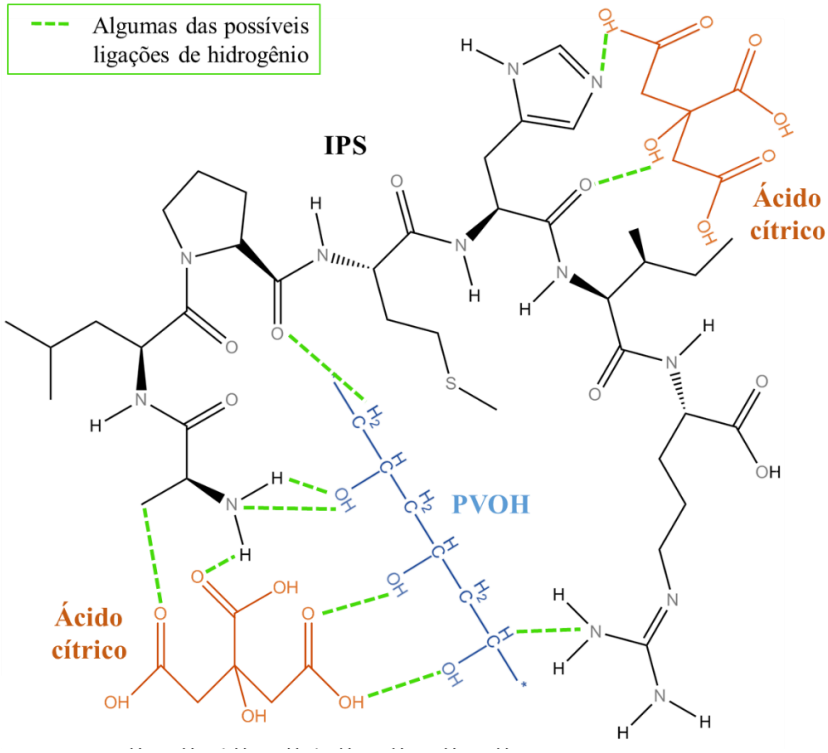

Fonte: Lara (2022).

2.11 Processamento de filmes compósitos com matriz de proteínas de soro

Desde as primeiras pesquisas relacionadas à produção de filmes compósitos contendo nanomateriais em matriz de biopolímeros termoplásticos, até as mais recentes, destaca-se a utilização do método de *casting* dada a sua simplicidade. Neste método, o biopolímero é solubilizado em água ou outro solvente, dispersa-se a nanocarga e, finalmente, a mistura líquida resultante é vertida em placas para que haja a evaporação do solvente e posterior retirada do filme sólido formado. Vale ressaltar que, a utilização do *casting* é bastante positiva em escala laboratorial, quando existe limitação quanto à quantidade de materiais e equipamentos, já que este é um método simples e que não requer estruturas dispendiosas para produção dos filmes. Entretanto, para maiores escalas, são mais utilizados outros métodos, como o de extrusão ou extrusão por sopro, por exemplo.

Quanto aos filmes de proteínas de soro de leite, esses podem ser obtidos através de dois processos principais: úmido ou seco. O processo úmido é o próprio *casting*, onde as proteínas

são dispersas em uma solução aquosa e, por aquecimento, é induzida a desnaturação das mesmas (JANJARASSKUL; TANANUWONG, 2019). Após solubilizadas, é possível fazer a adição de nanomateriais para formação de compósitos com propriedades diferentes àquelas dos filmes de proteínas puro. A dispersão destas cargas pode ser garantida por diferentes processos, associados ou não, como por exemplo, agitação mecânica, magnética, por ultrassom, entre outras. Durante a secagem do filme, fatores como a temperatura, a taxa e o tipo de secagem (natural, em estufa, micro-ondas, infravermelho) vão influenciar morfologia e propriedades do filme final.

Enquanto isso, o processo seco se baseia nas propriedades térmicas das proteínas, como transição vítrea e temperatura de escoamento. A formação do filme pode se dar pela extrusão ou extrusão com sopro, nas quais parâmetros como perfil de temperaturas do canhão, tempo de residência, taxa de alimentação e concentração de plastificantes vão determinar as propriedades químicas e físicas do filme final (JANJARASSKUL; TANANUWONG, 2019). Assim como no processo úmido, no seco é possível adicionar nanomateriais para modificação de propriedades do filme, sendo importante avaliar as características térmicas desta carga, garantindo que ela não seja degradada ou libere outros compostos durante a extrusão devido ao aquecimento. O processo a seco é mais efetivo em larga escala e, apesar de solicitar um gasto maior de energia, dispensa a utilização do solvente e possui maior taxa de produção.

A laminação de filmes, por sua vez, consiste em formar filmes com duas ou mais camadas de polímeros, iguais ou não, para obtenção de propriedades específicas, com a utilização ou não de aditivos químicos ou processos físicos para garantia da aderência entre as camadas. Trabalhos recentes têm provado a efetividade da utilização do processo de laminação de camadas de polímeros através do método de *casting*, tornando assim possível o estudo preliminar das propriedades obtidas por filmes bicamadas.

Hanani *et al*. (2018) produziram filmes ativos laminados de polietileno (PE) e gelatina. Os autores utilizaram uma camada já seca de PE, a qual recebeu a solução de gelatina e, com o solvente desta evaporado, obtiveram o filme bicamada. Nenhum processo físico ou aditivo químico foi utilizado entre as camadas. Zhou *et al*. (2019), enquanto isso, produziram um filme com uma primeira camada de amido de ervilha por *casting*, e uma segunda de poli (ácido lático) colocada acima da primeira e também utilizando *casting*, para aplicação como embalagens de tomate cereja. Os autores também não utilizaram nenhum tratamento químico ou físico na superfície do filme de amido antes do recebimento da segunda camada. Foi observado que o

filme bicamada teve maior barreira à umidade e ao oxigênio quando comparado aos filmes monocamadas de amido e poli (ácido lático), atrasando o processo de maturação do tomate cereja.

Como citado anteriormente, a adição de PVOH ao IPS, formando uma blenda, produziu um material mais dúctil, com flexibilidade nove vezes maior comparado ao filme de IPS puro produzido, apesar de não ter provocado modificações na barreira à umidade (LARA *et al*., 2019). Além da adição de nanocargas, a mistura do PVOH ao IPS, não na forma de um compósito convencional, mas pela utilização de filmes bicamada, constitui-se em uma alternativa para modificação das propriedades em geral. A formação de um filme laminado com uma primeira camada de PVOH e uma segunda de IPS ainda não foi reportada na literatura até então. Além disso, pode-se explorar a possibilidade de utilização de mecanismos para garantia da aderência entre as camadas, como, por exemplo, a descarga corona.

2.12 Tratamento corona

O tratamento de descarga por corona é uma técnica de modificação de superfície usada para tratar materiais poliméricos buscando melhorar suas propriedades de adesão, possibilitar laminação com outros polímeros e aumentar molhabilidade em aplicações como revestimento (JOO *et al*., 2018). O tratamento corona consiste em submeter um material à uma descarga elétrica contínua produzida por uma diferença de potencial alta aplicada entre eletrodos assimétricos, como, por exemplo, uma ponta metálica e uma superfície plana (SUN; ZHANG; WADSWORTH, 1999). Superfícies tratadas com descarga corona apresentam um aumento da adesão à substância polares, o que pode ser explicado por diferentes teorias já propostas: carregamento eletrostático, eliminação de camadas superficiais, aumento de rugosidade, mas, principalmente, pela teoria da introdução de grupos polares devido à oxidação (JOO *et al*., 2018; MAZZOLA, 2010). Partindo da teoria mais aceita, a de que a descarga corona introduz grupos polares ao material (FIGURA 8), um polímero tratado com corona apresenta um aumento na energia e na polaridade superficiais, as quais tendem a diminuir com o tempo pós-tratamento.

Figura 8 – Introdução de grupos polares na superfície de filmes após aplicação de corona

Fonte: Adaptado (DAI; XU, 2019).

As propriedades adesivas resultantes em superfícies poliméricas tratadas com corona, por sua vez, vão depender de variáveis usadas na descarga, como potência, tempo e distância de aplicação, a atmosfera utilizada, além das propriedades originais do material tratado. No caso de filmes laminados, a adesão entre as camadas é de suma importância para garantir a integridade do filme final e, o corona, pode ser usado para aumentar esta adesão. Com a aplicação da descarga, à medida que a polaridade da superfície aumenta, as forças intermoleculares e a força de adesão entre as camadas aumentam (JOO et al., 2018). Cinelli *et al*. (2016) produziram filmes multilaminados de polietileno tereftalato (PET), IPS e PE, utilizando tratamento corona nas camadas substrato de PET e PE para recebimento da camada de IPS. Os autores afirmam que a descarga garantiu a substancial adesão entre as camadas.

No que se refere aos propostos filmes laminados de PVOH/IPS, ao avaliar a grande quantidade de grupos polares presentes no PVOH altamente hidrolisado (um grupo OH por monômero), entende-se que a aplicação do tratamento corona em filmes deste material será capaz de modificar consideravelmente a energia superficial. A alta molhabilidade proporcionada pode permitir o melhor espalhamento da solução de IPS que irá formar a segunda camada. Além disso, o aumento da polaridade da superfície permite que sejam mais intensas e numerosas as interações dos os grupos polares do PVOH com os das proteínas e demais compostos da solução filmogênica da segunda camada. Desta forma, entende-se que o efeito corona tem potencial para garantir a adesão entre as camadas de PVOH e IPS, e portanto, a integridade do laminado final.

2.13 Propriedades mecânicas de tração

Conhecer propriedades mecânicas de tração de materiais poliméricos destinados a embalagens é de extrema importância, visto que, além das solicitações sofridas no durante o processamento da embalagem (estiramento, laminação, impressão, etc.), o próprio peso do

produto embalado e o manuseio por parte do consumidor exigem resistência apropriada. Usualmente, segue-se a norma ASTM D882-02 de 2002 (*Standard Test Method for Tensile Properties of Thin Plastic Sheeting*), específica para materiais com espessura menor que 1.0 mm, para avaliação das propriedades de tração de filmes para embalagens.

Materiais plásticos, como os filmes utilizados para embalagens, apresentam um comportamento de deformação simultaneamente, elástico e plástico. Portanto, ao serem submetidos ao teste de tração, a curva característica do gráfico de tensão (σ) *versus* deformação (ε) expõe de forma clara esses dois comportamentos característicos (FIGURA 9). As propriedades mecânicas de maior interesse em se tratando de filmes flexíveis são o limite de resistência à tração (LRT), o módulo de elasticidade (E) e a porcentagem de deformação ou alongamento suportada pelo filme (D) (GUIMARÃES JR. *et al*., 2015). O LRT corresponde à máxima tensão suportada pelo filme antes da ruptura, enquanto o E corresponde ao coeficiente angular da porção elástica da curva σ *versus* ε, e representa a medida de rigidez do filme. Por outro lado, a D corresponde ao alongamento percentual, ou seja, à relação entre o comprimento final e o comprimento inicial do filme. A deformação (D) ou alongamento pode ser associada à ductilidade ou grau de deformação plástica suportada pelo filme.

Figura 9 – Gráfico tensão versus deformação característico de materiais plásticos.

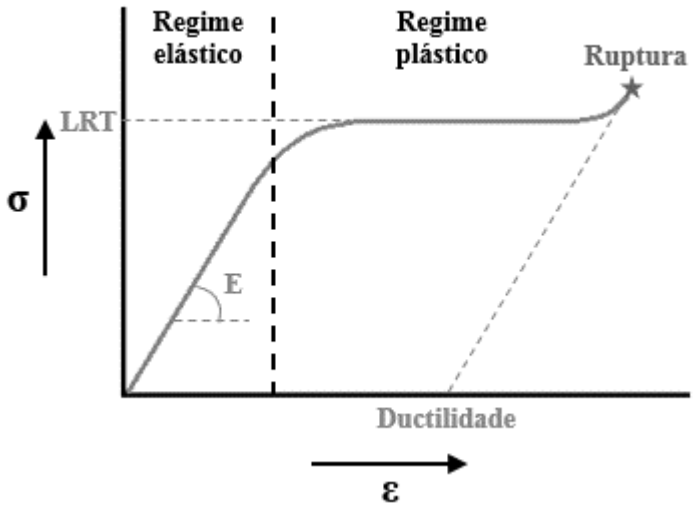

Fonte: Lara (2018).

A depender do alimento a ser acondicionado e de fatores como tempo necessário de conservação, tipo de transporte, entre outros, exige-se propriedades diferentes de resistência à tração, capacidade de deformação e flexibilidade às embalagens. Desta forma, confirma-se a

importância do estudo das propriedades de tração de novos filmes destinados ao uso como embalagens alimentícias para que se consiga definir a aplicação adequada.

2.14 Propriedades físicas de interação com a água

Em se tratando de embalagens, conhecer o comportamento de interação com a água é de extrema importância, visto que muitos alimentos requerem proteção quanto à entrada e saída de umidade da embalagem. A medida da permeabilidade ao vapor de água de filmes é usualmente medida seguindo a norma ASTM E96 / E96M-16 de 2016 (*Standard Test Methods for Water Vapor Transmission of Materials*).

O teste poder ser realizado utilizando-se amostras circulares de filme com uma área conhecida (area – A), fixadas em cápsulas contendo, por exemplo, sílica gel, adotando-se como zero a umidade da atmosfera em contato com a face inferior da amostra (*relative humidity* 1 – RH_1) (FIGURA 10). As cápsulas são então inseridas em dessecadores herméticos com um valor de umidade relativa conhecido e controlado (*relative humidity* 2 – RH_2). O ganho de massa da cápsula ao longo do tempo corresponde à quantidade de umidade que atravessa a amostra de filme (método gravimétrico). A norma ASTM E96 / E96M (2016) pede que, no mínimo, seis pontos sejam utilizados para plotar o gráfico de massa adquirida (*weight gain* – Wg) versus tempo (time - t) e, portanto, no mínimo sete pesagens devem ser feitas incluindo a pesagem inicial.

Figura 10 – Esquema da análise de permeabilidade ao vapor d'água pelo método gravimétrico utilizando cápsulas com sílica e dessecador.

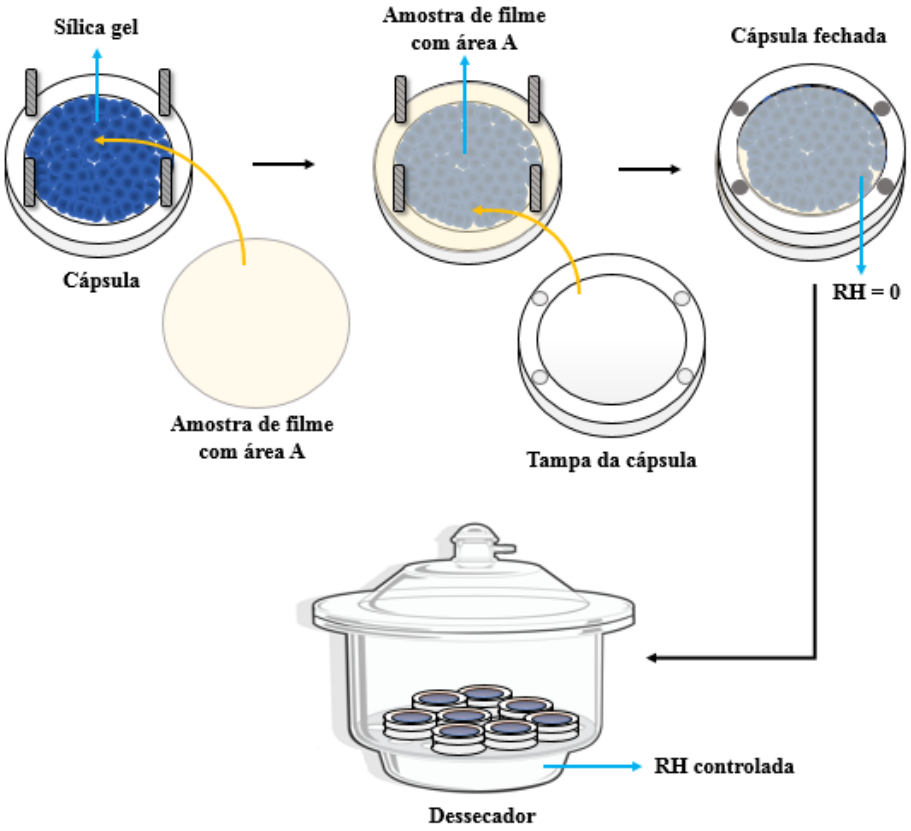

Fonte: Lara (2018).

A taxa de permeabilidade ao vapor de água *(water vapor permeability rate* – WVPR) pode então ser calculada através da Equação 1, enquanto a permeabilidade ao vapor de água *(water vapor permeability* – WVP) é obtida a partir da Equação 2, a qual leva em consideração a espessura da amostra (*thickness* – ti) e a pressão de saturação da água na temperatura do teste (ρs).

$$WVPR = \frac{Wg}{t\,A} \tag{1}$$

$$WVP = \frac{WVPR.ti}{\rho s\,(RH_1 - RH_2)} \tag{2}$$

Uma vez que a permeação de água através do filme é influenciada, tanto pela solubilidade da molécula de água na superfície do material, quanto pela velocidade da penetração das moléculas de água no material, justifica-se o conhecimento dos coeficientes de solubilidade e difusividade de água no filme para melhor compreender o comportamento de barreira do mesmo.

O coeficiente de difusividade está relacionado à velocidade de permeação das moléculas de água através do material, e pode ser calculado através da variação da Lei de Fick para membranas finas e planas (EQUAÇÃO 3), considerando-se: (i) a espessura das amostras de compósito como sendo constantes, (ii) a difusão da água ocorrendo em ambas as faces das amostras, e (iii) a concentração inicial de água na superfície como sendo nula.

$$\frac{M_t}{M_\infty} = 1 - \frac{8}{\pi^2}\sum_{n=0}^{\infty}\frac{1}{(2n+1)^2}\ exp\left[\frac{-(2n+1)^2\pi^2 Dt}{\delta^2}\right] \quad (3)$$

Na equação, D corresponde ao coeficiente de difusividade (cm^2s^{-1}), M_t/M_∞ é a quantidade de água difundida no tempo t, dividida pela quantidade de água difundida no equilíbrio (tempo infinito), e δ é a espessura de cada filme.

Enquanto isso, o coeficiente de solubilidade (S) está relacionado à interação das moléculas de água na superfície do filme. Considerando-se que: (i) a difusão está em estado estacionário; (ii) a relação concentração-distância através do filme é linear (iii) a difusão ocorre em apenas uma direção (através do filme); e (iv) D e S não dependem da concentração, é possível utilizar a Equação 4 para estimar S conhecendo-se os valores de P (WVP) e D (ROBERTSON, 2013; JANJARASSKUL; TANANUWONG, 2019).

$$S = P/D \quad (4)$$

2.15 Isotermas de sorção de água

A submissão de filmes biopoliméricos aos testes de isotermas de sorção de água auxilia na previsão do comportamento de interação com a umidade do material em diferentes atividades de água internas e externas às embalagens e, portanto, é desejável para a adequação das condições de aplicação do filme. Além disso, a submissão de filmes hidrofílicos para embalagens aos experimentos de isotermas é desejável, uma vez que, suas propriedades mecânicas, térmicas e físicas são sensíveis à umidade, influenciando, portanto, sua funcionalidade (YANG; PAULSON, 2000). O gráfico de isoterma de sorção é obtido através de dados experimentais de teor de umidade do filme no equilíbrio em atividades de água pré-determinadas e a uma dada temperatura.

Fennema (2000), afirma que em uma isoterma típica de material biológico, enquadrando-se aqui os filmes de biopolímeros, podem ser distinguidas três zonas, as quais indicam a forma como a água encontra-se ligada ao material (FIGURA 11).

Figura 11 – Zonas (I, II e III) características de isotermas de sorção de água de material biológico.

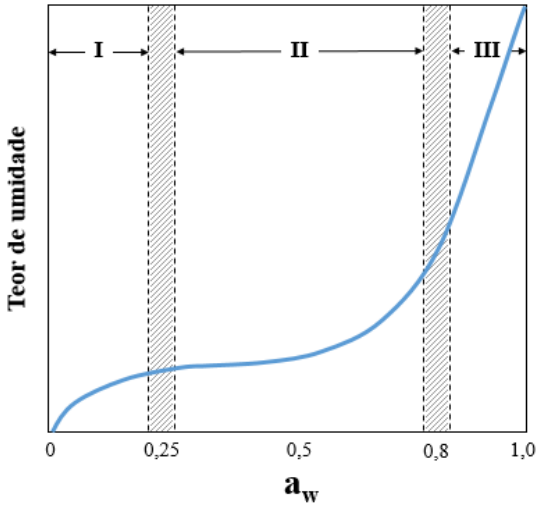

Fonte: Lara (2018); Adaptado de FENNEMA (2000).

A zona I representa a adsorção da água que estará mais fortemente ligada e com menor mobilidade por estar fixa aos grupos polares de certos compostos do material. O limite entre as Zonas I e II pode ser entendido como o teor de umidade necessário para que se forme uma monocamada sobre os grupos polares e acessíveis do material. A zona II, por sua vez, se refere à água das camadas de hidratação de constituintes solúveis do material, como proteínas, açúcares, amidos, sais etc., qual pode estar ligada tanto por interações intermoleculares (ligações de hidrogênio ou dipolo-dipolo) quanto fisicamente retida em microcapilares (FENNEMA, 2000). A transição entre a zona II e a zona III dá início a processos de dissolução, de forma que a água começa a promover o inchamento da matriz do material. Finalmente, a zona III representa a água menos ligada e com maior mobilidade, disponível para o desenvolvimento dos microrganismos e das reações químicas, cuja retenção é determinada pelo pH e pelas forças iônicas.

Dentre os diversos modelos empíricos e semiempíricos desenvolvidos para predição do comportamento das isotermas, o modelo de GAB (EQUAÇÃO 5) em trabalho prévio, conseguiu descrever com qualidade o comportamento de sorção de filmes de IPS e PVOH (VAN DER BERG, 1984; LARA *et al*., 2020).

$$Y_e = \frac{Y_m C K a_w}{(1-Ka_w)(1-Ka_w+CKa_w)} \quad (5)$$

onde Y_e é o conteúdo de umidade no equilíbrio (base seca, g/g); Y_m é o conteúdo de água na monocamada molecular (base seca, g/g); a_w é a atividade de água, C e K são constantes.

Através do estudo de isotermas é possível extrair, também, parâmetros termodinâmicos que nos informam sobre a estabilidade do material testado, bem como sobre a espontaneidade ou não do processo de adsorção de água. De acordo com Liébanes *et al*. (2006), parâmetros termodinâmicos diferenciais revelam informações qualitativas sobre os diferentes níveis de energia da adsorção de água, enquanto os parâmetros termodinâmicos integrais fornecem informações quantitativas sobre o sistema. É desejável conhecer parâmetros integrais em projetos de processos térmicos, por exemplo, para processos de secagem de alimentos. No caso da análise de sorção de água em embalagens, os parâmetros termodinâmicos diferenciais são os de maior interesse, uma vez que a compreensão das interações entre a água e o material é mais importante do que a quantificação de energia envolvida (LARA *et al*., 2018).

Para o cálculo de propriedades termodinâmicas do processo de sorção de água, assume-se as hipóteses: (i) de que o processo de adsorção de água ocorre em um sólido inerte, já que o equilíbrio de umidade entre as moléculas de água adsorvidas na superfície do material e o vapor de água circundante é alcançado; (ii) e de que o vapor de água tem um comportamento de gás ideal, uma vez que apenas a água (adsorvida fisicamente) ocupa a superfície do filme (LIÉBANES *et al*., 2006).

A entalpia diferencial de sorção (ΔH_{dif}) pode ser utilizada como um indicador das forças de atração intermoleculares entre o vapor de água e os sítios de sorção do filme. ΔH_{dif} (J/mol) é definida como diferença entre um calor total de sorção (Q_{st}) e o calor latente de vaporização de água pura (λ) (TAO *et al*., 2018). Os valores de ΔH_{dif} podem ser determinados a partir da Equação 6 de Clausius-Clapeyron:

$$\left[\frac{\partial ln(a_w)}{\partial \frac{1}{T}}\right]_{Y_e} = -\frac{Q_{st}-\lambda}{R} = -\frac{\Delta H_{dif}}{R} \quad (6)$$

A Equação 7 de Gibbs-Helmholtz pode ser usada para determinar a entropia diferencial de sorção (ΔS_{dif}, $Jmol^{-1}K^{-1}$), visto que mudanças na energia livre de um processo de sorção são geralmente acompanhadas por mudanças nos valores de entalpia e entropia.

$$[-\ln(a_w)]_{Y_e} = \frac{\Delta H_{dif}}{RT} - \frac{\Delta S_{dif}}{R} \quad (7)$$

Um gráfico de $-\ln(a_w)$ *versus* 1/T para determinado conteúdo de umidade de equilíbrio (Y_e) pode ser utilizado para calcular ΔH_{dif} e ΔS_{dif}. Os valores de ΔH_{dif} e ΔS_{dif} são obtidos, respectivamente, pelo coeficiente angular ($\Delta H_{dif}/R$) e linear ($-\Delta S_{dif}/R$) da regressão linear deste gráfico, conforme mostrado na Figura 12. Repetindo-se a plotagem para diferentes valores de Ye é possível estabelecer a dependência entre a entropia e entalpia diferenciais e o conteúdo de umidade (TAO *et al*., 2018).

Figura 12 – Pontos experimentais de $\ln(a_w)$ *versus* 1/T, para três temperaturas (T_1, T_2 e T_3) ajustados para obtenção dos coeficientes angular (ΔH_{dif} /R) e linear ($\Delta S_{dif}/R$).

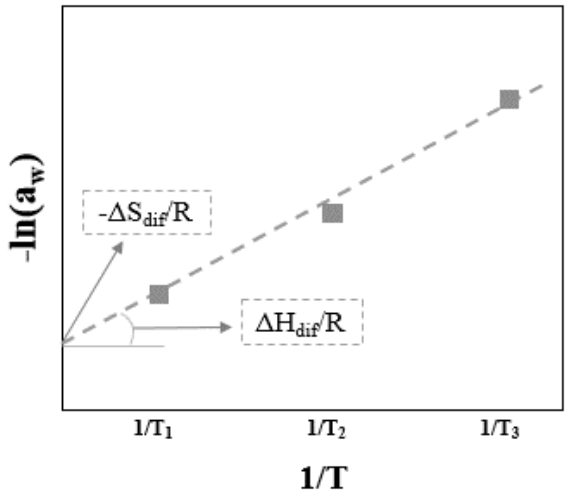

Fonte: Lara (2018).

Uma relação linear entre entalpia diferencial e entropia diferencial é proposta pela Teoria da Compensação Entalpia-Entropia, a qual é dada pela Equação 8, onde T_β é a temperatura isocinética e pode ser expressa como a inclinação do gráfico ΔS_{dif} versus ΔH_{dif} mostrado na Figura 13 (VELÁZQUEZ-GUTIÉRREZ *et al*., 2015).

$$\Delta H_{dif} = T_\beta . \Delta S_{dif} + \Delta G_\beta \quad (8)$$

Figura 13 – Dados de ΔS_{dif} *versus* ΔH_{dif}, ajustados para obtenção dos coeficientes angular (T_β) e linear (ΔG).

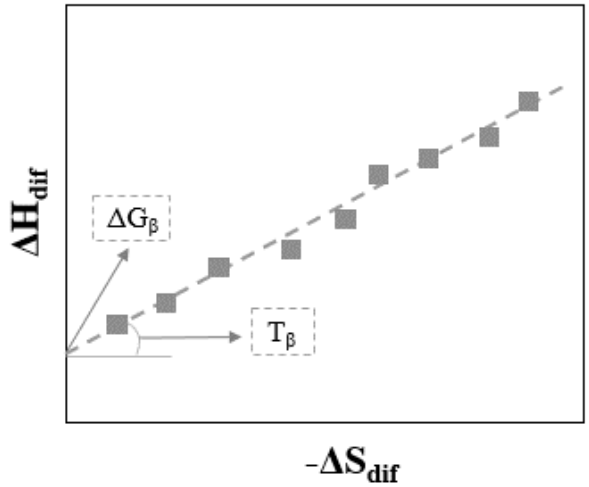

Fonte: Lara (2018).

À T_β, todas as reações ocorrem na mesma taxa para diferentes valores de $\ln(a_w)$, e nos casos em que $T_\beta \neq T_{hm}$, sendo T_{hm} a temperatura harmônica média, pode ser assegurada a ocorrência de compensação entalpia-entropia, indicando mudanças na interação molecular entre água e material (L'VOV, 2007). T_{hm} é calculada através da Equação 9, na qual n é o número de isotermas de sorção e T_i (K) é a temperatura da iésima isoterma.

$$T_{hm} = \frac{n}{\sum_{i=1}^{n}\left(\frac{1}{T_i}\right)} \tag{9}$$

A comparação entre T_β e T_{hm}, também permite a determinação do mecanismo que rege a sorção. Em casos onde $T_\beta > T_{hm}$, a sorção é guiada pela entalpia, e as interações entre a água e o material são mais influentes que o número de sítios de sorção disponíveis no mesmo (TELIS *et al.*, 2000). Por outro lado, se $T_\beta < T_{hm}$, a sorção é regida por fenômenos entrópicos, e o número de sítios de sorção exerce mais influência no processo do que as forças de ligação entre a água e o material. A existência da compensação entre entalpia e entropia permite a obtenção da energia livre de Gibbs associada à temperatura isocinética (ΔG_β) através do cálculo do coeficiente linear do gráfico de ΔS_{dif} *versus* ΔH_{dif}, conforme mostrado na Figura 11. ΔG_β pode fornecer informações sobre a espontaneidade do processo de sorção de acordo com a composição do filme analisado.

3 CONSIDERAÇÕES FINAIS DO REFERENCIAL TEÓRICO

No setor de embalagens para alimentos, é desejável a existência de fontes alternativas de matéria-prima, considerando-se o consumo de montantes de materiais poliméricos diariamente. Blendas formadas por IPS e PVOH, biodegradáveis e de origem renovável, podem ser utilizadas como potenciais substituintes dos polímeros de origem fóssil no setor de embalagens flexíveis para alimentos. Entretanto, para que essa substituição seja efetiva, é necessário aproximar mais as propriedades mecânicas e de barreira à umidade dessas blendas àquelas pertencentes às poliolefinas comumente utilizadas como embalagens. A rigidez e fragilidade apresentada pelo IPS, bem como a forte interação do mesmo e também do PVOH com umidade são limitadores desta aproximação. Nano-materiais, neste contexto, como a nano-sílica coloidal, podem ser utilizados como melhoradores de resistência mecânica e de barreira, quando bem dispersos nos espaços entre as cadeias poliméricas. Além disso, comumente a formação de filmes compósitos, utilizando-se métodos convencionais de processamento, não cessa o leque de propriedades possíveis de serem obtidas pela combinação dos materiais usados. Isto porque, a utilização de um novo método e/ou variação nas fases do compósito com certeza amplia as possibilidades de propriedades apresentadas pelo material. É o caso da produção de filmes laminados, com aplicação de processos químicos ou físicos para garantir boa aderência entre as fases. Sendo sempre desejável a mínima formação de resíduos descartáveis, com menor gasto de água e outros materiais, o uso do efeito corona como melhorador das propriedades adesivas de polímeros é perfeitamente adequado. Portanto, o estudo de novos biocompósitos de IPS/PVOH/nano-sílica, convencionais e laminados, vem agregar às pesquisas relacionadas à materiais para embalagens como um novo material alternativo às poliolefinas. Ressalta-se a novidade deste estudo tanto em relação à composição ainda não estudada, quanto devido à inédita laminação com descarga corona proposta para a estrutura IPS/PVOH.

REFERÊNCIAS

ABRE, A. B. de E. **Estudo abre macroeconômico da embalagem e cadeia de consumo**. Disponível em: https://www.abre.org.br/dados-do-setor/2020-2/. Acesso em: 10 jul. 2020.

ALIZADEH SANI, M.; EHSANI, A.; HASHEMI, M. Whey protein isolate/cellulose nanofibre/TiO2 nanoparticle/rosemary essential oil nanocomposite film: Its effect on microbial and sensory quality of lamb meat and growth of common foodborne pathogenic bacteria during refrigeration. **International Journal of Food Microbiology**, v. 251, p. 8–14, 19 jun. 2017.

AZEVEDO, V. M. *et al.* Whey protein isolate biodegradable films: Influence of the citric acid and montmorillonite clay nanoparticles on the physical properties. **Food hydrocolloids**, v. 43, p. 252–258, 2015.

AZEVEDO, V. M. *et al*. Effect of replacement of corn starch by whey protein isolate in biodegradable film blends obtained by extrusion. **Carbohydrate Polymers**, v. 157, p. 971–980, 2017.

BERTOLINI, A. C. **Biopolymers Technology**. São Paulo: Cultura Acadêmica, 2007.

BRASIL. **Portaria no 53 de 10 abril de 2013.** Cria o Regulamento técnico de identidade e qualidade de soro de leite. Disponível em: http://www.terraviva.com.br/clique/minuta.htm. Acesso em: 10 ago. 2021.

CANEVAROLO JUNIOR, S. V. **Ciência dos polímeros: um texto básico para tecnólogos e engenheiros**. 2. ed. São Paulo: Artliber, 2006.

CAZÓN, P.; VELAZQUEZ, G.; VÁZQUEZ, M. Characterization of mechanical and barrier properties of bacterial cellulose, glycerol and polyvinyl alcohol (PVOH) composite films with eco-friendly UV-protective properties. **Food hydrocolloids**, *[s.l.]*, v. 99, 2019.

CHAVAN, R. S. *et al*. Whey Based Beverage: Its Functionality, Formulations, Health Benefits and Applications. **J Food Process Technol**, *[s.l.]*, v. 6, n. 10, 2015.

CHIELLINI, E. *et al*. **Biodegradation of poly (vinyl alcohol) based materials**. *[s.l]*, *[s.n.]*. v. 28.

CINELLI, P. *et al*. Recyclability of PET/WPI/PE Multilayer Films by Removal of Whey Protein Isolate-Based Coatings with Enzymatic Detergents. **Materials (Basel, Switzerland)**, v. 9, n. 6, 14 jun. 2016.

DAI, L.; XU, D. Polyethylene surface enhancement by corona and chemical co-treatment. 2019.
EPRO, P. E. **Plastics – the Facts 2020**. Disponível em: https://plasticseurope.org/knowledge-hub/plastics-the-facts-2020/. Acesso em: 10 ago. 2020.

FAO; OECD; OECD; FAO. Agricultural Outlook 2018 - 2027**. Chapter 7:** Dairy and dairy products. Rome: OECD Publishing, Paris/Food and Agriculture Organization of the United Nations, 2018.

FENNEMA, O. **Quimica de los Alimentos**. 2 ed. Espanha: Acribia, 2000. 1258 p.

FERNANDES, A. F. **Utilização de concentrado e de isolado proteico de soro lácteo na extrusão de milho**. 2010. 280 p. Tese (Doutorado em Ciência dos Alimentos) - Universidade Federal de Lavras, Lavras, 2010.

GHAANI, M. *et al.* An overview of the intelligent packaging technologies in the food sector. **Trends in Food Science & Technology**, *[s.l.]*, v. 51, p. 1–11, 2016.

GIANNAKAS, A. *et al*. Preparation, characterization, mechanical, barrier and antimicrobial properties of chitosan/PVOH/clay nanocomposites. **Carbohydrate Polymers**, *[s.l.]*, v. 140, p. 408–415, 2016.

GÖKKAYA ERDEM, B.; DIBLAN, S.; KAYA, S. Development and structural assessment of whey protein isolate/sunflower seed oil biocomposite film. **Food and Bioproducts Processing**, *[s.l.]*, v. 1, n. 9, p. 270–280, 2019.

GONZÁLEZ-SISO, M. I. *et al*. Improved bioethanol production in an engineered Kluyveromyces lactis strain shifted from respiratory to fermentative metabolism by deletion of NDI1. **Microbial biotechnology**, *[s.l.]*, v. 8, n. 2, p. 319–30, mar. 2015.

GUIMARÃES, M. *et al*. High moisture strength of cassava starch/polyvinyl alcohol-compatible blends for the packaging and agricultural sectors. **Journal of Polymer Research**, *[s.l.]*, v. 22, n. 10, 2015.

HALIMA, N. BEN. Poly(vinyl alcohol): review of its promising applications and insights into biodegradation. **The Royal Society of Chemistry**, *[s.l.]*, v. 6, p. 39823–39832, 2016.

HANANI, Z. A. N. *et al*. Effect of different fruit peels on the functional properties of gelatin/ polyethylene bilayer films for active packaging. **Food Packaging and Shelf Life**, *[s.l.]*, v. 18, p. 201–211, 2018.

HASSANNIA-KOLAEE, M. *et al*. Development of ecofriendly bionanocomposite: Whey protein isolate/pullulan films with nano-SiO2. **International Journal of Biological Macromolecules**, *[s.l.]*, v. 86, p. 139–144, 1 maio 2016.

HUNTRAKUL, K.; HARNKARNSUJARIT, N. Effects of plasticizers on water sorption and aging stability of whey protein/ carboxy methyl cellulose films. **Journal of Food Engineering**, *[s.l.]*, v. 272, n. 109809, 2020.

IUPAC. International Union of Pure and Applied Chemistry. **Compendium of Chemical Terminology**. 2. ed. Oxford: Blackwell Scientific Publications, 1996.

JANJARASSKUL, T.; TANANUWONG, K. **Role of Whey Proteins in Food Packaging Reference Module in Food Sciences**. 2019. Disponível em: https://doi.org/10.1016/B978-0-08-100596-5.22399-8. Acesso em: 2 set. 2019

JOO, E. *et al*. Whey protein-coated high oxygen barrier multilayer films using surface pretreated PET substrate. **Food Hydrocolloids**, *[s.l.]*, v. 80, p. 1–7, 2018.
KALOGERAS, I. M.; BROSTOW, W. Glass Transition Temperatures In Binary Polymer Blends. **Polym Sci Part B:** Polym Phys, *[s.l.]*, v. 47, p. 80–95, 2008.

LANGE, B. J.; WYSER, Y. Lange_et_al-2003-Packaging_Technology_and_Science. **Packaging Technology and Science**, *[s.l.]*, v. 16, p. 149–158, 2003.

LARA, B. R. B. *et al*. **Morphological, mechanical and physical properties of new whey protein isolate/ polyvinyl alcohol blends for food flexible packaging**. Disponível em: https://linkinghub.elsevier.com/retrieve/pii/S2214289418301777. Acesso em: 17 fev. 2021.

LARA, B. R. B. *et al*. Water Sorption Thermodynamic Behavior Of Whey Protein Isolate/ Polyvinyl Alcohol Blends For Food Packaging. **Food Hydrocolloids**, *[s.l.]*, v. 103, n. 105710, p. 9, 2020.

LARA, B. R. B. **Development of wpi and pva blends aiming their use as flexible plastic packaging for food.** 2018. 138 p. Dissertação (Mestrado em Engenharia de Biomateriais) – Universidade Federal de Lavras, Lavras, 2018.

LIÉBANES, M. D.; ARAGÓN, J. M.; PALANCAR, M. C.; ARÉVALO, G. JIMÉEZ, D. Equilibrium moisture isotherms of two-phase solid olive oil by-products: Adsorption process thermodynamics**. Colloids and Surfaces A**: Physicochem. Eng. Aspects, 2006. p. 282-283, p. 298-306.

LI, T. *et al*. Surface hydrophobicity and functional properties of citric acid cross-linked whey protein isolate: The impact of pH and concentration of citric acid. **Molecules**, *[s.l.]*, v. 23, p. 1–11, 2018.

L'VOV, B. V. **Thermal decomposition of solids and melts:** new thermochemical approach to the mechanism, kinetics, and methodology. *[s.l.]* Springer, 2007.

MACHADO AZEVEDO, V. *et al*. Effect of whey protein isolate films incorporated with montmorillonite and citric acid on the preservation of fresh-cut apples. **Food Research International**, *[s.l.]*, v. 107, p. 306–313, 2018.

MAGRINI, A. *et al.* **Impactos Ambientais Causados pelos Plásticos:** Uma discussão abrangente sobre os mitos e os dados científicos. Rio de Janeiro: e-papers, 2012.

MAZZOLA, N. C. **Study of surface degradation caused by corona treatment on propylene/ethylene copolymers and its influence on heat sealing behavior**. 2010. 135 f. Dissertação (Mestrado em Ciências Exatas e da Terra) - Universidade Federal de São Carlos, São Carlos, 2010.

MESQUITA, A. C. **Estudo da polimerização de acetato de vinila utilizando a radiação ionizante**. 2002. 90 p. Dissertação (Mestrado em Ciências na Área de Tecnologia Nuclear-Aplicação) - Instituto de Pesquisas Energéticas e Nucleares, São Paulo, 2002.

NCBI. National Center For Biotechnology Information. **PubChem Compound Database; CID=9988076**. Disponível em: https://pubchem.ncbi.nlm.nih.gov/compound/9988076. Acesso em: 9 jan. 2020.

OSÉS, J. *et al*. Stability of the mechanical properties of edible films based on whey protein isolate during storage at different relative humidity. **Food Hydrocolloids**, *[s.l.]*, v. 23, n. 1, p. 125–131, 1 jan. 2009.

OYMACI, P.; ALTINKAYA, S. A. Improvement of barrier and mechanical properties of whey protein isolate based food packaging films by incorporation of zein nanoparticles as a novel bionanocomposite. **Food Hydrocolloids**, *[s.l.]*, v. 54, p. 1–9, 1 mar. 2016.

OZAKI, S. K. **Compósitos biodegradáveis de resíduos de madeira-PVA modificado por anidrido ftálico**. 2004. 210 p. Tese (Doutorado em Ciências de Materiais) - Universidade de São Paulo, São Carlos, SP, 2004.

QAZANFARZADEH, Z.; KADIVAR, M. Properties of whey protein isolate nanocomposite films reinforced with nanocellulose isolated from oat husk. **International Journal of Biological Macromolecules**, *[s.l.]*, v. 91, p. 1134–1140, 2016.

RABELLO, M.; DE PAOLI, M. A. **Aditivação de termoplásticos**. São Paulo: Artliber, 2013.

RAJAK, D. K. *et al*. Recent progress of reinforcement materials: a comprehensive overview of composite materials. **Journal of Materials Research and Technology**, *[s.l.]*, v. 8, n. 6, p. 6354–6374, 2019.

RAMOS, Ó. L. *et al*. Antimicrobial activity of edible coatings prepared from whey protein isolate and formulated with various antimicrobial agents. **International Dairy Journal**, *[s.l.]*, v. 25, p. 132–141, 2012.

RAMOS, Ó. L. *et al*. Effect of whey protein purity and glycerol content upon physical properties of edible films manufactured therefrom. **Food hydrocolloids**, *[s.l.]*, v. 30, p. 110–122, 2013.

ROBERTSON, G. L.**Food Packaging Principles and Practice**, 3rd ed. CRC Press, Boca Raton. 2013.

SAMADANI, F.; BEHZAD, T.; SAEID ENAYATI, M. Facile strategy for improvement properties of whey protein isolate/walnut oil bio-packaging films: Using modified cellulose nanofibers. **International Journal of Biological Macromolecules**, *[s.l.]*, v. 139, p. 858–866, 2019.

SCHMID, M. Whey Protein Edible Coatings: Recent Developments and Applications. **Materials (Basel, Switzerland)**, *[s.l.]*, v. 6, n. 8, p. 3254–3269, 2013.

SCHMID, M. *et al*. Effect of thermally induced denaturation on molecular interaction-re. **Progress in Organic Coatings**, *[s.l.]*, v. 104, p. 161–172, 2017.

SEYFI, J. *et al*. Enhanced hydrophobicity of polyurethane via non-solvent induced surface aggregation of silica nanoparticles. **Journal of Colloid and Interface Science**, *[s.l.]*, v. 478, p. 117–126, 2016.

SHEBANI, A. *et al*. The Influence of LDPE Content on the Mechanical Properties of HDPE/LDPE Blends. **Research & Development in Material Science**, *[s.l.]*, v. 7, n. 5, p. 791–797, 2018.

SILVA, K. S. *et al.* Synergistic interactions of locust bean gum with whey proteins: Effect on physicochemical and microstructural properties of whey protein-based films. **Food Hydrocolloids**, *[s.l.]*, v. 54, p. 179–188, 2016.

SILVA, K. S. *et al.* Physicochemical and microstructural properties of whey protein isolate-based films with addition of pectin. **Food Packaging and Shelf Life**, *[s.l.]*, v. 16, p. 122–128, 2018.

SILVÉRIO, H. A. **Extração e caracterização de nanocristais de celulose a partir de sabugo de milho, e sua aplicação como agente de reforço em nanocompósitos poliméricos utilizando poli(álcool vinílico) com matriz.** 2013. 121 p. Dissertação **(Mestrado em Química) -** Universidade Federal de Uberlânida, Uberlândia, MG, 2013.

SUN, C.; ZHANG, D.; WADSWORTH, L. Corona Treatment of Polyolefin Films – A Review. **Advances in Polymer Technology**, *[s.l.]*, v. 18, p. 171–180, 1999.

TAO, Y. *et al.* Thermodynamic sorption properties, water plasticizing effect and particle characteristics of blueberry powders produced from juices, fruits and pomaces. **Powder Technology**, *[s.l.]*, v. 323, p. 208–218, 2018.

TANG, X.; ALAVI, S. Recent advances in starch, polyvinyl alcohol based polymer blends, nanocomposites and their biodegradability. **Carbohydrate Polymers**, *[s.l.]*, v. 85, n. 1, p. 7–16, 2011.

TELIS, V. R. N.; GABAS, A. L.; MENEGALLI, F. C.; TELIS-ROMERO, J. Water sorption thermodynamic properties applied to persimmon skin and pulp. **Thermochimica Acta**, *[s.l.]*, v. 343, 49–56, 2000.

THOMAS, S.; MISHRA, R.; KALARIKKAL, N. *In*: RAGHVENDRA, K. M.; SABU, T. NANDAKUMAR, K. **Micro and nano fibrillar composites (MFCs and NFCs) from polymer blends.** Disponível em: https://lib.ugent.be/catalog/ebk01:3710000001410607. Acesso em: 10 ago. 2021.

VAN DER BERG, C. Description of water activity of foods for engineering purposes by means of the GAB model of sorption. *In***:** Engineering and Food. London: B. M. Mckenna Elsevier Applied Science, 1984. V. 1. p.311-321.

VELÁZQUEZ-GUTIÉRREZ, S. K.; FIGUEIRA, A. C.; RODRÍGUEZ-HUEZO, M. E.; ROMÁN-GUERRERO, A.; CARRILLO-NAVAS, H.; PÉREZ-ALONSO, C. Sorption isotherms, thermodynamic properties and glass transition temperature of mucilage extracted from chia seeds (Salvia hispanica L.), **Carbohydrate Polymers**, *[s.l.]*, v. 121, p. 411–419, 2015.

VIEIRA, M. G. A. *et al*. Natural-based plasticizers and biopolymer films: A review. **European Polymer Journal**, *[s.l.]*, v. 47, n. 3, p. 254–263, 2011.
VIVERO-ESCOTO, J. **Silica Nanoparticles: Preparation, Properties and Uses**. *[s.l.]:* Nova Science Publishers, 2012.

YANG, L.; PAULSON, A. T. Mechanical and water vapour barrier properties of edible gellan films. **Food Research International**, *[s.l.]*, v. 33, p. 563–570, 2000.

YAO, K. *et al*. Structure and properties of starch/PVA/nano-SiO 2 hybrid films. **Carbohydrate Polymers**, v. 86, p. 1784–1789, 2011.

YOUNES, M. *et al*. Re-evaluation of silicon dioxide (E 551) as a food additive. **EFSA Journal**, *[s.l.]*, v. 16, n. 1, p. 1–70, 2018.

ZHOU, X. *et al*. Development and characterization of bilayer films based on pea starch/ polylactic acid and use in the cherry tomatoes packaging. **Carbohydrate Polymers**, *[s.l.]*, v. 222, 2019.

ZOLFI, M. *et al.* Development and characterization of the kefiran-whey protein isolate-TiO2 nanocomposite films. **International Journal of Biological Macromolecules**, *[s.l.]*, v. 65, p. 340–345, 1 abr. 2014.

SEGUNDA PARTE – ARTIGOS*

1 DELINEAMENTO GERAL DA TESE

Esta tese foi desenvolvida em duas partes principais: (i) produção de compósitos convencionais (uma única camada) de Isolado proteico de soro de leite (IPS) e Poli (álcool vinílico) (PVOH), com cinco diferentes concentrações de nano-sílica (NS) (0%, 1%, 2%, 3% e 4%), e caracterização destes segundo as propriedades de espessura e gramatura, morfológicas (Microscopia Eletrônica de Varredura – MEV), mecânicas de tração, interacionais entre componentes (Fourier transform infrared – FT-IR), sorção de água, permeabilidade ao vapor de água, coeficientes de difusividade e solubilidade, ângulo de contato com a água e energia de superfície, comportamento de sorção de água (isotermas de sorção); (ii) produção de compósitos laminados, com uma primeira camada de PVOH/NS e uma segunda camada de IPS/NS, utilizando-se a concentração de NS definida como ideal na parte (i) (4%), aplicando-se diferentes tempos de descarga corona entre as camadas (0s, 30s, 60s e 90s), e caracterização da primeira camada quanto às alterações nos grupos funcionais (FT-IR), molhabilidade (ângulo de contato com a água) e energia superficial, assim como do compósito laminado final quanto às propriedades mecânicas de tração, permeabilidade ao vapor de água e coeficientes de difusividade e solubilidade. As análises e resultados foram divididos em três artigos, conforme disposto no fluxograma da Figura 1.

Figura 1 – Fluxograma com a divisão e delineamento geral da tese

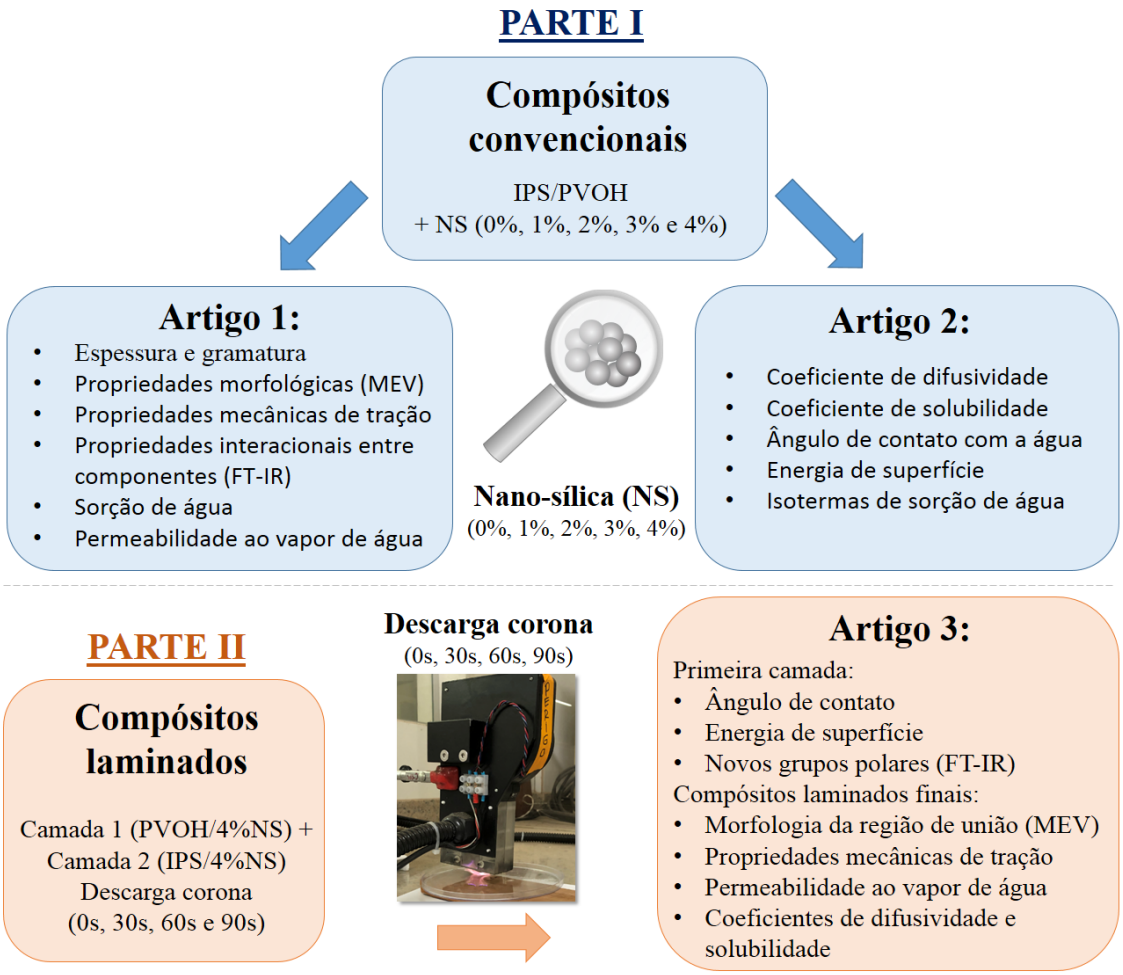

Fonte: Da autora (2022).

ARTIGO 1

Publicado na Revista Journal of Polymers and the Environment
(https://doi.org/10.1007/s10924-020-02033-x)

NOVEL WHEY PROTEIN ISOLATE/POLYVINYL BIOCOMPOSITE FOR PACKAGING: IMPROVEMENT OF MECHANICAL AND WATER BARRIER PROPERTIES BY INCORPORATION OF NANO-SILICA

Bruna Rage Baldone Lara[a*], Paulo Sérgio de Andrade[a], Mario Guimarães Junior[b], Marali Vilela Dias[a], Lizzy Ayra Pereira Alcântara[a]

[a] Federal University of Lavras - UFLA / Department of Food Science, University Campus - PO Box: 3037 - CEP: 37200-000, Lavras - MG, Brazil.

[b] Federal Center of Technological Education of Minas Gerais – CEFET-MG / Department of Electromechanics – CEP 38180-510, Araxá - MG, Brazil.

*Corresponding author. E-mail: brunabaldone@hotmail.com; Phone: +55 35 38322321; Mailing address: Federal University of Lavras – UFLA, University Campus - PO Box: 3037 - CEP: 37200-000, Lavras - MG, Brazil.

Running head:

IMPROVEMENT OF MECHANICAL AND WATER BARRIER PROPERTIES OF WPI/PVOH FILMS BY INCORPORATION OF NANO-SILICA

Abstract

The current global proposal for withdrawing polymers with high resistance to degradation and from fossil sources from disposable appliances, as well as the increasing trend of cheese production and whey generation, are some of the incentives for using whey proteins to produce biodegradable packaging films. Brittleness and poor water barrier limit the application of whey protein isolate (WPI) films in the food packaging sector. The addition of polyvinyl alcohol (PVOH) to WPI film, making a blend, improves flexibility but maintains poor water barrier and tensile strength. In this work, to make WPI/PVOH blends more suitable for food packaging applications, films of WPI/PVOH were reinforced with up to 4% of colloidal nano-silica (NS) for improvement of mechanical resistance and water vapor barrier, thus producing a novel biocomposite in terms of composition. At 4% of NS, the values obtained for tensile strength and tensile modulus were 10.2 and 78.2 MPa, being suitable for food packaging application when compared to commercial polymers currently used as packaging. An expressive reduction of water sorption (17% of decrease) and water vapor permeability (40% of reduction) was

observed at 4% of NS, increasing the efficiency in keeping integrity during application and leading to a material with a higher water vapor barrier. The addition of 4% of NS in WPI/PVOH films is indicated to improve tensile strength and water barrier, thus increasing its application potential as food packaging.

Keywords: Whey protein isolate; Polyvinyl alcohol; Colloidal nano-silica; Biocomposite; Food packaging.

1 Introduction

There is a current trend of the gradual withdrawal of non-biodegradable plastics from the composition of disposable plates, cups, trays, and cutlery to decrease their accumulation in the environment. Countries such as France, Costa Rica, and recently Brazil, has already decided to accomplish the full replacement of these plastics for biodegradable materials until 2020, 2021, and 2028, respectively, leading to an expected growth in biodegradable polymers demand [1]. In this context, researches related to the use of renewable proteins or polysaccharides as biopolymers in the food packaging sector has gained attention. Packaging films of proteins isolated from whey, a cheese production by-product, have been showing better mechanical and oxygen barrier characteristics when compared to other proteins or polysaccharides due to their structure which confers high intermolecular binding potential [2–4]. The current market shows an increasing trend of the milk global production of 9% in developed countries until 2027, from which 37% refers to cheese production [5]. Besides that, a high amount of whey, 9 kg, is generated by each kg of cheese produced, which makes its use very attractive, especially to isolate its proteins for biodegradable packaging production [1, 2, 6–9].

Despite the nutritional property, good oxygen barrier, colorless, transparent, and flavorless properties, whey protein isolate (WPI) films usually present low tensile strength, intrinsic brittleness and poor water barrier properties, which are the major limitations in protein materials use [10, 11]. The hydrophilic nature of the protein molecules and their heating during film formation, providing intermolecular disulfide bonds between cysteine amino acids, are responsible for this hydrophilic and brittle behavior of WPI films. Blending WPI with other biopolymers can be an efficient method to achieve desirable properties [8]. The addition of polyvinyl alcohol (PVOH) to the WPI matrix, forming a blend, can improve flexibility and thus reduce the film brittleness, but the properties of low tensile strength and water barrier are still limitations for application in the food packaging sector [1]. Adding a compatible nanofiller could be a possible alternative to increase both strength and water barrier, making the WPI/PVOH blend appropriate for food packaging.

The reduction of silica, an abundant material, to nanometric sizes, provides a material with high specific surface area and high surface energy with unsaturated chemical bonds [12]. Besides that, it was published in the European Food Safety Authority (EFSA) Journal that no adverse effect with nano-silica

(NS) was observed in oral toxicity studies available in vivo, until the time of the referent publication, in March 2018, not preventing its use as a food additive [13]. In polymeric films, NS can maintain acceptable levels of sensorial and physiological qualities and longer storage life for food [14]. Another advantage of this nanostructure, when incorporated into the polymeric matrices, is its reflectivity for ultraviolet light, in the order of 70-80% (wavelength ≤ 490 nm). This property allows the film to resist ultraviolet aging and thermal aging [15, 16]. Despite these advantages, there are few studies related to the addition of colloidal NS and NS powder in packaging systems. It was reported that the addition of NS powder in polyurethane films using ethanol as a non-solvent has caused the formation of a superhydrophobic top layer [17]. The addition of NS powder to WPI/pullulan films increased tensile strength and water barrier and water resistance [12]. Besides morphological, mechanical, and barrier changes, the addition of NS powder improved the thermal stability of PVOH/xylan films by producing a compact structure [18]. It has been also observed that the addition of colloidal NS to pullulan-coated BOPP films is an effective strategy for improving the general performance of the material for food packaging applications [19].

Until the present time, no research evaluating the addition of NS to WPI/PVOH films has been reported, representing the WPI/PVOH/NS a novel biocomposite in terms of composition. In this work, NS was selected to improve the properties of PVOH/WPI films due to its unique properties (large specific surface area, lightweight, and high dispersion into the matrix). Furthermore, NS promotes great improvement in mechanical and moisture absorption properties with lower addition compared with other nanofillers [20]. Good interaction among NS, WPI proteins, and PVOH is expected, mainly through hydrogen bonds, improving the matrix cohesiveness, and leading to a material with higher tensile strength and water barrier. Since the high surface energy can encourage NS to aggregate in polymeric matrices, citric acid can be used as a surface modifier to prevent NS agglomeration, as well as to add a functional characteristic of food preservative to the biocomposites [21].

In previous works, it was verified that the addition of 30% of PVOH to the WPI matrix was able to improve flexibility and thus reduce the WPI film brittleness, however, decreased its tensile strength and increased the water sorption process spontaneity [1, 22]. Therefore, this work aimed to evaluate the influence of NS addition to the mechanical and water vapor barrier properties of films with 70% of WPI and 30% of PVOH intended to be applied as flexible food packaging. For this purpose, new biocomposite films of 70% of WPI, 30% of PVOH and 0, 1, 2, 3 and 4% of NS had the following properties evaluated: thickness and basis weight, morphology (SEM), mechanical (tensile and puncture), interaction phenomena (FT-IR), glass transition temperature (DSC), water sorption behavior and water vapor permeability.

2 Material and Methods

2.1 Material

Whey Protein Isolate (WPI 9400) with 90% of proteins was purchased from Hilmar Ingredients; polyvinyl alcohol with high molecular weight (Mw = 130.000 g/mol) and highly hydrolyzed (99%), from Sigma-Aldrich; glycerol (≥ 99.5%, density 1.26 g/mL), as plasticizing agent, produced by Sigma-Aldrich; granulated anhydrous citric acid from Cargill Agrícola S.A was used to guarantee a good distribution of NS; and NS from colloidal solution Bindzil 2034DI (Akzo Nobel), with 34% in weight of NS (average particle size of 15 nm and surface area of 200 m^2g-1).

2.2 Preparation of the biocomposites

Initially, a WPI and a PVOH solution were separately prepared using a concentration of 6% m/v [1]. For the WPI solution, WPI (12 g) was dissolved in 200 mL of distilled water, added with glycerol (30% m/m of WPI), citric acid (8% m/m of WPI), and kept under agitation for 30 min (250 rpm) at room temperature (25 °C). The solution had the pH adjusted to 8 using a NaOH solution (3 M) and was then submitted to a water bath at 90 °C for 30 min to guarantee protein denaturation [23]. In another beaker, the PVOH solution was produced by dissolving PVOH (12 g) on 200 mL of distilled water and keeping under agitation for 24 h (100 rpm) to hydrate the PVOH [24]. Glycerol (30% m/m of PVOH) and citric acid (8% m/m of PVOH) were added and the PVOH solution was kept under agitation for more 30 min (250 rpm). Then, it was submitted to the water bath at 90 °C for 60 min. WPI and PVOH solutions were merged in a volume ratio of 70/30 (140 mL from WPI solution and 60 mL from PVOH solution), leading to 200 mL of merged solution. This volume ratio was used here since, in a previous work that evaluated blends of WPI and PVOH, the 70/30 produced the best tensile properties [1]. After cooled at room temperature, nano-silica (Bindzil 2034DI) was added in five different concentrations: 0, 1, 2, 3 and 4% m/m of polymer (Table 1). Since each film had 12g of polymer (6%) and Bindzil has a concentration of 34% in weight of NS, for 0, 1, 2, 3 and 4% of concentration, it was added, respectively, 0, 0.35, 0.70, 1.1, and 1.4 g of Bindzil per film. The final solution of each treatment was homogenized in Ultra Turrax (Kika Labortchnik) for 20 min (450 rpm) and after sonified (Sonifier Cell Disruptor Branson – Model 450D, Manchester, UK) using a probe with 100 mm of diameter, at 60% of amplitude (270 W), for 10 min (600 s) in a continuous assay, using an ice bath to avoid heating, resulting in ultrasonic energy applied of 810 $J.mL^{-1}$.

Final solutions were shed on rectangular Teflon plates (750 cm^2), perfectly level, and conditioned at room temperature (25 °C) for spontaneous drying (48 h). Three replicates of each treatment were performed. The dried biocomposites were conditioned under controlled temperature and relative humidity (RH) (25±1 ºC and 50 % RH ±2 %) for 48h before characterization.

Table 1 – Biocomposites produced: fixed content of polymers/citric acid/glycerol and variations in nano-silica content.

Treatment	WPI (% m/m of polymers)	PVOH (% m/m of polymers)	Glycerol (% m/m of polymers)	CA (% m/m of polymers)	NS content (% m/m of polymers)
0%NS	70	30	30	8	0
1%NS	70	30	30	8	1
2%NS	70	30	30	8	2
3%NS	70	30	30	8	3
4%NS	70	30	30	8	4

2.3 Characterization of the biocomposites

2.3.1 Thickness and basis weight

Thickness (mm) was measured using a digital micrometer (Digimess) with a resolution of 0.001 mm, taking five random measurements per specimen. Basis weight ($g.m^{-2}$) was obtained from specimens of 100 cm^2, weighed on an analytical balance with a resolution of 0.001g. One specimen from each replicate was tested by biocomposite to obtain average thickness and basis weight.

2.3.2 Scanning Electron Microscopy (SEM)

SEM microscopies were obtained to evaluate the biocomposites morphology, looking for flaws, clusters of NS, phase separation or other any other effect which could be related to the mechanical and water barrier results. The analysis was conducted on a LEO 1430 VP (England) with an accelerating voltage of 20 kV, obtaining microscopies with 1500X of magnification. To observe the morphology at the cross-section, the specimens were previously frozen in liquid nitrogen and fractured, and then gold (Au)-coated using vapor deposition.

2.3.3 Tensile mechanical Properties

Tensile test was performed to verify the influence of the NS on strength, flexibility, ductility of the biocomposites when submitted to stretching stress. The maximum tensile strength (TS), the tensile modulus (TM) and the maximum elongation (E) of the biocomposites were measured according to ASTM D882-02 (2002), using a texturometer (Stable Microsystems, model TATX2i, England) with a load cell of 1 kN and a speed of 10 $mm.s^{-1}$. Specimens of 5 mm of width and 100 mm of length were tested at 23 ± 1 °C. TM was calculated through the tangent of the initial linear function of the stress-strain curve, which was considered as an elastic behavior. By dividing the maximum tensile by the film transversal section area and through the percentage relation between the final and initial length of the specimen, respectively, TS and E were obtained. Five repetitions were used for each replicate of the five different biocomposites.

2.3.4 Fourier transform infrared (FT-IR) analysis

To understand the interactions among the biocomposites constituents and to evaluate the structural changes resulted from NS addition, samples were characterized by absorption spectroscopy on the region of infrared through an FTS 3000 Excalibur Digilab (United States), in Total Attenuated Reflection (ATR) mode, equipped with a KBr detector. The analysis range was from 4000 to 400 cm^{-1} with 64 scans.

2.3.5 Differential Scanning Calorimetry (DSC) analysis

The DSC analysis was performed to determine the glass transition temperature (Tg), and then relate this transition to the behavior of the biocomposites through the mechanical and barrier results. According to a previous performed thermogravimetric analysis, the temperature of the first main degradation for WPI/PVOH/NS biocomposites starts at 200 °C. Therefore, DSC analysis was conducted on a DSC 60H (Shimadzu), with samples of 4 mg, at a heating rate of 10 $°Cmin^{-1}$ and adopting the following heating/cooling sequence: 1) an initial heating run from 25 °C to 110 °C was performed, then maintaining the sample at 150 °C for 10 min to eliminate thermal history; 2) sample was cooled from 150 °C to -50 °C with a cooling rate of 10 $°Cmin^{-1}$; and 3) a second heating run was performed until 190 °C.

2.3.6 Water sorption

A water sorption test was performed to understand the sorption behavior of the biocomposites when placed in an atmosphere at 25 °C and 75% of relative humidity (RH), as the one used for water vapor permeability test. Rectangular specimens of 6 cm^2 were dried on a vacuum oven (70 °C, 24h) and placed in small plastic containers (inert to moisture). Three specimens for each film were balanced into a hermetic pot containing a saturated saline solution of NaCl, assuring a water activity (a_w) of 0.753. The sorption kinetics was evaluated by periodically measuring the weight increment per hour of the specimens concerning the dry biocomposites with a balance accurate to 0.001 g, from 0 h to 8 h. The water gain (WG) was calculated as follows:

$$\%WG = \frac{w_t - w_{dry}}{w_{dry}} \times 100 \quad (1)$$

where w_t is the weight of the biocomposite at time *t*, and w_{dry} is the weight of the dry biocomposite.

2.3.7 Water vapor permeability

Water vapor permeability (WVP) was determined by the gravimetric method, following the ASTM E96/E96M-10 (2010) and using circular specimens with 80 mm of diameter. The specimens were fixed in circular capsules with 5.2 cm of effective permeation area. In the capsules interior, it was added silica gel, setting a low humidity, which was considered as 0 (zero) in the atmosphere in contact with the specimen's lower face [1]. The capsules were placed in hermetic desiccators at 25 ± 1 °C with a sodium chlorate saturated solution, setting the humidity to 75%. Weight gain measurements were taken

by weighing the capsules (Analytical balance, resolution 0.001 g) each 24 h for 7 days. A plot of weight gained (Wg) versus time (t) was used to determine the WVP through Equation 2:

$$WVP = \frac{Wg \times ti}{t \times A \times \rho_s (RH_1 - RH_2)} \quad (2)$$

Where: *WVP* is given in g.mm.m^{-2}.day^{-1}.kPa^{-1}; A is the permeation area of the specimen (m^2); *ti* is the medium specimen thickness (mm); ρs is the water vapor saturation pressure at the test temperature (3,169 kPa); RH_1 is the relative humidity of the desiccator chamber (0,75) and RH_2 (0,00) is the relative humidity inside the capsule. Three repetitions were performed for each biocomposite.

2.3.8 Statistical analysis

Sisvar 5.0 was used to perform statistical analysis of the results by comparing the means through Scott-Knott test, with 95 % of confidence level. The test was used for thickness, basis weight, mechanical, WVP and water sorption results.

3 Results and Discussion

3.1 Thickness and basis weight

In order to understand if the thickness and the mass of material by area could be parameters of influence on the mechanical and water barrier results, the thickness and the basis weight properties of the biocomposites were evaluated. All biocomposites presented similar values of thickness, despite the different amounts of nano-silica added, while basis weight was increased at higher amounts of NS (Table 2). Both thickness and basis weight can be related to the mechanical and barrier properties of films. For example, starch films had their tensile strength increased by 100% (from 2 to 4 MPa) when they increased thickness from 0.3 to 1.0 mm (230%) [27]. When analyzing the influence of thickness on PVOH film mechanical properties, some authors observed that at 25°C, tensile strength and deformation capacity increased, respectively, from 9.1 MPa to 16.2 MPa (78%), and from 76.4% to 167.4% (119%) when the film thickness change from 0.050 to 0.170 mm (an increase of 240%), corroborating the trend of improving mechanical properties with the thickness increment [28]. The water barrier is also usually higher for films with higher thickness. The permeability of gases and vapors is decreased when the thickness of a polymeric film increases, but it cannot be eliminated only by increasing the material thickness [29]. For the biocomposites produced, it can be assumed that other parameters than thickness will influence mechanical and barrier properties, such as the film morphology, the amount of free volume, the temperature of application or even the basis weight, since thickness were not significantly different ($p \geq 0.05$) for all tested treatments.

Basis weight or grammage is the amount of film mass by area, usually expressed in g.m^{-2} and used to specify papers [30]. Its measure is commercially used to predict the general properties and yield of polymeric materials. As expected, the weight basis of the biocomposites increased with the increment of NS. It occurs since the amount of polymer for all treatments was the same and, at the nano-scale, NS

can enter into the free volumes among the polymeric chains. Therefore, there is a higher mass for the same film area. Films with 3 and 4% of NS presented the highest values of basis weight, probably indicating a higher filling of the free volumes in the film matrix, which certainly will influence glass transition, mechanical and water barrier properties of these biocomposites.

Table 2 – Values of thickness, basis weight, glass transition temperature (Tg) from DSC and WVP from permeation test

Treatment	**Thickness (mm)**	**Basis weight ($g.m^{-2}$)**	**Tg (°C)**	**WVP ($g.mm.m^{-2}.day^{-1}.kPa^{-1}$)**
0%NS	0.211 ± 0.02a	126 ± 7.36a	19	2.70 ± 0.28b
1%NS	0.227 ± 0.00a	144 ± 5.38b	18	3.06 ± 0.43b
2%NS	0.212 ± 0.03a	160 ± 6.79b	18	2.68 ± 0.44b
3%NS	0.216 ± 0.03a	186 ± 9.84c	21	2.41 ± 0.27b
4%NS	0.211 ± 0.01a	189 ± 10.5c	26	1.62 ± 0.10a

At vertical columns, different letters represent significantly different values at ($p \geq 0.05$) using the Scott-Knott test.

3.2 Scanning Electron Microscopy (SEM)

SEM micrographs of the biocomposites are shown in Figure 3. For all the treatments, it was observed a compact structure with few pores, bubbles, flaws or cracks. It possibly indicates compatibility between WPI and PVOH, as previously stated by [1, 22]. Despite the unique major phase observed, there were dark spots at the cross-section of all biocomposites, and these spots were increased with the NS content increment. Films of WPI/PVOH/glycerol produced under the same conditions did not show these dark spots [1]. Apparently, the addition of citric acid (CA) caused the emergence of these spots at the WPI/PVOH/glycerol/CA films produced.

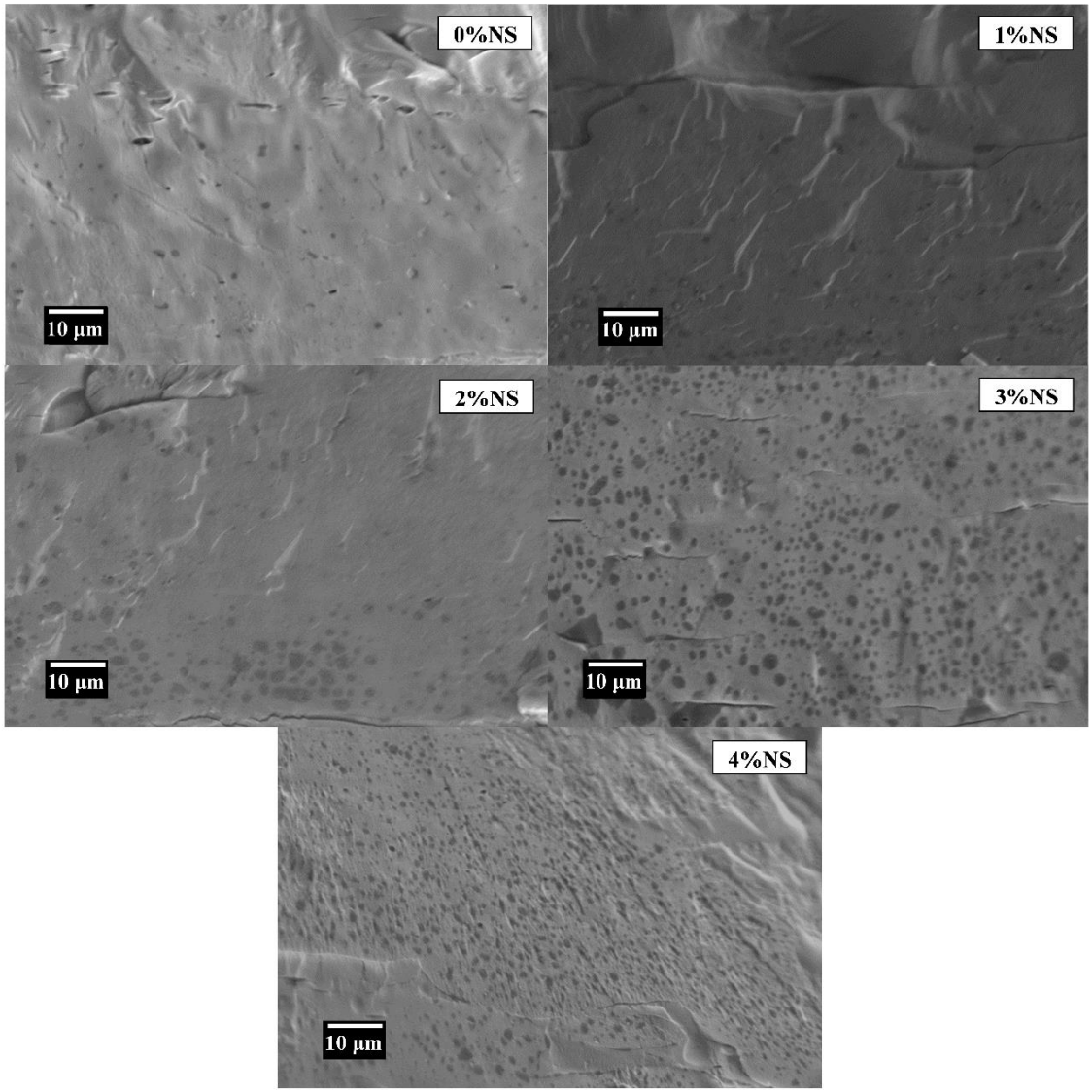

Figure 3. SEM cross-section micrographs of the biocomposites: 0%NS, 1%NS, 2%NS, 3%NS and 4%NS.

In the food products, CA is widely used as a food preservative due to its antibacterial and acidulant effect, the ability of reinforcing of the antioxidant action of other substances and the improvement of flavors [31]. CA can be used in WPI films for packaging to provide active antioxidant and/or antimicrobial effect, to produce cross-link interactions between WPI chains, or even to improve nanomaterial dispersion in the WPI matrix [3, 32–34]. In the present work, CA (Figure 2.c) was added: (i) to guarantee a good distribution of NS in the WPI/PVOH matrix, by introducing functional groups to the NS surface which are able to interact by hydrogen bonds with the amine and hydroxyl of proteins (Figure 2.a) and PVOH (Figure 2.b) chains, thus stabilizing the NS high surface energy [21]; and (ii) as a bio-safe molecule able to add a functional characteristic of food preservative to the biocomposites, which can possibly be explored in a future study with them applied to fresh fruits.

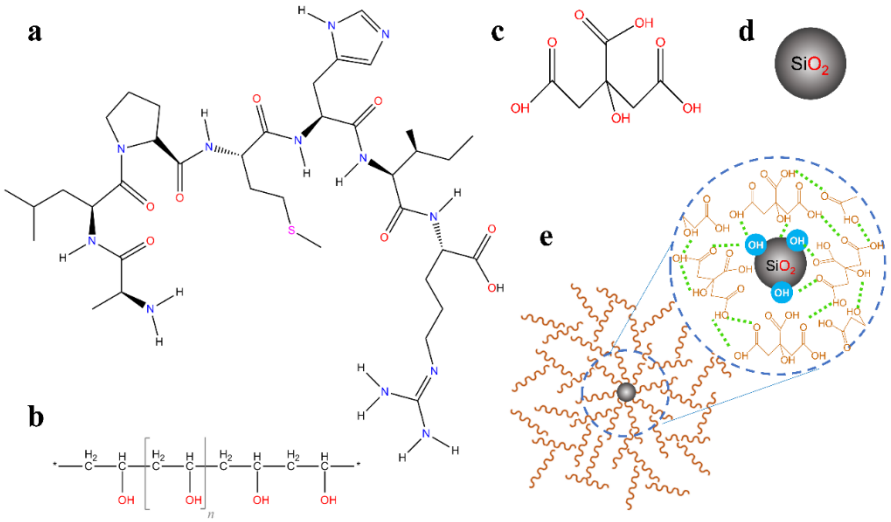

Figure 2. Representation or structure of: a) a chain segment (primary structure) with seven amino acid residues (H-Ala-Leu-Pro-Met-His-Ile-Arg-OH, 142–148) from β-lactoglobulin, the major protein of ruminants milk whey, representing the WPI chemical structure; b) the PVOH highly hydrolyzed; c) the citric acid; d) a silica nanoparticle; e) the micrometric cluster formed by CA and NS and some possible interactions.
Source: Adapted from [21, 35, 36].

To guarantee cross-linkage of WPI chains by CA addition usually is necessary a higher time of agitation in the bath of these two components together than that used on this work (30 min). In researches where a WPI/CA gel was submitted to annealing at 37°C for 48h, or where a WPI/CA solution was agitated for 6h at 50°C, the macromolecules cross-linking was achieved [33, 37]. Therefore, it is pertinent to suppose that only a small part of CA was capable to cross-link WPI chains, while most of it remained in solution. However, at pH 8, both whey proteins and citric acid molecules are negatively charged, occurring electrostatic repulsion between them [23]. Thus, is possible that CA molecules in solution were affected by the ultrasound energy applied, which was capable to form phase separation at the micrometric scale. Possibly, the dark spots observed in Figure 3 for the 0%NS biocomposite are these phases of CA. With the NS increment, the amount and distribution of these spots are changed. When 1% or 2 % of NS is added, the number of spots is increased and they are poorly distributed. Meanwhile, with 3% and 4% of NS, the number of spots was highly increased, with good distribution. Therefore, is reasonable to link the spots not only to the CA but also with the amount of NS in the biocomposites.

In the present work, certainly, the CA was able to interact with the NS surface through numerous hydrogen bonding with the oxygen atoms and silanol groups (Si-O-H), forming CA/NS clusters (Figure 2.e)., which appeared as dark spots in the macrographs (Figure 3). Similar results were obtained when other researchers modified NS by adding CA to its surface to prevent aggregation: particles of NS with CA at nanometric sizes dispersed in the PVOH matrix, which appeared as dark spheres in TEM micrographs [21]. The referred authors used much higher ultrasound energy (15,000 $J.mL^{-1}$) and a lower

CA amount (0.083% w/v) than those used in this work (810 $J.mL^{-1}$ and 0.480% w/v), which possibly guaranteed the nanometric size of the particles of CA/NS. For the biocomposites produced in this work, a lower energy applied and a higher amount of CA led to micrometric, but not nanometric clusters of CA/NS. NS surface was probably modified by CA molecules, encouraging the clusters to be adsorbed onto WPI/PVOH matrix, being hydrogen bond the driving force responsible for this adsorption [21]. These clusters were best distributed and with the smallest size of 236 nm when there was 4% of NS on the WPI/PVOH matrix.

3.3 Tensile Mechanical Properties

The analysis of tensile properties of biocomposite films is essential to predict the packaging stability under forces and deformations required during storage and handling. When analyzing experimental results of strength and deformation, is important to consider the film morphology, since the mechanical properties are closely related to the biocomposite microstructure [38]. Results from the tensile test of the biocomposites of WPI/PVOH/NS are exposed in Figure 3.

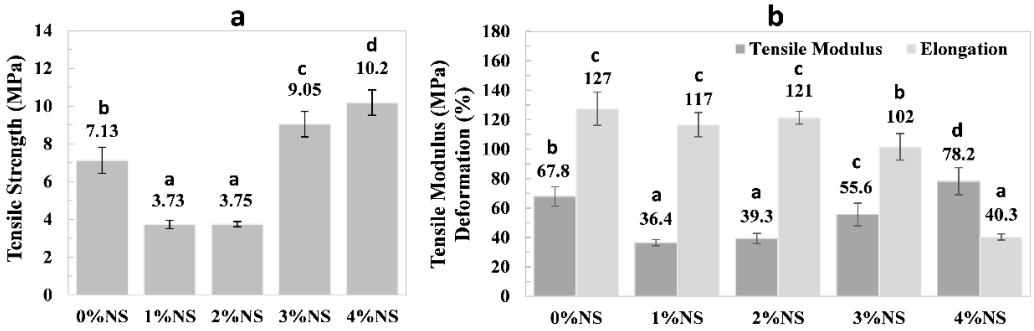

Figure 3. Average and standard deviation values of tensile properties: (a) maximum TS; (b) TM and E obtained by the tensile test of the biocomposites. Different letters represent significantly different values at ($p \geq 0.05$) using Scott-Knott test.

The addition of NS as a filler to the WPI/PVOH matrix significantly ($p \geq 0.05$) affects the TS results. Maximum tensile strength of 10.2 MPa was obtained when 4% of NS was added to the WPI/PVOH film. This is a good value when it comes to food flexible packaging since it is similar to that strength from low-density polyethylene (LDPE), widely used to produce packaging, around 10 MPa [35]. For low amounts of NS (1 and 2%) added to the WPI/PVOH matrix, is observed a reduction in strength when compared to the film without NS (48% of reduction). Possibly, the poor distribution and dispersion of the clusters of CA/NS observed on SEM micrographs (Figure 3 – 1%NS and 2%NS), as well as the low amount of NS added, led to lower results of tensile strength. Otherwise, when higher amounts (3% and 4% of NS) were added to the structure, good dispersion and distribution were provided, as observed in Figure 3, which certainly caused an increase in the TS.

In WPI/pullulan films with NS, it was observed an increase in TS from 2.07 to 3.51 MPa when 3% of NS was added as a consequence of a three-dimensional bond matrix among WPI, pullulan, and NS [12]. In the present work, the addition of 4% of NS to the WPI/PVOH film led to a biocomposite approximately 43% more resistant to tensile loads when compared to that film without NS. The strong interfacial bonding between the nanofiller and the polymeric matrix may have contributed substantially to the load transfer from the matrix to the reinforcement, which leads to a tougher composite [36]. As previously stated, possibly there was a modification of the NS surface by CA, forming CA/NS clusters, which increased the affinity of NS with the protein and PVOH chains. The good affinity and distribution of these clusters, as well as the formation of a three-dimensional hydrogen bond interaction matrix, certainly contributed to a higher strength.

Flexible food packaging widely used on market, such as LDPE and linear low-density polyethylene (LLDPE), usually presents low values of tensile modulus (TM), varying between 130 and 300 MPa [25, 37–39]. The addition of 30% of PVOH to the WPI film is known by the ability to reduce this film stiffness, decreasing the TM 64% [1]. By adding 1% or 2% of NS to the WPI/PVOH, the TM was reduced further, leading to a biocomposite around 70% less rigid than the least rigid of the polyethylenes cited, which can be desired in specific applications when super flexible and stretchable packaging is needed. The 3%NS and 4%NS biocomposites showed TM values of 55.6 and 78.2 MPa, respectively, still above the TM of the commercial polymers used as flexible food packaging and, therefore, less rigid. In relative low concentration, nanoparticles can reveal a plasticizing effect on the polymer chains, which increases mobility among these macromolecules by attenuating the effect of interactions [34]. Possibly, 1 and 2% of NS caused this plasticizing effect, and therefore decreasing TS and TM. Meanwhile, when 4% of NS was used, certainly occurred a mobility restriction that provided a more rigid biocomposite.

When 1% or 2% of NS is added, the WPI/PVOH film does not have its elongation significantly modified ($p \geq 0.05$), keeping strain capability above 100% of its initial length. However, higher amounts of NS seem to decrease ductility. The 3%NS biocomposites showed a reduction in E of 19.7% when compared to the 0%NS. However, a remarkable change in ductility was observed when 4% of NS was added: a reduction of 68.5% of the strain ability under tensile stress.

3.4 Fourier transform infrared (FT-IR) analysis

Figure 4 presents spectra on the infrared region for all the biocomposites. The main absorptions occurred on bands: from 3700 to 2400 cm^{-1} and from 1770 to 400 cm^{-1}. These specific regions of the general spectra (Figure 4.a) can be better observed in Figure 4.b and 4.c.

All films presented the band localized on approximately 3255 cm^{-1}, which is related to the existence of the N-H bond (from WPI proteins), to the stretch of OH groups, to the water existence for all the biocomposites, as well as to the presence of OH groups in the NS surface [24, 39, 40]. The bands

at 2920 cm^{-1} are associated with C-H bond stretch from PVOH and CH_2 groups from citric acid [21, 24, 40]. The 0%NS and the biocomposites with 1% and 2% of NS had vibrations around 3433 cm^{-1}, corresponding to the Si-OH bonds in NS surface. These vibrations did not occur for 3%NS and 4%NS possibly because, at higher concentrations, NS performed a high number of intermolecular hydrogen bonds with CA, forming the CA/NS clusters (Figure 2.e) and restricting the Si-OH bond vibration at the NS surface.

The 0%NS film showed an absorption band at 3247 cm^{-1} and, with NS increment, there was a dislocation of this band to higher wavenumbers (3257 cm^{-1} for 1%NS, 3261 cm^{-1} for 2%NS and, approximately 3266 cm^{-1} for 3%NS and 4%NS). This dislocation indicates a decrease in hydrogen bonds, possibly because, upon saturation of the reaction between the free OH of NS surface with CA molecules, the OH from CA/NS clusters competed for the hydrogen bonds formed within the WPI proteins and the PVOH molecules, as well as for those formed between the WPI proteins and PVOH molecules [41, 42]. Consequently, intra/intermolecular hydrogen bonds were broken while new intermolecular hydrogen bonds were formed between CA/NS clusters and WPI or between CA/NS clusters and PVOH. It acted disrupting the orientational structure formed by intermolecular hydrogen bond association, and therefore, shifting the absorption band to higher wavenumbers [41].

The non-observance of bands at 1719 cm^{-1} or 1730 cm^{-1} proves the high hydrolyzed PVOH used in the biocomposites preparation, indicating the absence of acetyl groups and leading to a high number of OH groups available to perform intermolecular hydrogen bonds among all the biocomposites constituents. At 1576 cm^{-1}, there was a significant reduction in the band intensity with the NS addition, being the 3%NS and 4%NS the biocomposites with more expressive reduction. The same reduction occurred at 1392 cm^{-1}, 1275 cm^{-1}, 735 cm^{-1} and 574 cm^{-1}. It suggests new interactions among all the biocomposites components when NS was added. The band at 1392 cm^{-1} is related to the CH and CH_2 deformation vibrations, which were less intense for 3%NS and 4%NS in which the biocomposite constituents were performing a higher number of hydrogen bonds that restricted the deformations [40]. Bands between 1320 cm^{-1} and 1180 cm^{-1} are related to the combination of N-H in-plane bending with C-N stretching vibrations (amide III from WPI proteins) [39]. Once again, possibly the high number of hydrogen bonds formed when 3% or 4% of NS was added acted restricting stretching of bonds, now from proteins, explaining the lower absorbance at 1275 cm^{-1}. Bands from 1180 cm^{-1} to 800 cm^{-1} can be attributed to the glycerol, corresponding to vibrations of C-C and C-O bonds, but also to the Si-O bonds of NS, explaining the higher absorptions for the 3%NS and 4%NS biocomposites at 1056 cm^{-1}, which have higher contents of NS [21, 40]. The band at 470 cm^{-1} is related to the flexural vibration of the Si-O-Si bond from NS, and that is why it did not appear for 0%NS [40].

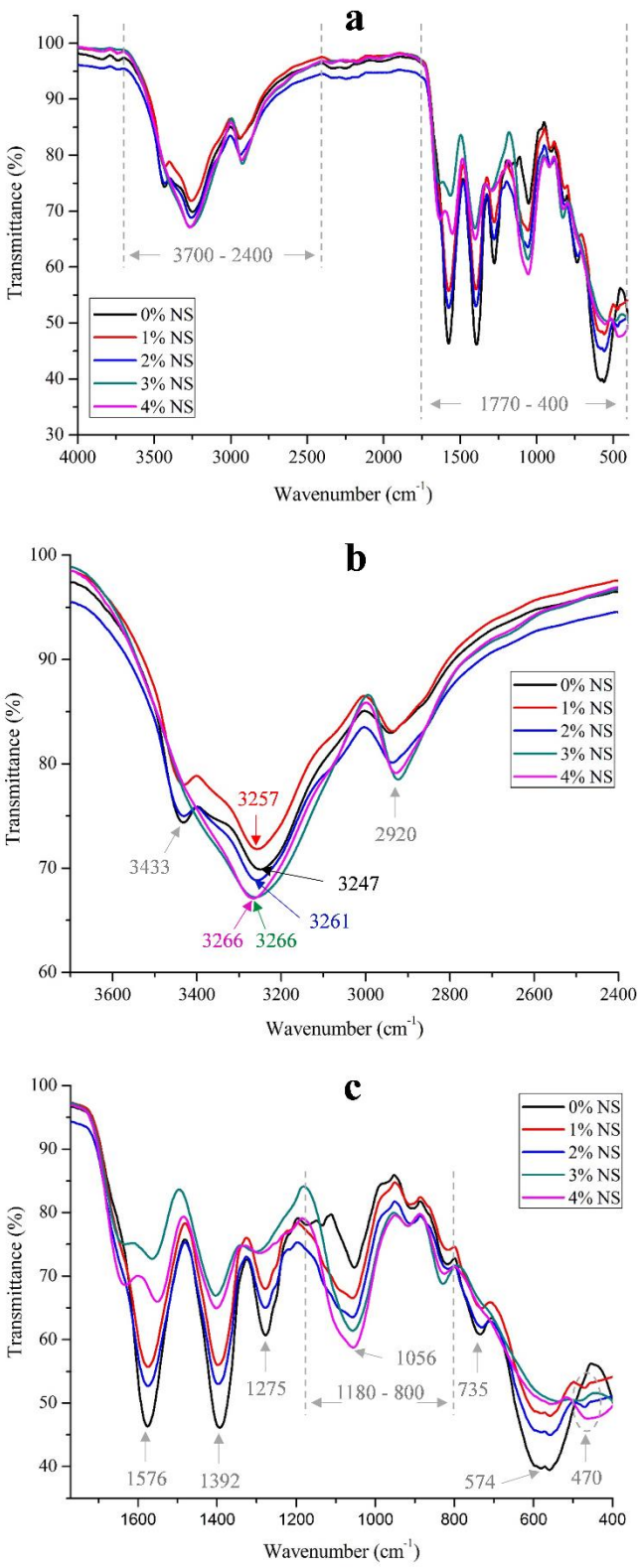

Figure 4. FT-IR spectra of the biocomposites: (a) general spectra from 4000 cm^{-1} to 400 cm^{-1}; (b) range from 3700 cm^{-1} to 2400 cm^{-1} and (c) range to 1770 cm^{-1} to 400 cm^{-1}.

3.5 Differential Scanning Calorimetry (DSC) analysis

The effect of the NS amount on the Tg of the biocomposites was evaluated through DSC analysis, and the resulting Tg's are exposed in Table 2. Tg is the temperature at which a polymer changes from a rigid and brittle behavior to a soft and rubbery condition, where chains have more mobility [43]. This property is directly related to the free volume among polymers chains. Below Tg, the free volume is relatively constant, while above Tg, there is an additional expansion from the free volume itself and an expansion due to an increased amplitude in the chemical bond thermal vibrations [44]. Therefore, it is appropriate to understand that the addition of a filler that can fit among polymer chains decreasing the free volume among them, such as nanoparticles in a composite, provides an increase in Tg since more energy is necessary to guarantee chain mobility and a rubbery condition.

The biocomposites with 1% and 2% of NS showed Tg values (18°C and 18°C, respectively) slightly lower than that from the pure WPI/PVOH film, of 19°C. The Tg reduction for 1%NS and 2%NS biocomposites corroborates the cited hypothesis that, at these low concentrations, the NS modified by CA molecules provided a plasticizing effect, increasing mobility among WPI and PVOH macromolecules and, therefore, reducing Tg. It explains the reduction in tensile strength and tensile modulus since at the test temperature (23°C), these biocomposites were above its Tg, at which a softer and less rigid behavior was guaranteed.

The 3%NS and the 4%NS biocomposites presented Tg values of 21 °C and 26 °C, respectively, which indicates that at these concentrations, NS was able to enter into the free volumes among the polymeric chains, decreasing the matrix total free volume and thus restricting chain mobility. This free volume filling from well distributed CA/NS clusters in the WPI/PVOH matrix is according to the higher basis weight results when 3 and 4% of NS were used. Besides that, for the 4%NS films, the mechanical test temperature (23 °C) is below Tg (26 °C), which is in agreement with the more rigid and less ductile behavior presented by this biocomposite. A similar phenomenon was observed by other researchers when adding 3% of NS to a WPI/pullulan matrix: Tg increased from 29.08 to 34.06°C [12]. These authors understood that at 3%, NS provided an increase of the intermolecular interactions between silanol groups and the polymer chains and, therefore decreased the mobility and increased Tg.

3.6 Water sorption

Figure 5 presents the weight gain (related to the water uptake) of the biocomposites versus time, at 25°C and 75% of RH. The knowledge of the moisture sorption behavior of packaging materials is important since, in certain polymers, the water acts as an internal lubricant, decreasing the energy barrier for chain mobility [29]. In the WPI/PVOH matrix, water sorption is heavily influenced by the strong interactions between these macromolecules and water molecules [22]. All the films, previously dried, achieved moisture sorption equilibrium in 8 h. Until the 2nd hour of the experiment, the 0%NS showed higher weight gain than all the other biocomposites, but after 3h, 1%NS and 2%NS showed a sorption

behavior similar to that without NS. A more expressive reduction, with significantly different results ($p \geq 0.05$) of water sorption was observed only when 4% of NS was added, with lower weight gain during the entire test, until equilibrium achievement. It corroborates the hypothesis that there was a free volume filling from well distributed CA/NS clusters in the WPI/PVOH matrix (Figure 2.e) when 4% of NS was used, which allowed fewer water molecules entering the biocomposite structure. Besides that, it is possible that at 4% of NS, the WPI and PVOH polar groups were preferentially interacting with the CA/NS clusters. This water sorption reduction is positive, whereas with lower water uptake when applied as packaging, the 4%NS will be less affected by the lubricant effect from water molecules and certainly keep its integrity more efficiently than the other biocomposites tested and, mainly, than the films of WPI/PVOH without NS.

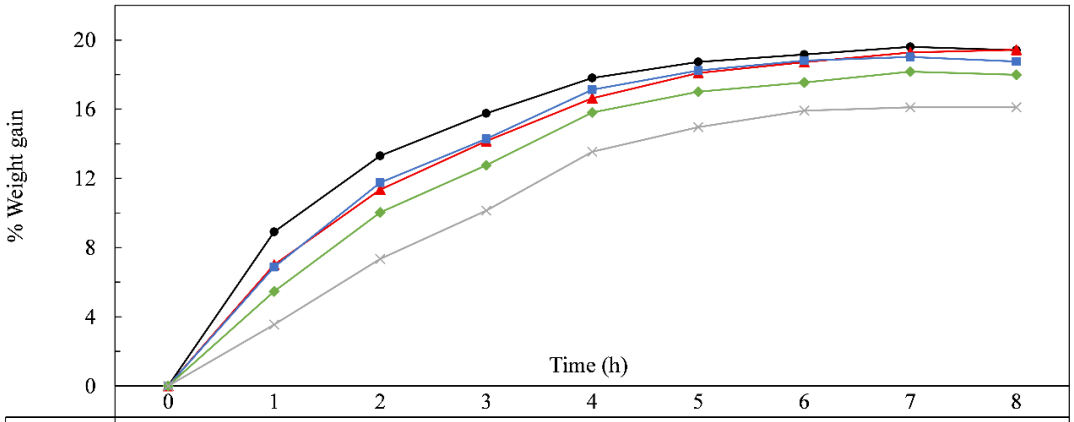

0%NS	0	8.91 ± 0.51d	13.3 ± 0.78b	15.8 ± 1.10b	17.8 ± 0.80b	18.7 ± 0.93b	19.2 ± 0.97b	19.6 ± 1.09b	19.4 ± 1.15b
1%NS	0	7.00 ± 0.61c	11.3 ± 0.96b	14.2 ± 1.38b	16.6 ± 0.95b	18.1 ± 0.95b	18.7 ± 0.81b	19.3 ± 0.76b	19.4 ± 0.84b
2%NS	0	6.88 ± 0.00b	11.8 ± 0.66b	14.4 ± 1.41b	17.1 ± 0.92b	18.2 ± 1.25b	18.8 ± 1.39b	19.0 ± 1.49b	18.8 ± 1.55b
3%NS	0	5.47 ± 0.68b	10.0 ± 0.75b	12.8 ± 0.82b	15.8 ± 0.49b	17.0 ± 0.64b	17.5 ± 0.53b	18.2 ± 0.80b	18.0 ± 0.93b
4%NS	0	3.55 ± 0.08a	7.34 ± 0.02a	10.1 ± 0.00a	13.5 ± 0.26a	15.0 ± 0.05a	15.9 ± 0.14a	16.1 ± 0.14a	16.1 ± 0.05a

Figure 5. Water sorption behavior of the WPI/PVOH/NS biocomposites at 25°C and 75% of RH. Different letters for the same time of test represent significantly different values at ($p \geq 0.05$) using Scott-Knott test.

3.7 Water vapor permeability (WVP)

WVP test is essential for new materials intended to be applied as food packaging, which is the case of the WPI/PVOH/NS composites developed. The permeability results showed that only at 4% of NS addition, there was a significantly ($p \geq 0.05$) change on the WPI/PVOH film barrier. The 4%NS biocomposite provided WVP 40% lower when compared to the 0%NS, leading to a material with a higher water vapor barrier. This result is in accordance with the lower moisture sorption found for this biocomposite, since permeability takes both sorption and diffusion of water into consideration. The increase in water barrier can be explained by the mentioned filling of free volumes by the CA/NS clusters, which allowed fewer water molecules to pass through the film structure.

When comparing the WVP value of the 4% NS to those from commercial packaging materials, it is still a poor barrier for food packaging applications. The WVP of a polyethylene (PE) at 23°C and 85% of RH can vary from 0.21 to 0.84 $g.mm.m^{-2}.day^{-1}.kPa^{-1}$ at 25 °C [45]. The WVP from 4%NS (1.62 $g.mm.m^{-2}.day^{-1}.kPa^{-1}$) is still around 10 times higher than the cited WVP of PE. However, the 4% NS presented an excellent result of WVP when compared to other biofilms intended to be used in food packaging sector as alternative to those from fossil sources: chitosan (7.84 $g.mm.m^{-2}.day^{-1}.kPa^{-1}$, 237% higher), starch (20.1 $g.mm.m^{-2}.day^{-1}.kPa^{-1}$, 11.4 times higher) and poly(lactic acid) (PLA, 2.69 $g.mm.m^{-2}.day^{-1}.kPa^{-1}$, 66% higher), for example [46–48].

4 Conclusion

The addition of 3% and 4% of NS to the WPI/PVOH films provided the formation of well-distributed micrometric clusters of CA/NS, which filled the free volumes in the film matrix, promoting intense intermolecular interactions. The 4%NS biocomposites presented tensile strength of 10.2 MPa and tensile modulus of 78.2 MPa (43% and 15% of enhance, respectively, when compared to the 0%NS) making it suitable for food packaging application in terms of tensile properties. An expressive reduction of water sorption (17%) of WPI/PVOH films was observed when 4% of NS was added, increasing the efficiency in keeping integrity during application. Besides that, a reduction of 40% in WVP was obtained for 4% of NS addition, making the biocomposite produced more resistant to water vapor barrier. Therefore, the addition of 4% of NS in WPI/PVOH films is indicated to improve tensile strength and water vapor barrier properties.

Declaration of competing interest

The authors declare no competing interest.

Acknowledgments

This work was financed by the Coordenação de Aperfeiçoamento de Pessoal de Nível Superior (CAPES) – Brazil (Finance Code 001), the Conselho Nacional de Desenvolvimento Científico e Tecnológico (CNPq) – Brazil, and the Fundação de Amparo à Pesquisa do Estado de Minas Gerais (FAPEMIG) – Brazil. The authors extend their appreciation for all support provided by the Universidade Federal de Lavras (UFLA) – Brazil, especially by the Central de Análise e Prospecção Química (*CAPQ, UFLA*) – Brazil, and the Laboratório de Microscopia Eletrônica e Análise Ultraestrutural (LME, *UFLA) – Brazil.*

5 References

1. Lara BRB, Araújo ACMA, Dias MV, et al (2019) Morphological, mechanical and physical properties of new whey protein isolate/ polyvinyl alcohol blends for food flexible packaging. In: Food Packag. Shelf Life. https://linkinghub.elsevier.com/retrieve/pii/S2214289418301777
2. Samadani F, Behzad T, Saeid Enayati M (2019) Facile strategy for improvement properties of whey protein isolate/walnut oil bio-packaging films: Using modified cellulose nanofibers. Int J

Biol Macromol 139:858–866. https://doi.org/10.1016/j.ijbiomac.2019.08.042

3. Machado Azevedo V, Vilela Dias M, Helena de Siqueira Elias H, et al (2018) Effect of whey protein isolate films incorporated with montmorillonite and citric acid on the preservation of fresh-cut apples. Food Res Int 107:306–313. https://doi.org/10.1016/j.foodres.2018.02.050
4. Wittaya T (2012) Application of protein-based edible films. In: Protein-Based Edible Films: Characteristics and Improvement of Properties. InTech
5. FAO, OECD (2018) OECD‐FAO Agricultural Outlook 2018‐2027. Chapter 7: Dairy and dairy products. OECD Publishing, Paris/Food and Agriculture Organization of the United Nations, Rome
6. González-Siso MI, Touriño A, Vizoso Á, et al (2015) Improved bioethanol production in an engineered Kluyveromyces lactis strain shifted from respiratory to fermentative metabolism by deletion of NDI1. Microb Biotechnol 8:319–30. https://doi.org/10.1111/1751-7915.12160
7. Weizman O, Dotan A, Nir Y, Ophir A (2017) Modified whey protein coatings for improved gas barrier properties of biodegradable films. Polym Adv Technol 28:261–270. https://doi.org/10.1002/pat.3882
8. Huntrakul K, Harnkarnsujarit N (2020) Effects of plasticizers on water sorption and aging stability of whey protein/ carboxy methyl cellulose films. J Food Eng 272:109809. https://doi.org/10.1016/j.jfoodeng.2019.109809
9. Gökkaya Erdem B, Dıblan S, Kaya S (2019) Development and structural assessment of whey protein isolate/sunflower seed oil biocomposite film. Food Bioprod Process 1:270–280. https://doi.org/10.1016/j.fbp.2019.09.015
10. Azevedo VM, Silva EK, Pereira CFG, et al (2015) Whey protein isolate biodegradable films: Influence of the citric acid and montmorillonite clay nanoparticles on the physical properties. Food Hydrocoll 43:252–258. https://doi.org/10.1016/j.foodhyd.2014.05.027
11. Carvalho RA, Santos TA, de Azevedo VM, et al (2018) Bio-nanocomposites for food packaging applications: effect of cellulose nanofibers on morphological, mechanical, optical and barrier properties. Polym Int 67:386–392. https://doi.org/10.1002/pi.5518
12. Hassannia-Kolaee M, Khodaiyan F, Pourahmad R, Shahabi-Ghahfarrokhi I (2016) Development of ecofriendly bionanocomposite: Whey protein isolate/pullulan films with nano-SiO2. Int J Biol Macromol 86:139–144. https://doi.org/10.1016/J.IJBIOMAC.2016.01.032
13. Younes M, Aggett P, Aguilar F, et al (2018) Re-evaluation of silicon dioxide (E 551) as a food additive. EFSA J 16:1–70. https://doi.org/10.2903/j.efsa.2018.5088
14. Zhang R, Wang X, Cheng M (2018) Preparation and characterization of potato starch film with various size of nano-SiO2. Polymers (Basel) 10:1–16. https://doi.org/doi.org/10.3390/polym10101172

15. Tabatabaei RH, Jafari SM, Mirzaei H, et al (2018) Preparation and characterization of nano-SiO2 reinforced gelatin-k-carrageenan biocomposites. Int J Biol Macromol 111:1091–1099. https://doi.org/doi.org/10.1016/j.ijbiomac.2018.01.116
16. Ritamäki M, Rytöluoto I, Lahti K, Karttunen M (2015) Effects of thermal aging on the characteristic breakdown behavior of Nano-SiO2 -BOPP and BOPP films. In: Proceedings of the 11th International Conference on the Properties and Applications of Dielectric Materials (ICPADM). Sydney, pp 19–22
17. Seyfi J, Hejazi I, Jafari SH, et al (2016) Enhanced hydrophobicity of polyurethane via non-solvent induced surface aggregation of silica nanoparticles. J Colloid Interface Sci 478:117–126. https://doi.org/10.1016/j.jcis.2016.06.005
18. Liu X, Chen X, Ren J, et al (2019) Effects of nano-ZnO and nano-SiO 2 particles on properties of PVA/xylan composite films. Int J Biol Macromol 132:978–986. https://doi.org/10.1016/j.ijbiomac.2019.03.088
19. Cozzolino CA, Castelli G, Trabattoni S, Farris S (2016) Influence of colloidal silica nanoparticles on pullulan-coated BOPP film. Food Packag Shelf Life 8:50–55. https://doi.org/10.1016/j.fpsl.2016.03.003
20. Wang C, Wei J, Xia B, et al (2013) Effect of silica on the mechanical, thermal, and crystalline properties of poly(vinyl alcohol)/nano-silica films. J Appl Polym Sci 128:1652–1658. https://doi.org/doi.org/10.1002/app.38277
21. Mallakpour S, Naghdi M (2016) Design and preparation of poly(vinyl alcohol) flexible nanocomposite films containing silica nanoparticles with citric acid and ascorbic acid linkages as a novel nanofiller through a green route. Int J Polym Anal Charact 21:2943. https://doi.org/10.1080/1023666X.2016.1091541
22. Lara BRB, Dias MV, Guimarães Junior M, et al (2020) Water Sorption Thermodynamic Behavior Of Whey Protein Isolate/ Polyvinyl Alcohol Blends For Food Packaging. Food Hydrocoll 103:9. https://doi.org/10.1016/j.foodhyd.2020.105710
23. Albano KM, Cavallieri ÂLF, Nicoletti VR (2018) Electrostatic interaction between proteins and polysaccharides: Physicochemical aspects and applications in emulsion stabilization. Food Rev Int 35:54–89. https://doi.org/10.1080/87559129.2018.1467442
24. Guimarães M, Botaro VR, Novack KM, et al (2015) High moisture strength of cassava starch/polyvinyl alcohol-compatible blends for the packaging and agricultural sectors. J Polym Res 22:. https://doi.org/10.1007/s10965-015-0834-z
25. ASTM D882-02 (2002) Standard Test Method for Tensile Properties of Thin Plastic Sheeting
26. ASTM E96/E96M-10 (2010) Standard Test Methods for Water Vapor Transmission. 4:1–12
27. Jansson A, Thuvander F (2004) Influence of thickness on the mechanical properties for starch

films. Carbohydr Polym 56:499–503. https://doi.org/10.1016/j.carbpol.2004.03.019

28. Aksakal B, Yargı Ö, Şahinturk U (2017) Uniaxial tensile and structural properties of poly(vinyl alcohol) films: The influence of heating and film thickness. J Appl Polym Sci 134:1–9. https://doi.org/10.1002/app.44915
29. Robertson GL (2013) Food Packaging Principles and Practice, 3rd ed. CRC Press, Boca Raton
30. Morris BA (2016) The Science and Technology of Flexible Packaging: Multilayer Films from Resin and Process to End Use. Matthew Deans, Cambridge, MA, United States
31. Park H-R, Chough S-H, Yun Y-H, Yoon S-D (2005) Properties of Starch/PVA Blend Films Containing Citric Acid as Additive. J Polym Environ 13:375–382. https://doi.org/10.1007/s10924-005-5532-1
32. Ramos ÓL, Santos AC, Leão M V, et al (2012) Antimicrobial activity of edible coatings prepared from whey protein isolate and formulated with various antimicrobial agents. Int Dairy J 25:132–141. https://doi.org/10.1016/j.idairyj.2012.02.008
33. Li T, Wang C, Li T, et al (2018) Surface hydrophobicity and functional properties of citric acid cross-linked whey protein isolate: The impact of pH and concentration of citric acid. Molecules 23:1–11. https://doi.org/10.3390/molecules23092383
34. Azevedo VM, Dias M V., Borges S V., et al (2015) Development of whey protein isolate bio-nanocomposites: Effect of montmorillonite and citric acid on structural, thermal, morphological and mechanical properties. Food Hydrocoll 48:179–188. https://doi.org/10.1016/J.FOODHYD.2015.02.014
35. NCBI (National Center for Biotechnology Information) (2017) PubChem Compound Database; CID=9988076. https://pubchem.ncbi.nlm.nih.gov/compound/9988076. Accessed 9 Jan 2020
36. Halima N Ben (2016) Poly(vinyl alcohol): review of its promising applications and insights into biodegradation. R Soc Chem 6:39823–39832. https://doi.org/10.1039/c6ra05742j
37. Farjami T, Madadlou A, Labbafi M (2015) Characteristics of the bulk hydrogels made of the citric acid cross-linked whey protein microgels. Food Hydrocoll 50:159–165. https://doi.org/10.1016/j.foodhyd.2015.04.011
38. Oymaci P, Altinkaya SA (2016) Improvement of barrier and mechanical properties of whey protein isolate based food packaging films by incorporation of zein nanoparticles as a novel bionanocomposite. Food Hydrocoll 54:1–9. https://doi.org/10.1016/J.FOODHYD.2015.08.030
39. Ramos ÓL, Reinas I, Silva SI, et al (2013) Effect of whey protein purity and glycerol content upon physical properties of edible films manufactured therefrom. Food Hydrocoll 30:110–122. https://doi.org/10.1016/j.foodhyd.2012.05.001
40. Tang S, Zou P, Xiong H, Tang H (2008) Effect of nano-SiO 2 on the performance of starch/polyvinyl alcohol blend films. https://doi.org/10.1016/j.carbpol.2007.09.019

41. Yao K, Cai J, Liu M, et al (2011) Structure and properties of starch/PVA/nano-SiO2 hybrid films. Carbohydr Polym 86:1784–1789. https://doi.org/10.1016/j.carbpol.2011.07.008
42. SILVERSTEIN RM, WEBSTER FX, KIEMLE D (1998) Spectrometric Identification of Organic Compounds, 6th ed. John Wiley & Sons, Ltd, New York
43. Ebnesajjad S (2016) Introduction to Plastics. In: Baur E, Ruhrberg K, Woishnis W (eds) Chemical Resistance of Engineering Thermoplastics. Elsevier Inc., pp xiii–xxv
44. Hale A (2002) Thermosets. In: Handbook of Thermal Analysis and Calorimetry. Elsevier Inc., pp 295–354
45. Lange BJ, Wyser Y (2003) Recent Innovations in Barrier Technologies for Plastic Packaging – a Review. Packag Technol Sci 16:149–158. https://doi.org/10.1002/pts.621
46. Moura CM De, Moura JM De, dos Santos JP, et al (2012) Evaluation of Mechanical Properties and Water Vapor Permeability in Chitosan Biofilms Using Sorbitol and Glycerol. Macromol Symp 319:240–245. https://doi.org/10.1002/masy.201100128
47. Monteiro MKS, Oliveira VRL, Santos FKG, et al (2018) Incorporation of bentonite clay in cassava starch fi lms for the reduction of water vapor permeability. Food Res Int 105:637–644. https://doi.org/10.1016/j.foodres.2017.11.030
48. Shankar S, Wang L, Rhim J (2018) Incorporation of zinc oxide nanoparticles improved the mechanical , water vapor barrier , UV-light barrier , and antibacterial properties of PLA-based nanocomposite fi lms. Mater Sci Eng C 93:289–298. https://doi.org/10.1016/j.msec.2018.08.002

ARTIGO 2

(Formatação segundo a revista Food Packaging and Shelf Life – ISSN: 2214-2894)

REDUCING SPONTANEITY OF WATER SORPTION PROCESS IN WHEY PROTEIN ISOLATE/ POLYVINYL ALCOHOL BIOCOMPOSITES THROUGH NANO-SILICA ADDITION

Bruna Rage Baldone Lara[a], Paulo Sérgio de Andrade[a], Mario Guimarães Junior[b], Natália Leite Oliveira[a*], Bruna de Souza Nascimento[a], Gustavo Henrique Denzin Tonoli[c], Marali Vilela Dias[a]

[a] Federal University of Lavras (UFLA) – Department of Food Science, Lavras (Minas Gerais), Brazil

[b] Federal Center of Technological Education of Minas Gerais (CEFET-MG) – Department of Electromechanics, Belo Horizonte, Minas Gerais, Brazil.

[c] Federal University of Lavras - UFLA / Department of Forest Science, University Campus - PO Box: 3037 - CEP: 37200-000, Lavras - MG, Brazil.

*Corresponding author. E-mail: bruna.lara@estudante.ufla.br

Graphical abstract:

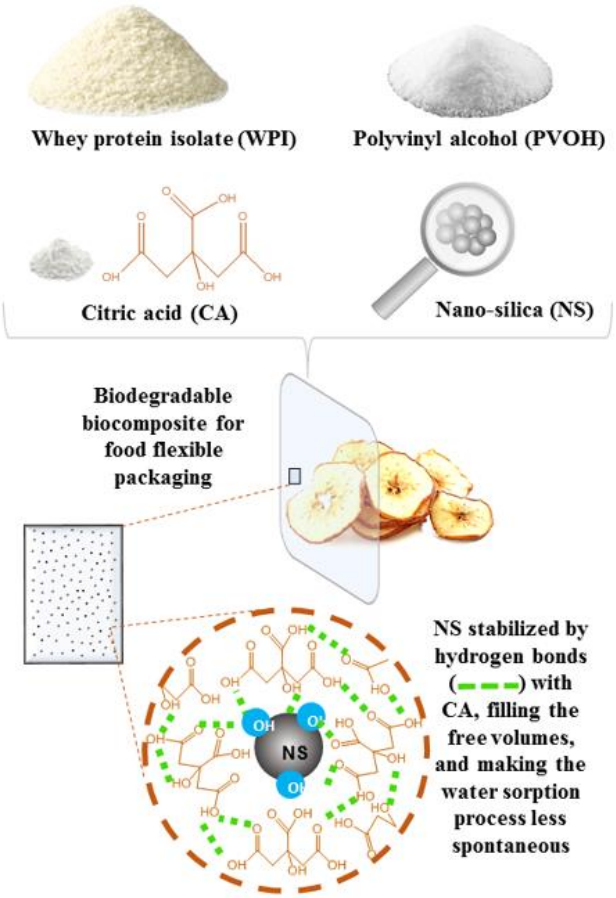

Abstract

To determine the best application of new materials for food packaging, the study of water permeation and sorption processes is essential since it allows to predict the film behavior under different moisture conditions inside and/or outside the packaging. This work aimed to investigate the interaction with water, and the water sorption, solubility, and diffusion behaviors of new biocomposites 70% of Whey Protein Isolate (WPI), 30% of Polyvinyl Alcohol (PVOH), and up to 4% of nano-silica (NS) intended to be applied as flexible food packaging. Water diffusion analysis indicated that the addition of NS to WPI/PVOH matrix was able to reduce diffusion of water through this material, mostly at 4% of NS (reduction of 58% when compared with the film without NS). Solubility coefficient values were not significantly different ($p \geq 0.05$) for all the biocomposites while wettability and surface energy were reduced with NS addition. The water sorption test provided curves with a more expressive increase of water sorption above $a_w = 0.75$ and higher equilibrium moistures at higher temperatures. Finally, the addition of NS to the WPI/PVOH matrix was able to make the water sorption process less spontaneous and, the biocomposite produced is potentially suitable for application as packaging for foods and chilled environments with until 0.75 of a_w.

Keywords: Whey protein isolate; Polyvinyl alcohol; Nano-silica; Biocomposite; Water sorption isotherms; Food packaging.

1 INTRODUCTION

In the food sector, packaging plays an important role in protecting the quality of foods, including the management of moisture ingress or regress. The food spoilage process and food texture and crispiness are affected by moisture. Besides the food characteristics, the chemical and physical properties of the film packaging are directly influenced by moisture (Jakubczyk, Marzec, & Lewicki, 2008; Pitt & Hocking, 2009). Therefore, it is very important to know the water sorption behavior of flexible films for food packaging, since it can be used to predict information about the stability and quality changes of the packed food product and to predict the film behavior under different moisture conditions inside and/or outside the packaging (Jagadish & Raj, 2011; Lara et al., 2020).

Water sorption isotherms are important to hydrophilic biomacromolecules for packaging since their films are water sensitive, besides the fact that the water content or the water activity (a_w) can strongly influence their functionality (Azevedo, Silva, Pereira, da Costa, & Borges, 2015; Huntrakul & Harnkarnsujarit, 2020). In previous work, it was observed that the addition of up to 30% of PVOH to the WPI matrix provided an increase in flexibility but made the water sorption process more spontaneous (Lara et al., 2019, 2020). To reduce the interaction of WPI/PVOH blends with water, new biocomposites of WPI/PVOH and nano-silica (NS) were produced, showing a 40% of reduction in water vapor permeability and a decrease of 17% in water sorption by NS adding (Lara, de Andrade, Guimarães Junior, Dias, & Alcântara, 2021). Seeking to define the most suitable application, it is necessary to better understand the interaction of these new WPI/PVOH/NS biocomposites with moisture, which can be accomplished by water contact angle and surface energy results, but mainly through sorption isotherms studies.

The general properties of biopolymeric films are strongly influenced by water content water activity (a_w) of both the food packaged and the external atmosphere and, therefore, water sorption isotherms tests of new packaging films are essential correctly determine conditions of application. However, few are the published works evaluating the sorption behavior of WPI biofilms or blends with WPI, and those published do not contemplate the study of thermodynamic properties, such as differential enthalpy (ΔH_{dif}), differential entropy (ΔS_{dif}), and Gibbs free energy (ΔG) (Azevedo et al., 2015; Huntrakul & Harnkarnsujarit, 2020). These parameters provides information about the material's microstructure and its behavior in respect to water, including the influence of the film composition in the spontaneity of the water sorption process (Echavarria, Torres, & Montoya, 2021). Besides the sorption behavior analysis, it is also important to know the diffusivity and solubility coefficients since the film's moisture gain in the sorption process is influenced by both the water molecule's solubility on the biocomposite surface and the penetration of water molecules into the material (Robertson, 2013).

The present study is a continuation of works (Lara et al., 2019, 2020, 2021), but now using a single concentration of WPI and PVOH (optimal condition obtained), and varied concentrations of NS. There are no published studies in the literature with the WPI/PVOH/NS mixture for the study of sorption isotherms, calculation of thermodynamic properties and diffusivity and solubility coefficients, and water contact angle test. Thus, the objective was to establish comparisons between films with NS at different concentrations and without NS with different concentrations of WPI and PVOH, as well as understanding the interaction with water and the water sorption, solubility, and diffusion behavior of new biocomposites 70% WPI and 30% PVOH and up to 4% NS intended to be applied as flexible food packaging. Therefore, the solubility and diffusivity coefficients, the contact angle with water and the surface energy, as well as the thermodynamic behavior of sorption of these materials were studied by means of water sorption isotherms under three different temperatures (5, 15, and 25°C).

2 MATERIAL AND METHODS

2.1 Material

Whey Protein Isolate (WPI 9400) with 90% of proteins from Hilmar Ingredients; polyvinyl alcohol with high molecular weight (Mw = 130.000 $g.mol^{-1}$) and highly hydrolyzed (99%) from Sigma-Aldrich; glycerol (≥ 99.5%, density 1.26 $g.mL^{-1}$), as a plasticizing agent, produced by Sigma-Aldrich; granulated anhydrous citric acid from Cargill Agrícola S.A was used to guarantee a good distribution of NS; and NS from colloidal solution Bindzil 2034DI (Akzo Nobel), with 34% in weight of NS (average particle size of 15 nm and 200 $m^2.g^{-1}$ of surface area).

2.2 Preparation of the biocomposites

Biocomposites were prepared following the same procedures from (Lara et al., 2021). WPI and PVOH solutions were separately prepared using a polymer concentration of 6% w/v, and adding 30% of glycerol (w/w of polymer), and 8% of citric acid (w/w of polymer). Both solutions were agitated and conducted to water bath at 90°C. WPI and PVOH solutions were merged in a volumetric proportion of 70/30 and, after cooled at room temperature, nano-silica (Bindzil 2034DI) was added in five different concentrations: 0, 1, 2, 3, and 4% w/w of polymer (Table 1). The final solution of each treatment was homogenized in Ultra Turrax (Kika Labortchnik) resulting in ultrasonic energy applied of 810 $J.mL^{-1}$. Final solutions were shed on rectangular Teflon plates (750 cm²), perfectly level, and conditioned at room temperature (25 °C) for spontaneous drying (48 h). Three replicates of each treatment were

performed. The dried biocomposites were conditioned under controlled temperature and relative humidity (RH) (25 ± 1 ºC and 50% RH) for 48 h before characterization.

2.3 Characterization of the biocomposites

2.3.1 Determination of water diffusion coefficient

Effective diffusion coefficient (D_{eff}) of water was determined using the Fick's model for diffusion shown in Equation 1, which can be simplified when considering that the water diffusion occurs in a unique direction, as expressed as in Equation 2. Besides that, considering: (i) a membrane with uniform thickness (ii) and surfaces, x = −l and x = l, with a known constant concentration of water (C_0), and that (iii) concentration of water inside the film is zero, the diffusion equation can be expressed as Equation 3 [11]. For short periods, Equation 3 can be simplified as showed in Equation 4, which can be used to adjust the initial experimental points, when until 60% of the solute mass has been absorbed (Crank, 1975).

$$\frac{\partial C}{\partial t} = D_{eff}\left(\frac{\partial^2 C}{\partial x^2} + \frac{\partial^2 C}{\partial y^2} + \frac{\partial^2 C}{\partial z^2}\right) \quad (1)$$

$$\frac{\partial C}{\partial t} = D_{eff}\left(\frac{\partial^2 C}{\partial x^2}\right) \quad (2)$$

$$\frac{M_t}{M_\infty} = 1 - \frac{8}{\pi^2}\sum_{N=0}^{\infty}\frac{1}{(2N+1)^2}\exp\left[\frac{-D_{eff}(2N+1)^2\pi^2 t}{e^2}\right] \quad (3)$$

$$\frac{M_t}{M_\infty}(\leq 0{,}60) = 4\sqrt{\frac{D_{eff}.t}{e^2\pi}} \quad (4)$$

Where C is the water concentration (g.cm^{-3}), D_{eff} is the effective diffusion coefficient (cm^2.s^{-1}), *x*, *y* e *z* are the dimensions of the film with significant diffusivity (cm), *x* = thickness, *y* = 0 and *z* = 0 (when occurring in only one direction, x); M_t (g) is the total amount of diffusing substance which has entered the membrane at the time *t* (s), M_∞ (g) is the corresponding moisture amount after the infinite time (equilibrium moisture), *N* is the number of terms in the series and e is the thickness of the film (cm).

The experimental test was conducted by preparing specimens of 6 cm² in triplicate and submitting them to vacuum drying at 70 °C for 24 h. The samples were placed in a hermetic pot with a relative humidity of 75% (saturated saline solution of NaCl) at 25 °C to measure their moisture gain. All samples were weighted with an accuracy of 0.001 g from the time zero to equilibrium (approximately 8 days), in a 24 h interval. For the first 9 h, when there were significant changes in mass, weight was

measured at each hour. Through the moisture gain by time data and considering the thickness of each sample, it was possible to estimate the value of D_{eff} through a non-linear regression with Equation 3 (using several terms of the series truncated in N = 10).

2.3.2 Determination of water solubility coefficient

Besides the sorption behavior analysis, it is also important to know the diffusivity and solubility coefficients since the film's moisture gain in the sorption process is influenced by both the water molecule's solubility on the biocomposite surface and the penetration of water molecules into the material (Robertson, 2013). The determination of the solubility coefficient (S) takes considers: (i) biocomposite as a finite solid, where initially the film is free from vapor on the surface; (ii) a constant water diffusion which is independent of water concentration. Finally, considering that this film is then exposed to a pressure p_1 giving a concentration in the surface layer of c_1, is possible to find the amount of water vapor Q diffusing through the material with thickness X in a time t through Equation 5 (Robertson, 2013):

$$Q = \frac{Dc_1 t}{X} - \frac{c_1 X}{6} \tag{5}$$

D is the diffusion coefficient and the amount of water vapor passing through the biocomposite increases linearly with time once the steady-state has been reached. With the test of water permeability performed in previous work was possible to obtain the permeability coefficient (P), and the values of P are exposed in Table 1 (Lara et al., 2021). Finally, at steady-state diffusion, knowing P and D (D_{eff}), it was possible to obtain the solubility coefficient through Equation 6, considering four conditions: (i) diffusion is at steady-state; (ii) the relationship between concentration and distance through the biocomposite is linear (iii) diffusion occurs in only one direction; and (iv) both D and S are independent of the concentration (Janjarasskul & Tananuwong, 2019; Robertson, 2013).

$$S = P/D \tag{6}$$

2.3.3 Determination of the water contact angle and surface energy

For water contact angle measurement it was used the sessile drop method and a Goniometer (KRUSS, Drop Shape Analyzer-DSA25) in which, through a syringe, a drop of the standard liquid was applied on the surface to be characterized (Andrade et al., 2014; Wiacek, 2015). The static angle between the drop and the biocomposites surface was calculated through the slope of the tangent. The average of the left and right angles was obtained as the final value of the contact angle.

The contact angle analysis was performed fixing biocomposite samples on glass slides and attaching them to the equipment. A drop of the liquid was placed on the biocomposite surface and the goniometer carried out 10 angle measurements per second for 2 s (ASTM D7334-08, 2013). To determine the wettability, distilled water was used, while for surface energy, besides the distilled water, ethylene glycol and methane diode were used as well. The dispersion of surface energy was calculated following the procedure described by Owens-Wendt, considered universal for the calculation of surface energy (OWENS & WENDT, 1969). The existing relationship for surface energy was extended and the hydrogen bonds added in the non-dispersive component, renamed to the polar component (p) (Equation 7). It was assumed that the interaction between two materials is also a function of polar components and is described through a geometric mean, where only forces of the same nature interact (Equation 8) (OWENS & WENDT, 1969).

$$\gamma_i^T = \gamma_i^d + \gamma_i^p \tag{7}$$

$$\gamma_{i/j} = \gamma_i + \gamma_j - 2\left(\sqrt{\gamma_i^d + \gamma_j^d} + \sqrt{\gamma_i^p + \gamma_j^p}\right) \tag{8}$$

Where: γ is superficial free energy; γ^T is total surface free energy; *d* is the dispersive interactions and *p* is the polar component.

2.3.4 Water sorption isotherms

Sorption isotherms tests were performed at three different temperatures (5, 15, and 25 °C) and using film samples with 6 cm^2, placed in small plastic containers coated with foil. All samples were previously dried using a vacuum oven, at 70 °C for 24 h. The test was performed by balancing three samples for each film into six hermetic pots (static gravimetric method). Each one of these pots contained a different saturated saline solution (MgCl, K_2CO_3, $Mg(NO_3)_2$, NaCl, KCl, and K_2SO_4) with water activities between 0.328 to 0.985 and varying according to the temperature. A glass tube containing toluene was placed inside the pots to prevent fungi growth and samples were kept in the pots until the equilibrium (weight change ≤ 5%).

Since Guggenheim, Anderson, and Boer (GAB) model, showed in Equation 9, well described the water sorption behavior of WPI/PVOH blends, it was used in this work to adjust isotherm

experimental data of the biocomposites (Lara et al., 2020). Besides that, the GAB model is recognized as the most versatile sorption model, since it modifies the BET model to take into account the energies of interaction between the first and distant sorbet molecules at the individual sorption sites (Sandulachi, 2012). Solver tool from Microsoft Excel 2013 was used for the non-linear fitting of experimental data (Jiménez, Fabra, Talens, & Chiralt, 2013).

$$Y_e = \frac{Y_m C K a_w}{(1-Ka_w)(1-Ka_w+CKa_w)} \quad (9)$$

In Equation 10: Y_e is the water content at the equilibrium (dry basis, g water.100 g^{-1} film); Y_m is the water content of the molecular monolayer (dry basis, g water.100 g^{-1} film); aw is the water activity; *C* and *K* are constants.

2.3.5 Theory of Enthalpy-Entropy Compensation and ΔG_β

The Theory of Enthalpy-Entropy Compensation takes in consideration both physical and chemical phenomena and, therefore, can be used to identify mechanisms of water sorption of materials in different conditions (Echavarria et al., 2021). A graph of $-\ln(a_w)$ versus T^{-1} at different moisture content (Y_e) values were used to obtain the differential sorption enthalpy (ΔH_{dif}) and the differential entropy (ΔS_{dif}) to verify the enthalpy-entropy compensation and then obtain Gibbs free energy at the isokinetic temperature (ΔG_β) (Lara et al., 2021; Tao et al., 2018). A linear relation between differential enthalpy and differential entropy is proposed by the Theory of Enthalpy-Entropy Compensation and is given by Equation 10 (Velázquez-gutiérrez et al., 2015). T_β is isokinetic temperature and is expressed as the slope of the ΔS_{dif} versus ΔH_{dif} graph. At T_β, all reactions occur at the same rate for different values of $\ln(a_w)$, and in cases where $T_\beta \neq T_{hm}$, being T_{hm} (harmonic mean temperature), the enthalpy-entropy compensation is assured (L′vov, 2007). T_{hm} was obtained through Equation 11, in which *n* is the number of sorption isotherms and T_i (K) is the temperature of the ith isotherm. Once assured enthalpy-entropy compensation, ΔG_β can be obtained through the linear coefficient of the ΔS_{dif} versus ΔH_{dif} graph, ΔG_β can provide information about the spontaneity of the water sorption on the biocomposites tested according to the NS content.

$$\Delta H_{dif} = T_\beta . \Delta S_{dif} + \Delta G_\beta \quad (10)$$

$$T_{hm} = \frac{n}{\sum_{i=1}^{n}\left(\frac{1}{T_i}\right)} \quad (11)$$

2.4 Statistical analysis

The coefficient of determination (R^2) and the relative mean deviation (RMD) (Equation 12) were used to evaluate adequacy of the GAB model used for the description of sorption isothermal behavior. Besides that, the function between residual values and the levels of equilibrium moisture was to identify possible biased results.

$$RMD = \frac{100}{N}\sum_{i=1}^{N}\frac{\left|Y_{e_i} - Y_{e_{p,i}}\right|}{Y_{e_i}} \quad (12)$$

where N is the number of observations (which means the number of salts, six) Y_{ei} is the ith observation, and $Y_{ep,i}$ is the value predicted by the model for the ith observation.

To carry out statistical analysis of the P, D_{eff}, S, and water contact angle results by comparing the means, Sisvar 5.0 was used to apply Scott-Knott test, with 95% of confidence level.

3 RESULTS AND DISCUSSION

3.1 Water diffusion coefficient

Water diffusion coefficients obtained are exposed in Table 1. The effective diffusion coefficient (D_{eff}) can be understood as a kinetic term that represents the speed of water molecules which are moving through the polymer matrix (Janjarasskul & Tananuwong, 2019). The increase of NS content reduced the water diffusion through the biocomposite matrix, making it slower. NS can enter into the free volumes among the polymeric chains, and among the biocomposites tested, those with higher NS content (3 and 4%) provided a higher filling. In a previous work, the basis weight of the biocomposites were tested and it was concluded that NS acts filling free volumes among WPI and PVOH chains (Table 1) (Lara et al., 2021). With less free volume available, the speed of water molecules moving through the biocomposites matrix was reduced, leading to lower D_{eff} values.

Table 1 – Results of effective diffusion coefficient (D_{eff}), permeability coefficient (P), solubility coefficient (S) and Basis weight

Biocomposite	NS content (%)	D_{eff} ($cm^2.s^{-1}$)*10^{-9}	P ($g.cm.cm^{-2}.s^{-1}.kPa^{-1}$)*$10^{-10}$	S ($g.cm^{-3}.kPa^{-1}$) *10^{-1}	Basis weight ($g.m^{-2}$)
0%NS	0	2.37±0.26c	3.12±0.25b	1.38±0.31a	126 ± 7.36a
1%NS	1	1.93±0.11b	3.54±0.41b	1.97±0.07a	144 ± 5.38b
2%NS	2	1.56±0.09a	3.11±0.42b	1.97±0.38a	160 ± 6.79b
3%NS	3	1.23±0.12a	2.78±0.26b	2.36±0.46a	186 ± 9.84c
4%NS	4	1.00±0.02a	1.88±0.27a	1.88±0.07a	189 ± 10.5c

At vertical columns, different letters represent significantly different values at ($p \geq 0.05$) using the Scott-Knott test.

3.2 Water Solubility coefficient

Water solubility coefficient (S) was calculated through Equation 7 with the known values of P and D_{eff}, all expressed in Table 1. The solubility coefficient (S) indicates the number of water molecules dissolved in the polymer (Janjarasskul & Tananuwong, 2019; Robertson, 2013). Solubility coefficient values were not significantly different ($p \geq 0.05$) for all the biocomposites evaluated, meaning that NS has influenced the speed of water molecules moving through the polymer matrix, making it slower, but did not change the number of water molecules in the biocomposites matrix. The interaction among WPI/PVOH chains and water molecules was not affected by NS, while the filling of free volumes made it difficult for water to pass through the films.

3.3 Water contact angle and surface energy

The contact angle between water drop and the biocomposites surface was increased with the NS increment. 0%NS and 1%NS presented similar angles (28.9° and 28.3°, respectively), while 2%NS and 3%NS showed higher similar angles (43.4° and 43.7°, respectively). The highest, and therefore, less hydrophilic angle was showed by the 4%NS biocomposite (51.4°, 78% higher than that from 0%NS), but still an angle lower than 90°, which is a characteristic of hydrophilic materials. The WPI/PVOH matrix highly interacts with water, due to the nitrogen (N) and oxygen (O) atoms of β-lactoglobulin, the major whey protein of ruminants, and also because of the high number of -OH from highly hydrolyzed PVOH (Lara et al., 2019). Certainly, at the film surface, the NS was interacting through hydrogen bonds with the protein and PVOH chains, which allowed a lower number of interactions between the water drop and the film. Besides that, the filling of free volumes by the NS at the film surface also made increase the contact angle by reducing the water penetration. In a published work, it was reported that

the addition of 4% of NS in PVOH/xylan films increased the water contact angle by 136% due to a compact structure formed between nanoparticles and polymer matrix (Liu et al., 2019). In addition, the author explains that the NS on the film surface improved the smoothness, allowing the composites to capture more air on the surface, which acts blocking the penetration of water droplets.

The surface energy of the biocomposites was decreased with the NS addition, showing a reduction of the polar interactions energy and an increase of dispersion interactions energy. These results indicate that NS was able to reduce the wettability of the WPI/PVOH film surface. The 4%NS biocomposite showed surface energy 12% lower and a polar energy 40% lower than the 0%NS. The reduction is in accordance with the water contact angle results, corroborating the hypotheses that NS was able to reduce the number of interactions between the water drop and the film, as well as to difficult the penetration of water on the surface.

Table 2 – Results of water contact angle (CA), surface energy (SE), dispersive interactions energy (DE), polar interactions energy (PE), isokinetic temperatures (T_β) and free Gibbs energies at T_β (ΔG_β) and harmonic mean temperatures (T_{hm}) for each biocomposite

Biocomposites	**CA (°)**	**SE ($N.m^{-1}$)*10^{-3}**	**DE ($N.m^{-1}$)*10^{-3}**	**PE ($N.m^{-1}$)*10^{-3}**	**T_β (K)**	**ΔG ($J.mol^{-1}$)**	**T_{hm} (K)**
0%NS	28.9±2.88a	66.5±6.60	31.4±2.01	35.1±4.59	399±8.55	-2.00	288
1%NS	28.3±2.79a	53.6±5.19	27.8±4.05	25.9±3.14	360±2.86	-1.72	288
2%NS	43.4±3.23b	57.2±6.22	29.8±2.30	27.4±2.92	358±3.79	-1.39	288
3%NS	43.7±1.73b	59.3±6.08	35.4±3.80	23.9±2.29	347±5.38	-1.38	288
4%NS	51.4±3.97c	58.2±4.42	37.1±0.75	21.0±3.68	361±4.83	-0.95	288

At vertical columns, different letters represent significantly different values at ($p \geq 0.05$) using the Scott-Knott test.

3.4 Water sorption isotherms

Table 3 presents the results from models fitting to the experimental water sorption isotherm data for all the biocomposites under 5 °C, 15 °C, and 25 °C. GAB model was able to describe the moisture equilibrium data for all three different temperatures, confirmed by the high values for R^2 and low values of RMD. The GAB model was already used to well describe the sorption behavior of WPI films and WPI/PVOH blends by other authors (Azevedo et al., 2015; Lara et al., 2020). Besides that, all residual values tended to zero considering the GAB adjust performed, not including biased results. It corroborates the adequacy of the GAB model to adjust the water sorption experimental data from WPI/PVOH/NS biocomposites.

Table 3 - Calculated parameters for the isotherm GAB model for WPI/PVOH/NS biocomposites under 5 °C, 15 °C and 25 °C.

Isotherm temperature	**Biocomposites**	**Constants of linear fitting**			**R^2**	**RMD**
		Y_m $(g.100g^{-1})$	C	K		
5 °C	0%NS	20.36	0.36	0.88	1.00	8.21
	1%NS	20.94	0.33	0.88	1.00	9.22
	2%NS	21.82	0.29	0.88	1.00	8.95
	3%NS	14.51	0.55	0.90	1.00	7.75
	4%NS	21.06	0.40	0.87	1.00	9.44
15 °C	0%NS	10.64	0.96	0.93	1.00	7.27
	1%NS	6.93	2.02	0.95	0.99	7.81
	2%NS	12.80	0.77	0.91	1.00	5.22
	3%NS	9.88	1.00	0.93	1.00	6.74
	4%NS	13.35	0.72	0.91	1.00	9.63
25 °C	0%NS	10.98	0.48	0.97	1.00	9.15
	1%NS	11.77	0.41	0.96	1.00	9.35
	2%NS	11.63	0.48	0.96	1.00	8.58
	3%NS	10.71	0.58	0.96	1.00	6.05
	4%NS	9.47	0.62	0.97	1.00	7.97

Fig. 1 shows the water sorption isotherms under the three different tested temperatures, in which all the biocomposites presented a sigmoid type III isotherm format at 25 °C, 15 °C, and 25 °C according to the Brunauer's classification and observing values of K and C ($0 < K \leq 1$, $0 < C \leq 2$) of GAB model (Brunauer, Emmett, & Teller, 1938). This format refers to products with high protein content, which is the case of the biocomposites tested, with 70% of WPI (Brunauer et al., 1938; Echavarria et al., 2021).

The presence of NS did not influence the format of the isotherm or even the moisture content at the WPI/PVOH matrix. This result is in agreement with the similar solubility coefficient values found for all treatments. All the biocomposites, at all tested temperatures, presented a more expressive increase of water sorption above aw = 0.75. Similar behavior of slope increase of the isotherm curve above 0.75 of aw has been reported for WPI/PVOH blends with up to 30% of PVOH, for chitosan films, as well as blends of chitosan and PVOH (Aguirre-Loredo, Rodriguez-Hernandez, & Velazquez, 2017; Lara et al., 2020; Srinivasa, Ramesh, Kumar, & Tharanathan, 2003).

At higher water activity values, there is a larger amount of free water available to take part in chemical and physical reactions, and specifically above 0.70 of a_w, occurs condensation of water in the pores of the material followed by a dissolution of the material (Ghayal et al., 2013; Sandulachi, 2012). Thus, as the water content increases in higher aw values, water molecules can cause structural changes as plasticizing and swelling effect (Huntrakul & Harnkarnsujarit, 2020; Schmid, Reichert, Hammann, & Stäbler, 2015). These effects increase free volume among the biomacromolecules and facilitate the water entrance, which leads to higher amounts of sorbed water. Besides that, the sorption is directly affected by pressure because of the considerable interaction between the permeant and the polymers chains (water and proteins/PVOH chains) (Robertson, 2013). Since higher water activities mean higher water vapor pressure, in aw above 0.75, water sorption is higher not just because of the mentioned plasticizing effect caused by water molecules, but also due to the higher vapor pressure (Lara et al., 2020). Therefore, for the WPI/PVOH/NS biocomposite application as food packaging, is desirable a food, as well as an external environment, with aw below 0.75, due to the more stable bonds between the biocomposite and the water molecules, which allows better film stability. This WPI/PVOH/NS packaging would be suitable for storage of pasta, dry vegetables, and fruits, cereals, some candies, honey, and jams, for example, which have aw below 0.75 (Jay, Loessner, & Golden, 2006).

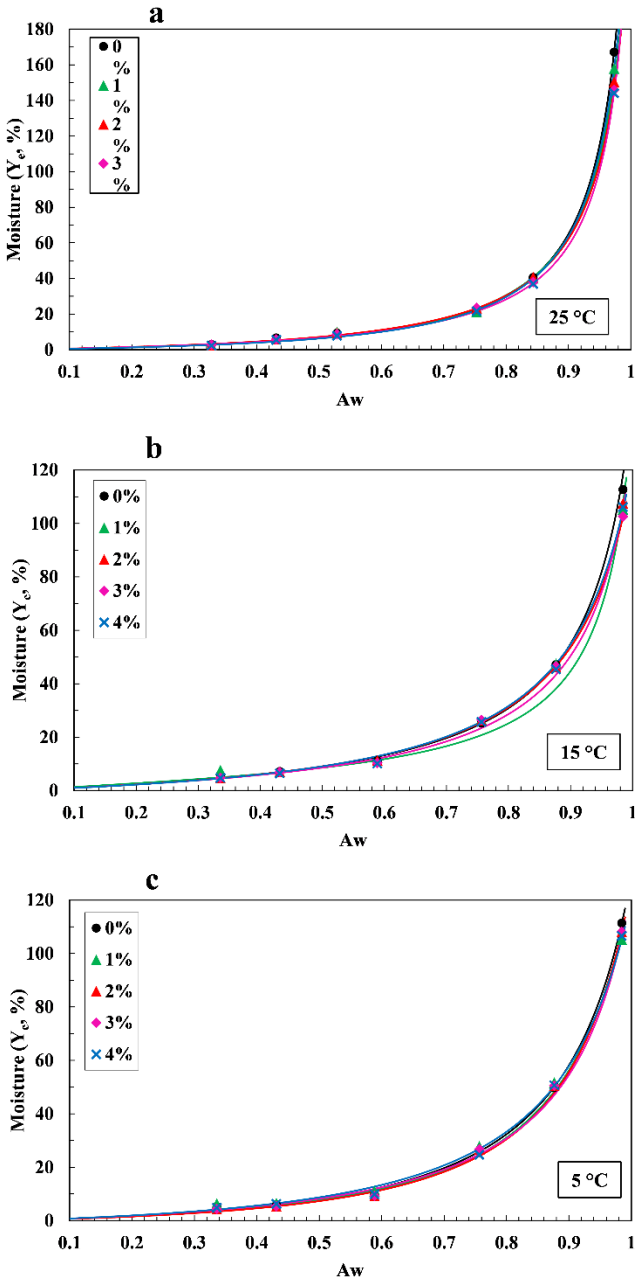

Figure 4 - Water sorption isotherms (% Moisture – g water.100g^{-1} film versus a_w) of WPI/PVOH/NS biocomposites under (a) 25 °C, (b) 15 °C and (c) 5 °C, adjusted through the GAB model.

Fig. 2 exposes the water sorption behavior of each biocomposite adjusted through GAB model, separately, now according to the different temperatures tested. All the biocomposites, above 0.9 of aw, presented the highest values of equilibrium moistures at 25 °C, the highest temperature tested. In fact, at higher temperatures, the excitation of water molecules decreases the interaction between themselves and them and the polymer, therefore decreasing the water sorption (Ramos, Mancini, & Mendes, 2015). However, a temperature of 25 °C is above or close to the biocomposites glass transition temperatures

(Tg). In previous work, the 0%NS, 1%NS, 2%NS, 3%NS, and 4%NS biocomposites showed Tg values of, respectively, 19 °C, 18 °C, 18 °C, 21 °C and 26 °C (Lara et al., 2021). With a temperature close to or above Tg, as at 25 °C, the WPI/PVOH macromolecules certainly had more mobility than at 5 °C or 15 °C, allowing more water filling and clustering into the biocomposite matrix and, therefore, presenting higher Y_e values (Echavarria et al., 2021). This results can indicate that the biocomposites tested are more suitable for application in chilled environments, where the packaging will be less subjected to water condensation at the film surface, or even to the swelling and plasticizing effect which can affect the film stability.

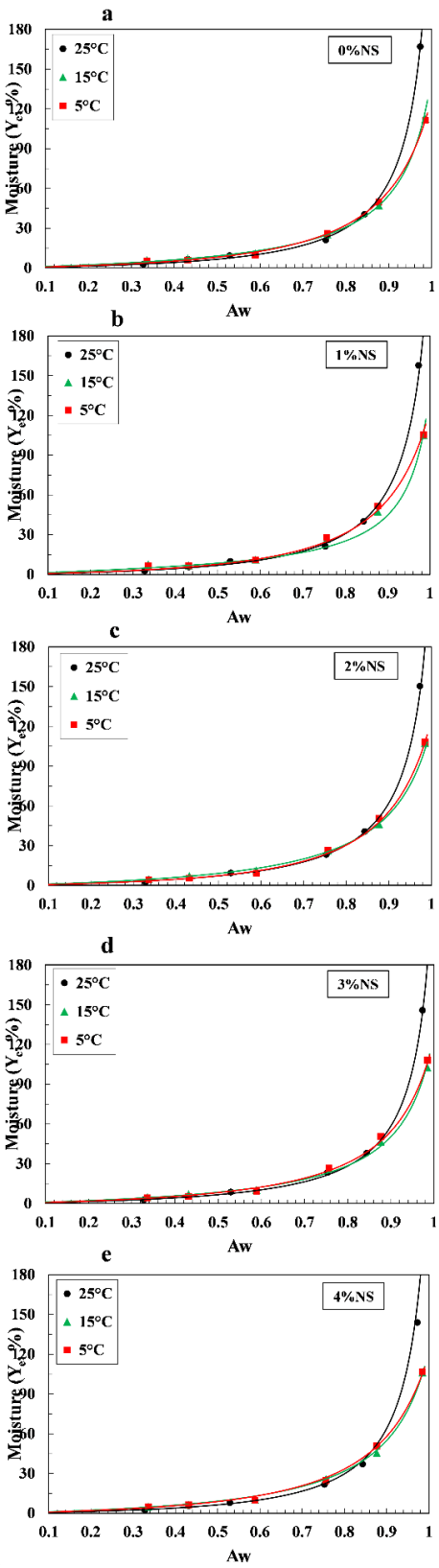

Figure 2 - Water sorption isotherms (% Moisture – g water.100g^{-1} film versus a_w) of (a) 0%NS, (b) 1%NS, (c) 2%NS, (d) 3%NS and (e) 4%NS under 5 °C, 15 °C and 25 °C, adjusted through GAB model.

3.4.1 Enthalpy-entropy compensation and ΔGβ

All the biocomposites showed a linear relation between differential enthalpy and differential entropy, with great coefficients of determination (R^2) varying from 0.97 to 1.00, as showed in Fig. 3. It indicates the occurrence of enthalpy-entropy compensation for all films, and allows the determination of the isokinetic temperatures (T_β) and free Gibbs energies at Tβ (ΔG_β) the adjusted lines of the ΔS_{dif} versus ΔH_{dif} graph. These variables, as well as the harmonic mean temperatures (T_{hm}) calculated are presented in Table 2.

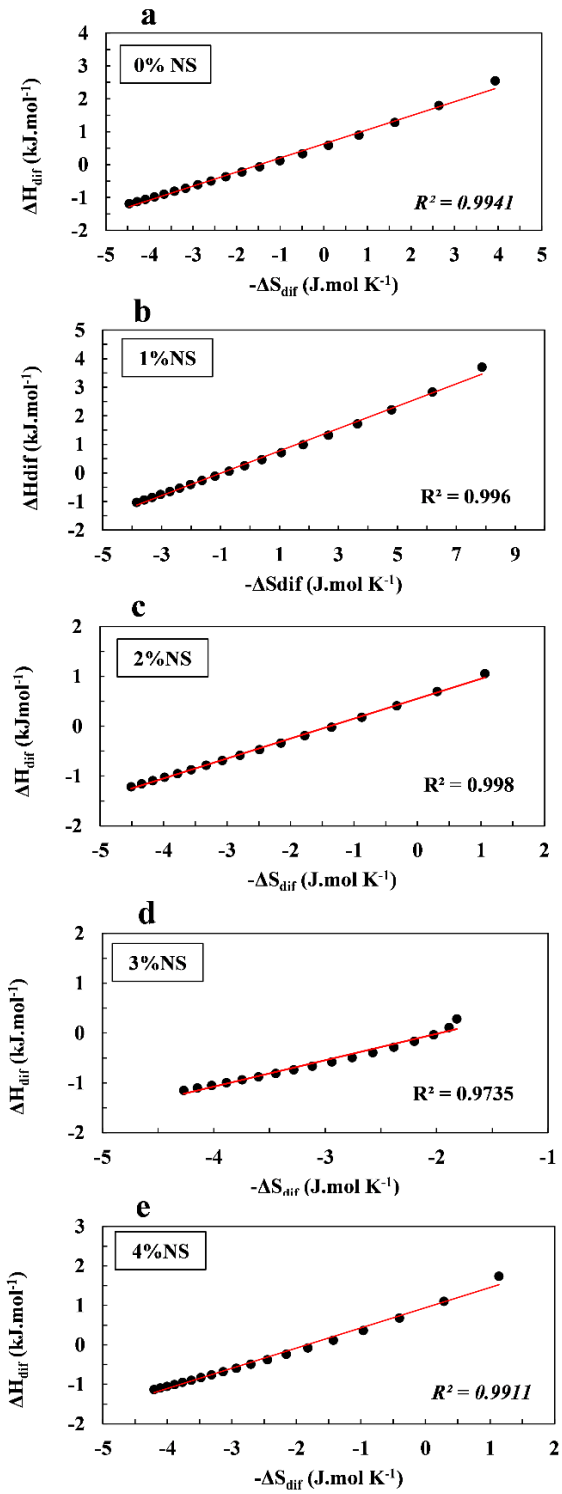

Figure 3 - Linear relation between differential enthalpy and differential entropy found for (a) 0%NS, (b) 1%NS, (c) 2%NS, (d) 3%NS and (e) 4%NS biocomposites.

The T_β values were different from the T_{hm} values for all the biocomposites, assuring the of enthalpy-entropy compensation occurrence, as predicted by the linear relation between these parameters,

and indicating that during the sorption process changes occurred in molecular interaction between water and the films. Besides that, enthalpy controlled the water sorption, since all films presented Tβ > Thm, indicating that energy interactions related to the material components (WPI/PVOH, NS, CA) are more influential than the number of available sorption sites for all biocomposites (Telis, Gabas, Menegalli, & Telis-Romero, 2000).

All the biocomposites presented a negative ΔG_β, indicating that water is spontaneously adsorbed to them, independently of the NS content. 0%NS showed the most spontaneous sorption process, with a ΔG_β of −2.00 J.mol^{-1}. With the NS increment, sorption became less spontaneous, being the 4%NS the biocomposite that presented the highest value of ΔG_β (−0.95 J.mol^{-1}). These results indicate that NS was able to reduce the tendency of the biocomposites surfaces to adsorb water molecules, which is desirable to maintain the integrity of the packaging material during food application.

4 CONCLUSION

The addition of 4% of NS to WPI/PVOH matrix was able to reduce the diffusion of water by 58%, which is desirable in most food packaging. Solubility coefficient values were not significantly different ($p \geq 0.05$) for all the biocomposites evaluated, meaning that NS has influenced the speed of water molecules moving through the polymer matrix, making it slower, but did not change the number of water molecules in the biocomposites matrix. The filling of free volumes by the NS at the biocomposites surface reduced both wettability and surface energy. GAB model was able to describe the water sorption experimental data, and all the biocomposites showed a more expressive increase of water sorption above a_w = 0.75 and higher equilibrium moistures at higher temperatures. For all the biocomposites enthalpy-entropy compensation was confirmed and energy interactions related to the composition were more influential in the sorption process than the number of available sorption sites. The hydrophilicity of the biocomposites was evidenced in thermodynamic sorption behavior, but the addition of NS to the WPI/PVOH matrix was able to make the water sorption process less spontaneous. Finally, the addition of 4% of NS in WPI/PVOH films is justified to produce biocomposite packaging with a less spontaneous water sorption behavior, suitable for application with foods and chilled environments with until 0.75 of a_w.

Acknowledgments

This work was financed by the Coordenação de Aperfeiçoamento de Pessoal de Nível Superior – Brasil (CAPES) (Finance Code 001), the Conselho Nacional de Desenvolvimento Científico e Tecnológico – Brasil (CNPq) and the Fundação de Amparo à Pesquisa do Estado de Minas Gerais –

Brasil (FAPEMIG). The authors extend their appreciation for all support provided by the Universidade Federal de Lavras - (UFLA).

REFERENCES

Aguirre-Loredo, R. Y., Rodriguez-Hernandez, A. I., & Velazquez, G. (2017). Modelling the effect of temperature on the water sorption isotherms of chitosan films. *Food Science and Technology*, *37*(1), 112–118. https://doi.org/10.1590/1678-457X.09416

Alfrey, T., Gurnee, E. F., & Lloyd, W. G. (1966). Diffusion in glassy polymers. *Journal of Polymer Science Part C: Polymer Symposia*, *12*(1), 249–261. https://doi.org/10.1002/polc.5070120119

Andrade, R., Skurtys, O., Osorio, F., Zuluaga, R., Gañán, P., & Castro, C. (2014). Wettability of gelatin coating formulations containing cellulose nanofibers on banana and eggplant epicarps. *LWT - Food Science and Technology*, *58*(1), 158–165. https://doi.org/10.1016/j.lwt.2014.02.034

ASTM D7334-08. (2013). Standard Practice for Surface Wettability of Coatings , Substrates and Pigments by Advancing Contact Angle Measurement. *Annual Book of ASTM Standards*. West Conshohocken, PA: ASTM International. https://doi.org/10.1520/D7334-08R13

Azevedo, V. M., Silva, E. K., Pereira, C. F. G., da Costa, J. M. G., & Borges, S. V. (2015). Whey protein isolate biodegradable films: Influence of the citric acid and montmorillonite clay nanoparticles on the physical properties. *Food Hydrocolloids*, *43*, 252–258. https://doi.org/10.1016/j.foodhyd.2014.05.027

Brunauer, S., Emmett, P. H., & Teller, E. (1938). Adsorption of Gases in Multimolecular Layers. *Journal of the American Chemical Society*, *60*(2), 309–319. https://doi.org/10.1021/ja01269a023

Crank, J. (1975). *The Mathematics of Diffusion* (2nd ed.). Clarendon Press.

Echavarria, J. A. C., Torres, A. M. R., & Montoya, J. E. Z. (2021). Sorption isotherms and thermodynamic properties of the dry silage of red tilapia viscera (Oreochromis spp .) obtained in a direct solar dryer. *Heliyon*, *7*(February).

Ghayal, G., Jha, A., Sahu, J. K., Kumar, A., Gautam, A., Kumar, R., & Rasane, P. (2013). Moisture sorption isotherms of dietetic Rabri at different storage temperatures. *International Journal of Dairy Technology*, *66*(4), 587–594. https://doi.org/10.1111/1471-0307.12083

Huntrakul, K., & Harnkarnsujarit, N. (2020). Effects of plasticizers on water sorption and aging stability of whey protein/ carboxy methyl cellulose films. *Journal of Food Engineering*, *272*, 109809. https://doi.org/10.1016/j.jfoodeng.2019.109809

Jagadish, R. S., & Raj, B. (2011). Properties and sorption studies of polyethylene oxideestarch blended films. *Food Hydrocolloids*, *25*, 1572–1580. https://doi.org/10.1016/j.foodhyd.2011.01.009

Jakubczyk, E., Marzec, A., & Lewicki, P. P. (2008). Relationship Between Water Activity of Crisp Bread and Its Mechanical Properties and Structure. *Polish Journal of Food and Nutrition Sciences*, *58*(1), 45–51.

Janjarasskul, T., & Tananuwong, K. (2019). Role of Whey Proteins in Food Packaging. *Reference Module in Food Sciences*. https://doi.org/10.1016/B978-0-08-100596-5.22399-8

Jay, M. J., Loessner, M. J., & Golden, D. A. (2006). *Modern food microbiology* (7th ed.). New York.

Jiménez, A., Fabra, M. J., Talens, P., & Chiralt, A. (2013). Phase transitions in starch based films containing fatty acids. Effect on water sorption and mechanical behaviour. *Food Hydrocolloids*, *30*, 408–418. https://doi.org/10.1016/j.foodhyd.2012.07.007

L′vov, B. V. (2007). *Thermal decomposition of solids and melts : new thermochemical approach to the mechanism, kinetics, and methodology*. Springer, Dordrecht. https://doi.org/https://doi.org/10.1007/978-1-4020-5672-7

Lara, B. R. B., Araújo, A. C. M. A., Dias, M. V., Guimarães, M., Santos, T. A., Ferreira, L. F., & Borges, S. V. (2019). Morphological, mechanical and physical properties of new whey protein isolate/ polyvinyl alcohol blends for food flexible packaging. *Food Packaging and Shelf Life*, *19*, 16–23. https://doi.org/10.1016/j.fpsl.2018.11.010

Lara, B. R. B., de Andrade, P. S., Guimarães Junior, M., Dias, M. V., & Alcântara, L. A. P. (2021). Novel Whey Protein Isolate/Polyvinyl Biocomposite for Packaging: Improvement of Mechanical and Water Barrier Properties by Incorporation of Nano-silica. *Journal of Polymers and the Environment*, *29*(8), 2397–2408. https://doi.org/10.1007/s10924-020-02033-x

Lara, B. R. B., Dias, M. V., Guimarães Junior, M., de Andrade, P. S., de Souza Nascimento, B., Ferreira, L. F., & Yoshida, M. I. (2020). Water sorption thermodynamic behavior of whey protein isolate/ polyvinyl alcohol blends for food packaging. *Food Hydrocolloids*, *103*(January). https://doi.org/10.1016/j.foodhyd.2020.105710

Liu, X., Chen, X., Ren, J., Chang, M., He, B., & Zhang, C. (2019). Effects of nano-ZnO and nano-SiO 2 particles on properties of PVA/xylan composite films. *International Journal of Biological Macromolecules*, *132*, 978–986. https://doi.org/10.1016/j.ijbiomac.2019.03.088

OWENS, D. K., & WENDT, R. C. (1969). Estimation of the Surface Free Energy of Polymers. *Journal Application of Polymers Science*, *13*, 1741–1747. https://doi.org/https://doi.org/10.1002/app.1969.070130815

Pitt, J. I., & Hocking, A. D. (2009). *Fungi and Food Spoilage* (3rd ed.). Springer US. https://doi.org/10.1007/978-0-387-92207-2

Ramos, B. A., Mancini, M. C., & Mendes, M. F. (2015). ISOTERMAS DE SORÇÃO E PROPRIEDADES TERMODINÂMICAS DO PINHÃO- MANSO (Jatropha curcas) MOISTURE SORPTION ISOTHERMS AND THERMODYNAMIC PROPERTIES OF JATROPHA (Jatropha curcas). *Revista Brasileira de Produtos Agroindustriais. Campina Grande.*, *17*(4), 371–380.

Robertson, G. L. (2013). *Food Packaging Principles and Practice*. *CRC Press* (3rd ed.). Boca Raton: CRC Press.

Sandulachi, E. (2012). Water Activity Concept and Its Role in Food Preservation. *Water Activity Concept and Its Role in Food Preservation*, 40–48.

Schmid, M., Reichert, K., Hammann, F., & Stäbler, A. (2015). Storage time-dependent alteration of molecular interaction–property relationships of whey protein isolate-based films and coatings. *Journal of Materials Science*, *50*(12), 4396–4404. https://doi.org/10.1007/s10853-015-8994-0

Sharma, P. K. (2001). *Surface studies relevant to microbial adhesion and bioflotation of sulphide minerals*. Luleå University of Technology.

Srinivasa, P. C., Ramesh, M. N., Kumar, K. R., & Tharanathan, R. N. (2003). Properties and sorption studies of chitosan – polyvinyl alcohol blend films. *Carbohydrate Polymers*, *53*, 431–438. https://doi.org/10.1016/S0144-8617(03)00105-X

Tao, Y., Wu, Y., Yang, J., Jiang, N., Wang, Q., Chu, D. T., … Zhou, J. (2018). Thermodynamic sorption properties, water plasticizing effect and particle characteristics of blueberry powders produced from juices, fruits and pomaces. *Powder Technology*, *323*, 208–218. https://doi.org/10.1016/j.powtec.2017.09.033

Telis, V. R. N., Gabas, A. L., Menegalli, F. C., & Telis-Romero, J. (2000). Water sorption thermodynamic properties applied to persimmon skin and pulp. *Thermochimica Acta*, *343*(1–2), 49–56.

Velázquez-gutiérrez, S., Figueira, A. C., Rodríguez-huezo, M. E., Roman-guerrero, A., Carrillo-Navas, H., & Pérez-Alonso, C. (2015). Sorption isotherms , thermodynamic properties and glass transition temperature of mucilage extracted from chia seeds (Salvia hispanica L .) temperature of mucilage extracted from chia seeds (Salvia hispanica L .). *Carbohydrate Polymers*, *121*(May), 411–419. https://doi.org/10.1016/j.carbpol.2014.11.068

Wiacek, A. E. (2015). Effect of surface modification on starch biopolymer wettability. *Food Hydrocolloids*, *48*, 228–237. https://doi.org/10.1016/j.foodhyd.2015.02.005

Yang, C., Xing, X., Li, Z., & Zhang, S. (2020). A Comprehensive Review on Water Diffusion in Polymers Focusing on the Polymer. *Polymers*, *12*(1).

ARTIGO 3

(Formatação Segundo a revista Journal of Polymers and the Environment – ISSN: 1566-2543)

HIGH TENSILE RESISTANT AND FLEXIBLE BILAYER BIOCOMPOSITES OF POLYVINYL ALCOHOL, WHEY PROTEIN ISOLATE, AND NANO-SILICA TREATED WITH CORONA DISCHARGE

Bruna Rage Baldone Lara[a*], Paulo Sérgio de Andrade[a], Mario Guimarães Junior[b], Lays Camila Matos[c], Gustavo Henrique Denzin Tonoli[c], Marali Vilela Dias[a]

[a] Federal University of Lavras - UFLA / Department of Food Science, University Campus - PO Box: 3037 - CEP: 37200-000, Lavras - MG, Brazil.

[b] Federal Center of Technological Education of Minas Gerais – CEFET-MG / Department of Electromechanics – CEP 38180-510, Araxá - MG, Brazil.

[c] Federal University of Lavras - UFLA / Department of Forest Science, University Campus - PO Box: 3037 - CEP: 37200-000, Lavras - MG, Brazil.

*Corresponding author. E-mail: brunabaldone@hotmail.com; Phone: +55 35 38322321; Mailing address: Federal University of Lavras – UFLA, University Campus - PO Box: 3037 - CEP: 37200-000, Lavras - MG, Brazil.

Running head:

HIGH TENSILE RESISTANT AND FLEXIBLE BILAYER BIOCOMPOSITES OF PVOH/WPI/NS TREATED WITH CORONA

Graphical Abstract:

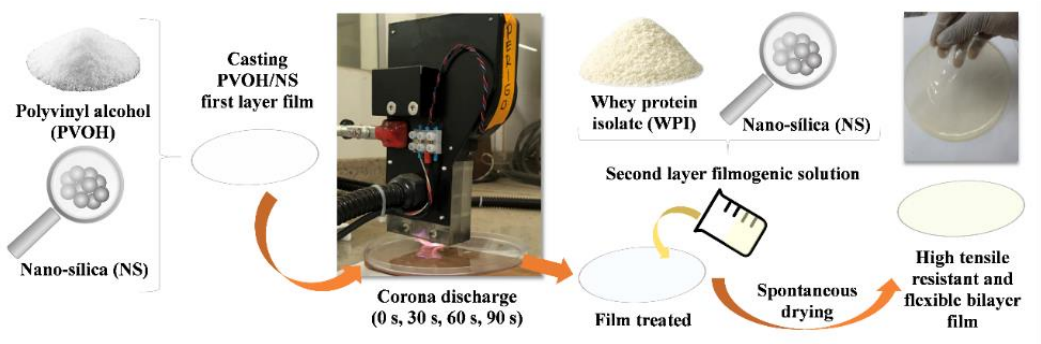

Abstract

In order to evaluate the influence of a different assembly of biocomposites of polyvinyl alcohol (PVOH), whey protein isolate (WPI), and nano-silica (NS), a new bilayer film treated with corona discharge was produced through a two-step lamination casting method. With the first layer of PVOH/NS, treated with up to 90 s of discharge, and the second layer of WPI/NS, the bilayer films had their morphology, tensile strength, and water barrier investigated and compared to a single layer PVOH/WPI/NS film. Corona discharge increased the wettability of the first layer improving the ability of the PVOH/NS surface to interact with the second layer of WPI/NS, thus increasing the adherence between these layers. Bilayer films treated with higher times of discharge showed an extremely homogeneous transition between phases, suggesting compatibility and adherence between layers provided by the treatment. At 90 s of corona discharge treatment, bilayer films showed a tensile strength 72% higher than the bilayer film not treated and also was 23% more resistant and 7.4 times more ductile than the single-layer film. The lamination process and corona treatment increase the affinity of the water with the film constituents, thus leading to a higher permeability. Finally, the use of corona discharge associated with the lamination of PVOH/WPI/NS biocomposites providing a bilayer film is justified to produce a more resistant, flexible and ductile biocomposite film for packaging.

Keywords: Bilayer packaging film; Polyvinyl alcohol; Whey protein isolate; Nano-silica; Corona discharge; Bicomposite.

1 INTRODUCTION

One of the biggest markets of plastics is that of packaging which is projected to grow at a compound annual growth rate of 4.2% from 2021 to 2026, being polyethylene and polypropylene the major raw materials used for the packaging applications [1, 2]. The high interest in biodegradable films as an alternative to these non-biodegradable petroleum-based film packaging is confirmed by the compound annual growth rate of 17.1% expected for the market of bioplastics from 2021 to 2028 [3]. In this context, more researches related to the use of renewable proteins as biopolymers in the food packaging sector has been performed [4].

Whey protein isolate (WPI) films have desirable film-forming and excellent gas barrier properties when compared to petroleum-based synthetic films, but presents low tensile strength and intrinsic stiffness [5]. Among the numerous methods proposed to overcome these inherent shortcomings of WPI films is possible to cite: blending with other biodegradable polymers, coating, lamination, plasticization, nanomaterials adding and cross-linking, for example. In previous works, it was proved that the addition of polyvinyl alcohol (PVOH) and colloidal nano-silica (NS) to the WPI matrix was effective in improving flexibility, strongly reducing stiffness, and also increasing the tensile strength of

the WPI matrix [4, 6]. In order to improve even more these tensile mechanical properties, a new assembly of the WPI/PVOH/NS biocomposite is proposed in this work.

One still poorly explored way to manipulate properties of the components is developing bilayer films [7]. With this different assembly, guarantying good adherence between layers, a bilayer film can achieve different properties of those from the single-layer film composed of the same raw materials. This adherence can be provided, for example, by a corona discharge treatment, which is a low cost and sustainable surface modification technology frequently used by the packaging industry able to increase surface energy and polarity of films, thus improving wettability and adhesion properties [8, 9].

In this study, a novel-designed bilayer film was developed through a two-step lamination casting method, with the first layer of PVOH/NS treated by 0 to 90 s of corona discharge and the second layer of WPI/NS. A film control of PVOH/WPI/NS with a single layer was also produced seeking to evaluate the effect of corona discharge and lamination in the tensile and water barrier properties of the biocomposites evaluated by tensile, permeability, and diffusion tests. The first layer was characterized with water contact angle, surface energy, and FT-IR analysis in order to understand changes provided by the different times of corona discharge. The morphology of the joining region between layers was evaluated through SEM micrographs. This study provides a worthwhile way for designing a novel bilayer PVOH/WPI/NS biocomposite with desired tensile properties.

2 MATERIAL AND METHODS

2.1 Material

Polyvinyl alcohol with high molecular weight (Mw = 130.000 $g.mol^{-1}$) and highly hydrolyzed (99%), from Sigma-Aldrich; whey protein isolate (WPI 9400) with 90% of proteins, from Hilmar Ingredients; glutaraldehyde solution (25% in H_2O), as PVOH crosslinking agent, from Sigma-Aldrich [10, 11]; glycerol (≥ 99.5%, density 1.26 $g.mL^{-1}$), as a plasticizing agent, produced by Sigma-Aldrich; granulated anhydrous citric acid from Cargill Agrícola S.A was used to guarantee a good distribution of NS [4]; and NS from colloidal solution Bindzil 2034DI (Akzo Nobel), with 34% in weight of NS (average particle size of 15 nm and200 m^2g^{-1} of surface area).

2.2 Experimental design and preparation of the biocomposites

This research was performed in two phases: a first one with the production of the first layer film of PVOH/NS, applying different periods of corona discharge (0s, 30s, 60s, 90s) and evaluating the first layer exactly after the discharge through water contact angle, surface energy, and Fourier transform infrared (FT-IR) analysis; and a second phase, with the production of the bilayer films (the first layer of PVOH/NS treated with the cited different periods of corona and the second layer of WPI/NS applied right after the discharge), which were analyzed through Scanning Electron Microscopy (SEM), tensile, and water barrier tests. The scheme shown in Figure 1 explains clearly the experimental design.

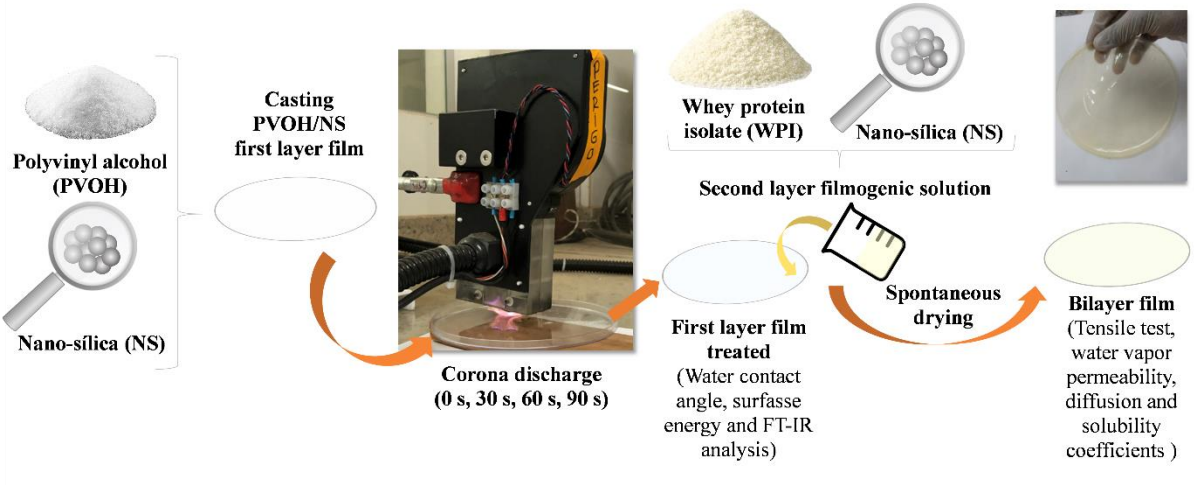

Figure 1 – Experimental design of preparation and tests of the biocomposites.

2.2.1 Bilayer biocomposites

2.2.1.1 Crosslinked PVOH/NS - First layer

The PVOH solution was prepared using a polymer concentration of 6% m.v^{-1}, and adding 30% of glycerol (m.m^{-1} of polymer), and 8% of citric acid (m/m of polymer). The solution was agitated for 30 min (250 rpm) and conducted to a water bath at 90°C for 1h until complete PVOH solubilization. After cooled at room temperature, nano-silica, NS, (Bindzil 2034DI) was added to the solution in 4% m/m of polymer. The final solution was homogenized in Ultra Turrax (Kika Labortchnik) for 20 min (450 rpm) and after sonified (Sonifier Cell Disruptor Branson – Model 450D, Manchester, UK) using a probe with 100 mm of diameter, at 60% of amplitude (270 W), for 10 min (600 s) in a continuous assay, using an ice bath to avoid heating, resulting in ultrasonic energy applied of 810 J.mL^{-1}. The sonicated solution was then crosslinked by adding 5% (m.m^{-1} of polymer) of glutaraldehyde and agitated for 15 min at 250 rpm. Final solutions were shed on circular acrylic plates (707 cm²), perfectly leveled, and conditioned at room temperature (25 °C) for spontaneous drying (48 h). The dried films were conditioned under controlled temperature and relative humidity (RH) (25±1 ºC and 50% RH) for 48h before corona treatment.

PVOH crosslinked with glutaraldehyde was chosen as the first layer since, in previous tests, WPI or PVOH not crosslinked films as first layers were not water-resistant enough to receive the second layer solution, solubilizing as showed in Figure 2.a and b.

Samples of the first layer films (of PVOH and nano-silica, crosslinked with glutataldehyde) were then submitted to the corona discharge, using a Corona Brasil equipment, (model PT) with a power of 0.5 kW, a discharge of 10 kV, an intensity of 60 μA, a frequency of 60 Hz, and an air-gap between the electrode and the sample film set at 15 mm. Four different treatments were produced varying the

period of corona discharge: 0 s, 30 s, 60 s and 90 s, corresponding, respectively, to the 0S, 30S, 60S, and 90S treatments. Three replicates of each treatment were performed.

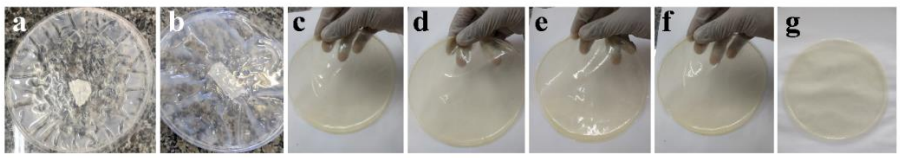

Figure 2 – Photo of tests and biocomposite films produced: (a) test with WPI solution as first layer and PVOH as second layer; (b) test with PVOH not crosslinked as first layer and WPI as second layer; (c) B0S; (d) B30S; (e) B60S; (f) B90S; (g) UNL.

2.2.1.2 WPI/NS - Second layer

WPI solution was prepared using a concentration of 6% m/v, added with glycerol (30% m/m of WPI), citric acid (8% m/m of WPI), and kept under agitation for 30 min (250 rpm) at room temperature (25 °C). The solution had the pH adjusted to 8 using a NaOH solution (3 M) and was then submitted to a water bath at 90 °C for 30 min to guarantee protein denaturation [12]. After cooled at room temperature, nano-silica, NS, (Bindzil 2034DI) was added at 4% m/m of polymer, and the solution was homogenized in Ultra Turrax (Kika Labortchnik) for 20 min (450 rpm) and after sonified (Sonifier Cell Disruptor Branson – Model 450D, Manchester, UK) using a probe with 100 mm of diameter, at 60% of amplitude (270 W), for 10 min (600 s) in a continuous assay, using an ice bath to avoid heating, resulting in ultrasonic energy applied of 810 $J.mL^{-1}$.

Final solutions were shed on top of the first layer films of PVOH and nano-silica and conditioned at room temperature (25 °C) for spontaneous drying (48 h). The dried bilayer biocomposites treated with corona discharge at 0 s, 30 s, 60 s, and 90 s were, respectively named as B0S, B30S, B60S and B90S, and conditioned under controlled temperature and relative humidity (RH) (25±1 ºC and 50 % RH ±2 %) for 48h before characterization. Photos of the bilayer films produced are exposed in Figure 2.(c – f).

2.2.2 Unlaminated film

The unlaminated biocomposite film (UNL), with a single layer, where prepared following the same procedures from [4]. WPI and PVOH solutions were separately prepared using a polymer concentration of 6% $m.v^{-1}$, and adding 30% of glycerol ($m.m^{-1}$ of polymer), and 8% of citric acid (m/m of polymer). Both solutions where agitated (30 min, 250 rpm, at room temperature of 25 °C) and conducted to water bath at 90°C (WPI solution for 30 min and PVOH solution for 60 min of bath). WPI and PVOH solutions were merged in a volumetric proportion 70/30 and, after cooled at room temperature, nano-silica (Bindzil 2034DI) was added in 4% m/m of polymer. This 70\30 volume ratio was used here since, in a previous work that evaluated blends of WPI and PVOH, those with 70% of WPI and 30% of PVOH produced the best tensile properties. Thus, this formulation was chosen as the

unlaminated control film to evaluate if the lamination and corona treatment is worth it to improve tensile properties. The final solution was homogenized in Ultra Turrax and after sonified under the same conditions that those from first and second layer of the bilayer films. Final solutions were shed on circular acrylic plates (707 cm²), perfectly leveled, and conditioned at room temperature (25 °C) for spontaneous drying (48 h). Three replicates were performed. The dried unlaminated biocomposites were conditioned under controlled temperature and relative humidity (RH) (25±1 ºC and RH ±2 %) for 48h before characterization. A photo of the unlaminated film produced are exposed in Figure 2.g.

2.3 Characterization of the biocomposites

2.3.1 First layer characterization

Exactly after the corona discharge, the film solution of the second layer (WPI and nano-silica) was shed on top of the first layers treated. Besides that, in a maximum time of 20 minutes after the corona discharge, samples of each treatment (0S, 30S, 60S, and 90S) were submitted to FT-IR, contact angle, and surface energy analysis to understand the surface modifications caused by the discharge.

2.3.1.1 Determination of the water contact angle and surface energy

The water contact angle measurement was performed to understand the modifications caused by the different times of corona discharge at the first layer film surface wettability. For this purpose, it was used the sessile drop method and a Goniometer (KRUSS, Drop Shape Analyzer-DSA25) in which, through a syringe, a drop of the standard liquid was applied on the surface to be characterized [13–19]. The static angle between the drop and the biocomposites surface was calculated through the slope of the tangent. The average of the left and right angles was obtained as the final value of the contact angle.

The contact angle analysis was performed by fixing biocomposite samples on glass slides and attaching them to the equipment. A drop of the liquid was placed on the biocomposite surface and the goniometer carried out 10 angle measurements per second for 2 seconds [20]. To determine the wettability, distilled water was used, while for surface energy, besides the distilled water, ethylene glycol and methane diode were used as well. Images of the drop at the film surface for each treatment were also captured by the equipment, and the average angle was indicated.

The dispersion of surface energy was calculated following the procedure described by Owens-Wendt (OWRK), considered as universal for the calculation of surface energy [21]. The existing relationship for surface energy was extended and the hydrogen bonds added in the non-dispersive component, renamed to the polar component (p) (Equation 1) [22]. It was assumed that the interaction between two materials is also a function of polar components and is described through a geometric mean, where only forces of the same nature interact (Equation 2) [22].

$$\gamma_i^T = \gamma_i^d + \gamma_i^p \quad (1)$$

$$\gamma_{i/j} = \gamma_i + \gamma_j - 2\left(\sqrt{\gamma_i^d + \gamma_j^d} + \sqrt{\gamma_i^p + \gamma_j^p}\right) \quad (2)$$

Where: γ is superficial free energy; γ^T is total surface free energy; *d* are the dispersive interactions and *p* is the polar component.

2.3.1.2 Fourier transform infrared (FT-IR) analysis

To understand the effects of the corona discharge at the surface, the first layer film samples were characterized by absorption spectroscopy on the region of infrared through an FTS 3000 Excalibur Digilab (United States), in Total Attenuated Reflection (ATR) mode, equipped with a KBr detector. The analysis range was from 4000 to 400 cm^{-1} with 64 scans.

2.3.2 Bilayer and unlaminated biocomposites characterization

2.3.2.1 Scanning Electron Microscopy (SEM)

SEM micrographs were obtained to evaluate the biocomposites morphology at the joining region of the two layers, looking for flaws, phase separation or any other effect which could be related to the mechanical and water barrier results. The analysis was conducted on a LEO 1430 VP (England) with an accelerating voltage of 20 kV, obtaining microscopies with 1000X of magnification. To observe the morphology at the cross-section, the specimens were previously frozen in liquid nitrogen and fractured, and then gold (Au)-coated using vapor deposition.

2.3.2.2 Tensile Properties

Tensile test was performed to verify the influence of lamination and corona discharge on strength, flexibility, ductility of the biocomposites when submitted to stretching stress. The maximum tensile strength (TS), the tensile modulus (TM) and the maximum elongation (E) of the biocomposites were measured according to ASTM D882-02 (2002), using a texturometer (Stable Microsystems, model TATX2i, England) with a load cell of 1 kN and a speed of 10 $mm.s^{-1}$. Specimens of 5 mm of width and 100 mm of length were tested at 23 ± 1 °C. TM was calculated through the tangent of the initial linear function of the stress-strain curve, which was considered as an elastic behavior. By dividing the maximum tensile by the film transversal section area and through the percentage relation between the final and initial length of the specimen, respectively, TS and E were obtained. Five repetitions were used for each replicate of the five different biocomposites. Thickness (mm) was measured using a digital micrometer (Digimess) with a resolution of 0.001 mm, taking five random measurements per specimen.

2.3.2.3 Water Vapor Permeability coefficient

Water vapor permeability coefficient (P) was determined by the gravimetric method, following the ASTM E96/E96M-10 (2010) and using circular specimens with 80 mm of diameter. The specimens were fixed in circular capsules with 5.2 cm of effective permeation area. In the capsules interior, it was added silica gel, setting a low humidity, which was considered as 0 (zero) in the atmosphere in contact with the specimen's lower face [6]. The capsules were placed in hermetic desiccators at 25 ± 1 °C with

a sodium chlorate saturated solution, setting the humidity to 75%. Weight gain measurements were taken by weighing the capsules (Analytical balance, resolution 0.001 g) each 24 h for 7 days. A plot of weight gained (Wg) versus time (t) was used to determine the WVP through Equation 3:

$$P = \frac{Wg \times ti}{t \times A \times \rho_s (RH_1 - RH_2)} \quad (3)$$

Where: P is given in g.cm.cm^{-2}.s^{-1}.kPa^{-1}; A is the permeation area of the specimen (cm²); ti is the medium specimen thickness (cm); ρs is the water vapor saturation pressure at the test temperature (3,169 kPa); RH_1 is the relative humidity of the desiccator chamber (0,75) and RH_2 (0,00) is the relative humidity inside the capsule. Three repetitions were performed for each biocomposite.

2.3.2.4 Determination of water diffusion and solubility coefficients

Effective diffusion coefficient (D_{eff}) of water was determined using the Fick's model for diffusion showed in Equation 4, which can be simplified when considering that the water diffusion occurs in a unique direction, as expressed as in Equation 5. Besides that, considering (i) a membrane with uniform thickness (ii) and surfaces, x = -l and x = l, with a known constant concentration of water (C_0), and that (iii) concentration of water inside the film is zero, the diffusion equation can be expressed as Equation 6 [25]. For short periods, Equation 3 can be simplified as showed in Equation 7, which can be used to adjust the initial experimental points, when until 60% of the solute mass has been absorbed [25].

$$\frac{\partial C}{\partial t} = D_{eff}\left(\frac{\partial^2 C}{\partial x^2} + \frac{\partial^2 C}{\partial y^2} + \frac{\partial^2 C}{\partial z^2}\right) \quad (4)$$

$$\frac{\partial C}{\partial t} = D_{eff}\left(\frac{\partial^2 C}{\partial x^2}\right) \quad (5)$$

$$\frac{M_t}{M_\infty} = 1 - \frac{8}{\pi^2}\sum_{N=0}^{\infty}\frac{1}{(2N+1)^2}\exp\left[\frac{-D_{eff}(2N+1)^2\pi^2 t}{e^2}\right] \quad (6)$$

$$\frac{M_t}{M_\infty}(\leq 0{,}60) = 4\sqrt{\frac{D_{eff} \cdot t}{e^2 \pi}} \quad (7)$$

Where: C is the water concentration (g.cm^{-3}), D_{eff} is the effective diffusion coefficient (cm^2.s^{-1}), x, y e z are the dimensions of film with significant diffusivity (cm), x = thickness, y = 0 and z = 0 (when occurring in only one direction, x), M_t (g) is the total amount of diffusing substance which has entered the membrane at the time t (s), M_∞ (g) is the corresponding moisture amount after infinite time (equilibrium moisture), N is the number of terms in the series and e is the thickness of film (cm).

The experimental test was conducted preparing specimens of 6 cm² in triplicate and submitting them to vacuum drying at 70 °C for 24h. The samples were placed in a hermetic pot with a relative humidity of 75 % (saturated saline solution of NaCl) at 25 °C in order to measure their moisture gain. All samples were weighted with an accuracy of 0.001 g from the time zero to equilibrium (approximately

8 days), in a 24h interval. For the first 9h, when there were significant changes in mass, weight was measured at each hour. Through the moisture gain by time data and considering the thickness of each sample, it was possible to estimate the value of D_{eff} through a non-linear regression with the Equation 7 (using a number of terms of the series truncated in N = 10).

Besides the diffusivity coefficient, is also important to know the solubility coefficient since the film's moisture permeability is influenced by both the penetration of water molecules into the material and the water molecule's solubility on the biocomposite matrix [26]. Considering the biocomposite as a finite solid, with a water vapor concentration-independent diffusion constant, where initially the film is free from vapor and one surface is then exposed to a pressure p_1 giving a concentration in the surface layer of c_1, the amount of water vapor *Q* diffusing through the material is with thickness *X* in a time *t* is [26]:

$$Q = \frac{Dc_1 t}{X} - \frac{c_1 X}{6} \quad (8)$$

where D is the diffusion coefficient. The amount of water vapor permeating through the biocomposite increases linearly with time once the steady-state has been reached. Considering a Fickian diffusion and sorption following Henry's law, at steady-state diffusion is possible to use the permeability coefficient (P) and the experimentally calculated diffusion coefficient (D_{eff}) to obtain the solubility coefficient through Equation 9 [26–28]:

$$S = P/D_{eff} \quad (9)$$

Is important to mention that, to obtain this P and S coefficients, four conditions were taken: (i) diffusion is at steady-state; (ii) the concentration–distance relationship through the biocomposite is linear (iii) diffusion takes place in only one direction (through the biocomposite); and (iv) both D and S are not dependent of the concentration [26]. The application of these conditions to the here considered materials is a simplification in order to obtain estimated values of P and S to better discuss about the influence of corona treatment at the water permeation process.

2.4 Statistical analysis

Sisvar 5.0 was used to perform statistical analysis of the results by comparing the means through Scott-Knott test, with 95 % of confidence level. The test was used for contact angle, tensile, water vapor permeability, water diffusion coefficient and water solubility coefficient results.

3 RESULTS AND DISCUSSION

3.1 Water contact angle and surface energy

The contact angle was verified to measure the wettability changes in the PVOH/NS surface after the different times of corona treatment: a smaller contact angle means better wettability to receive the second layer of WPI/NS, which can be directly related to water permeation and tensile properties of the bilayer biocomposites.

Table 1 – Results of water contact angle (WCA), Diiodo-methane contact angle (DCA), surface energy (SE), dispersive interactions energy (DE) and polar interactions energy (PE) for each first layer (PVOH/NS) film

Treatment	WCA (°)	SE $(N.m^{-1})*10^{-3}$	DE $(N.m^{-1})*10^{-3}$	PE $(N.m^{-1})*10^{-3}$
0S	105.92 ± 2.94^{c}	27.96 ± 3.44	27.81 ± 3.53	0.15 ± 0.03
30S	41.08 ± 2.92^{b}	59.87 ± 6.43	34.73 ± 3.80	25.14 ± 2.14
60S	29.55 ± 2.17^{a}	67.42 ± 7.60	35.91 ± 4.12	31.5 ± 2.78
90S	27.00 ± 2.27^{a}	70.48 ± 8.16	40.44 ± 5.41	31.04 ± 3.09

At vertical columns, different letters represent significantly different values at ($p \geq 0.05$) using the Scott-Knott test.

The angle between water drop and the biocomposites surface was decreased with the time of corona discharge increment, corroborating the ability of this treatment in increasing the wettability of the surface. The WCA results can be visually understood in Figure 3. The film surface not treated by corona (0S) presented a hydrophobic surface, with WCA higher than 90° (105.92°). The more time the surface was treated with corona, the more wettability of the WPI/NS film surface was increased. The lowest, and therefore, more hydrophilic angle was observed when the film surface was treated for the longest period of time, 90 seconds (27.00°). This result indicates that corona discharge improves the ability of the PVOH/NS surface to interact with the second layer of WPI/NS, increasing the adherence between these layers, which certainly influences the barrier and mechanical properties of the bilayer biocomposites.

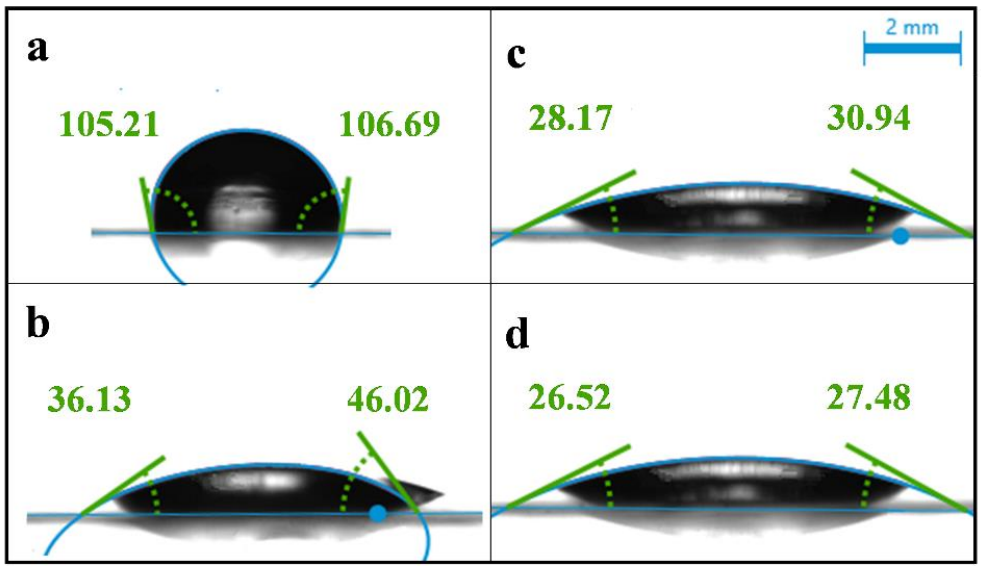

Figure 3 – Water contact angle (right and left) formed between the water drop and the first layer films: (a) 0S; (b) 30S; (c) 60S and (d) 90S.

The surface energy of the biocomposites was increased with the corona treatment, showing higher polar interactions energy and a slight increase of dispersion interactions energy. These results indicate that the discharge was able to improve the wettability of PVOH/NS film surface. The film with

90 seconds of corona discharge (90S) showed surface energy 152% higher and a polar energy 206 times higher than that with no corona discharge (0S). The reduction is in accordance with the water contact angle results, corroborating the hypotheses that the corona treatment is able to increase the adherence between the polymeric layers.

3.2 Fourier transform infrared (FT-IR) analysis

The corona treatment leads to chemical and structural changes in surface area, generating reactive oxidants, such as ozone, oxygen-free radicals, or oxygen atoms, through electron bombardment at the surface [8, 29]. As result, the treatment provides the creation of carbonyl, carboxyl, hydroxyl, or ester functional groups at the polymer surface, which allows the increase of wettability. The groups formed at the PVOH/NS surface after corona discharge will be discussed with the results from FT-IR analysis.

Figure 4 presents spectra on the infrared region of PVOH/NS films after different times of corona discharge. The main absorptions occurred on bands: from 3600 cm^{-1} to 2800 cm^{-1} and from 1800 cm^{-1} to 950 cm^{-1}. These specific regions of the general spectra (Fig. 3.a) can be better observed in Fig. 3.b and c.

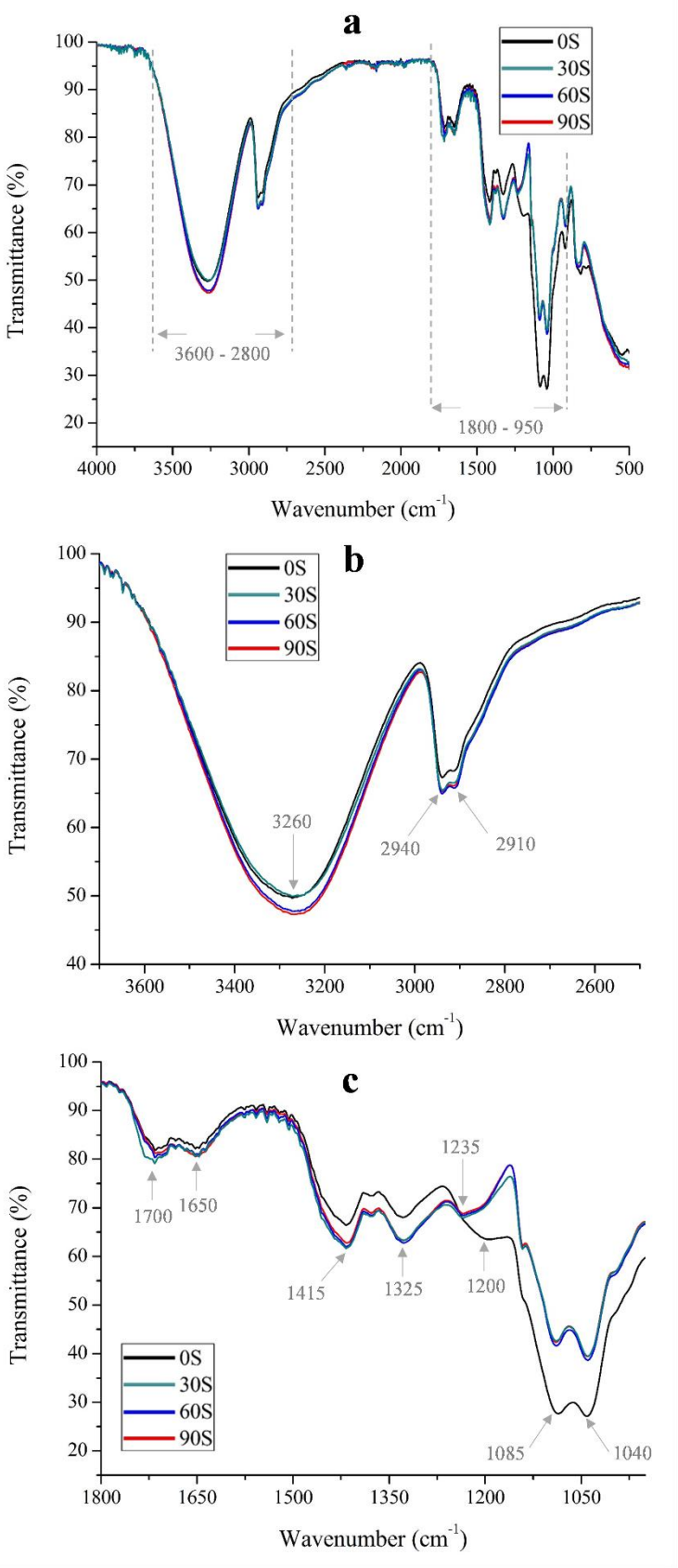
a
0S
30S
60S
90S
Transmittance (%)
3600 - 2800
1800 - 950
Wavenumber (cm-1)
b
0S
30S
60S
90S
Transmittance (%)
3260
2940
2910
Wavenumber (cm-1)
c
1700
1650
1415
1325
1235
1200
1085
1040
0S
30S
60S
90S
Transmittance (%)
Wavenumber (cm-1)

Figure 4 – FT-IR spectra of the first layer films treated under different times of corona discharge: (**a)** general spectra from 4000 cm^{-1} to 500 cm^{-1}; (**b)** range from 3600 cm^{-1} to 2800 cm^{-1} and (**c)** range to 1800 cm^{-1} to 950 cm^{-1}.

A broad band was observed for all treatments around 3260cm^{-1} corresponding to de –OH stretching. It can be observed a higher intensity of this band and a dislocation to lower wavenumbers for films treated with 60 s and 90 s of corona discharge. This result indicates an increase in –OH groups and hydrogen bonds with the higher times of discharge [4]. The two peaks at 2940 cm^{-1} and 2910 cm^{-1} related to the asymmetrical and symmetrical stretching of methylene groups, respectively [11].

Peaks at 1700 cm^{-1} and 1650 cm^{-1} can be related to the axial deformation of carbonyl (–C=O) groups, indicating their formation on the sample surface and contributing to the wettability increase [30]. At 1415 cm^{-1} and 1325 cm^{-1} absorbance can be assigned to the $–CH_3$ bending [28]. An important change, which corroborates the generation of polar groups at the film surface after corona is the disappearance of the peak at 1200 cm^{-1} (–C–O–C stretching) and reduction of the band intensity at 1085 cm^{-1} (–C–O– stretching) and 1040 cm^{-1} (–OH bending), with the subsequent new peak at 1235 cm^{-1} indicating the formation of –C=O groups [28, 30].

3.3 Scanning Electron Microscopy (SEM)

SEM micrographs of the biocomposites are shown in Figure 5, revealing clearly the individual layers. For all the treatments, it was observed a compact structure with few pores or cracks, but the joining region between the layers of the bilayer biocomposites was different according to the time of corona discharge applied. The transition between the layers is more evident and heterogeneous for the composite without the corona treatment (B0S), whereas the treatments with 60 s and 90 s of discharge (B60S and B90S) showed an extremely homogeneous transition. It suggests that the treatment increased compatibility between layers possibly by increasing hydrogen bonds interactions among the films constituents at the interface, providing good adherence [31].

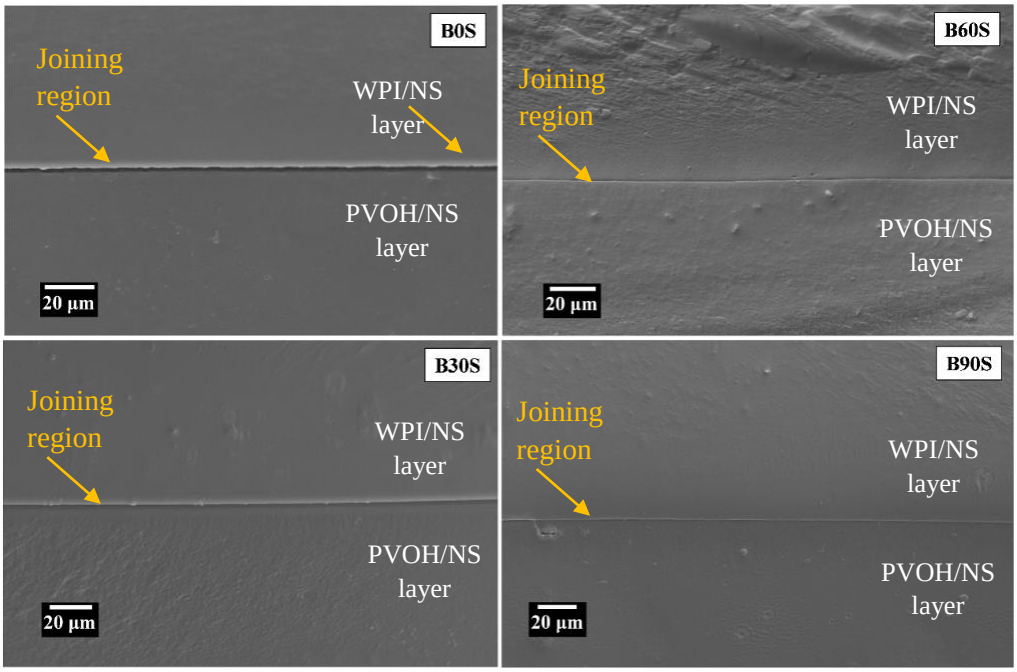

Figure 5 – SEM cross-section micrographs showing joining region between layers of the bilayer biocomposites: B0S, B30S, B60S and B90S.

3.4 Tensile Properties

Figure 6 presents the results obtained from the tensile test (TS, TM, and E), conducted until the film rupture. As observed in Figure 6-a, the lamination process without corona discharge reduces tensile strength by 28%: TS for UNL was 10.2 MPa while for B0S was 7.3 MPa. However, submitting the first layer film to 30 s of discharge provided a slight increase in TS and, at 90 s of corona discharge, TS achieved 12.6 MPa, being 72% more resistant than B0S and 23% stronger than UNL film. Certainly, the good adherence between layers provided by corona treatment and predicted through water contact angle, surface energy, and SEM results, allowed this higher strength. This 12.6 MPa of tensile strength for B90S is a great tensile resistance value when compared, for example, with LDPE, a material with widespread application in the food packaging sector, which presents (in different tests conditions) TS of 6.9 - 16 MPa [32, 33].

The tensile modulus of bilayer films was not affected by corona discharge at the periods of time used in this work (0 s, 30 s, 60 s or 90 s), meaning that the treatment did not affect the films rigidity. However, lamination provided films 60% more flexible when comparing the mean values of TM from B0S, B30S, B60S, and B90S whit the TM result from UNL. Flexible food packaging widely used on market, such as LDPE and linear low-density polyethylene (LLDPE), usually presents tensile modulus varying between 130 and 300 MPa which provides low stiffness and brittleness [26, 34–36]. In this work, all bilayer films showed a mean TM of 28.6 MPa, being up to 9 times less rigid than these commercial polymers. Although different conditions of test had been used in comparison with those

commercial materials cited, the results here obtained can be extremely positive for some applications when super flexible and stretchable packaging is needed [4].

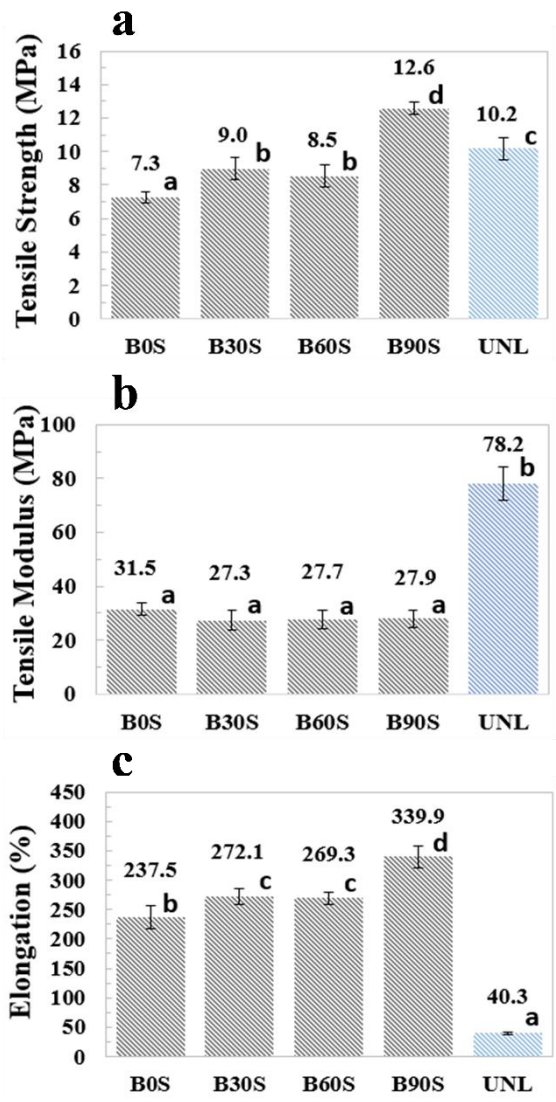

Figure 6 - Average and standard deviation values of tensile properties: (a) maximum TS; (b) TM and E obtained by the tensile test of the biocomposites. Different letters represent significantly different values at ($p \geq 0.05$) using Scott-Knott test.

By analyzing elongation results, is possible to notice a behavior much more ductile for films bilayer when compared to the unlaminated. Besides that, at 90 s of corona discharge, the treatment was able to provide a film 7.4 times more ductile when compared to UNL. Possibly, interactions between PVOH/PVOH chains and among film constituents on the first layer and between WPI/WPI chains and among film constituents on the second layer, as well as interactions between layers, were more numerous when compared to interactions between all film constituents in a single phase on UNL film, allowing higher deformation before rupture.

These results corroborated the capacity of corona discharge in providing more polar groups available to interact between layers and among the films constituents, and that is worth it to investigate composites and blends of different polymers not only in a single phase but also in separated phases using corona as an agent of adherence.

3.5 Water vapor permeability

WVP test is essential for new materials intended to be applied as food packaging such as the PVOH/WPI/NS bilayer biocomposites developed since is important to know how the film will manage moisture ingress or regress. Intending to apply this film packaging in dry vegetables and fruits or cereals, with a low water activity (a_w), the second layer of the film (WPI/NS) was chosen to be in contact with the interior of the capsule (a_w close to zero) in the water permeability test, and the second layer (PVOH/NS cross-linked with glutaraldehyde) to be the face in contact with the atmosphere (a_w of 0.75) [37]. This way, we avoided the food contact with possible traces of free glutaraldehyde and simulated similar conditions of the packaging inside and outside, respectively with the inside and the outside capsule environments. The permeability results (Table 2) showed that lamination, even without corona treatment, increased water permeability: B0S showed a P result 63.7% higher than the UNL film. Among bilayer films submitted to the corona discharge, there was no significant ($p \geq 0.05$) difference in P according to the times of discharge tested. Treatments with 30 s, 60 s, or 90s of discharge, on average showed a water permeability 19.6% higher than that not treated (B0S) and 96% higher than the unlaminated film (UNL).

Since permeability takes both sorption and diffusion of water into consideration, is important to evaluate coefficients of sorption and diffusion to better understand this raise in P when films were treated with the corona discharge.

Table 2 – Results of permeability coefficient (P), effective diffusion coefficient (D_{eff}), and solubility coefficient (S)

Biocomposite	Time of corona discharge (s)	Thickness (mm)	P ($g.cm.cm^{-2}.s^{-1}.kPa^{-1}$)*$10^{-10}$	D_{eff} ($cm^2.s^{-1}$)*10^{-6}	S ($g.cm^{-3}.kPa^{-1}$) *10^{-5}
B0S	0	0.190 ± 0.02a	3.39 ± 0.09b	4.05 ± 0.28c	8.52 ± 0.82b
B30S	30	0.206± 0.01a	4.12 ± 0.42c	4.30 ± 0.16c	9.57 ± 0.94b
B60S	60	0.219 ± 0.02a	3.89 ± 0.33c	3.51 ± 0.26b	10.3 ± 1.23b
B90S	90	0.226 ± 0.02a	4.16 ± 0.36c	2.55 ± 0.29a	16.3 ± 0.72c
UNL	-	0.223 ± 0.01a	2.07 ± 0.24a	4.40 ± 0.41c	4.29 ± 0.15a

At vertical columns, different letters represent significantly different values at ($p \geq 0.05$) using the Scott-Knott test.

3.6 Water diffusion and water solubility coefficients

Water diffusion and solubility coefficients obtained are exposed in Table 2. Permeation of water vapor through a polymer sheet is related to both diffusivity and solubility, where the effective diffusion

coefficient (D_{eff}) represents the speed of water molecules moving through the polymer matrix and solubility coefficient (S) is related to the affinity of the matrix with water molecules indicating the amount of water dissolved in the polymer [26, 27].

Lamination did not significantly ($p \geq 0.05$) change the diffusion coefficient, but lamination associated with corona treatment above 60 s acted decreasing D_{eff}. The B90S film showed a diffusion 37% and 42% lower than those from B0S and UNL, respectively. Regarding the water solubility, it was increased by lamination and even more by corona discharge. At 90s of discharge, the bilayer film had an S result 91% higher than that from the bilayer film without corona treatment (B0S) and 2.8 times higher than S from UNL. These results allow understanding those from water permeability.

Water solubility is increased by corona treatment since the discharge raises the number of polar groups in the bilayer film matrix, as proved on FT-IR results, increasing, therefore, the affinity between the film and polar water molecule. This affinity act by decreasing the speed of water permeating through the film, thus leading to lower values of D_{eff}. Despite this lower diffusion, observing the magnitude order of D_{eff} and S is possible to infer that solubility is more influent than diffusion at the water permeation process of the films tested. It indicates that corona treatment makes water pass slowly through the film, but highly increases the affinity of this permeant with the matrix making it more hygroscopic. Therefore, possibly the lower water barrier (higher P) obtained for films treated with the discharge is related with a higher water absorption at the film surface, and not with a higher water vapor permeation through the film.

In terms of the lamination process, it was possible to conclude that PVOH/WPI in separated layers (B0S) favored a higher affinity of the film constituents with water molecules (raising S) when compared to the single-phase biocomposite (UNL). Therefore, despite the unchanged D_{eff} ($p \geq 0.05$), lamination decreased water barrier.

4 CONCLUSION

In the bilayer biocomposites, corona discharge increased the wettability of the first layer surface by generating new polar groups, improving the ability of the PVOH/NS surface to interact with the second layer of WPI/NS, thus increasing the adherence between these layers. Besides that, bilayer films treated with higher times (60 s and 90 s) of discharge showed an extremely homogeneous transition between phases, suggesting compatibility and adherence between layers provided by the treatment. Bilayer films treated with 90 s of corona discharge showed a tensile 72% and 23% more resistant than the bilayer film not treated and than the single-layer film, respectively. Besides that, at 90 s of discharge, the bilayer film was 7.4 times more ductile when compared to unlaminated one. Regarding the water barrier, the lamination process and corona treatment make water pass slowly through the film, but increase the affinity of the water with the matrix thus leading to a lower water barrier. Finally, the use

of corona discharge associated with the lamination of PVOH/WPI/NS biocomposites providing a bilayer film is justified to produce a more resistant, flexible and ductile biocomposite film for packaging.

Declaration of competing interest

The authors declare no competing interest.

Acknowledgements

This work was financed by the Coordenação de Aperfeiçoamento de Pessoal de Nível Superior (CAPES) – Brasil (Finance Code 001), the Conselho Nacional de Desenvolvimento Científico e Tecnológico – Brasil (CNPq) and the Fundação de Amparo à Pesquisa do Estado de Minas Gerais – Brasil (FAPEMIG). The authors extend their appreciation for all support provided by the Universidade Federal de Lavras - (UFLA).

5 REFERENCES

1. Agarwal S (2021) Major factors affecting the characteristics of starch based biopolymer films. Eur Polym J 160:. https://doi.org/https://doi.org/10.1016/j.eurpolymj.2021.110788
2. Grand View Research (2021) Plastic Packaging Market Size, Share & Trends Analysis Report By Product (Flexible, Rigid), By Technology (Extrusion, Thermoforming), By Application (Food & Beverages, Pharmaceuticals), And Segment Forecasts, 2021 – 2028
3. Grand View Research (2021) Bioplastics Market Size, Share & Trends Analysis Report By Product (Biodegradable, Non-biodegradable), By Application (Packaging, Automotive & Transportation, Textile), By Region, And Segment Forecasts, 2021 – 2028.
4. Lara BRB, de Andrade PS, Guimarães Junior M, et al (2021) Novel Whey Protein Isolate/Polyvinyl Biocomposite for Packaging: Improvement of Mechanical and Water Barrier Properties by Incorporation of Nano-silica. J Polym Environ. https://doi.org/10.1007/s10924-020-02033-x
5. Oymaci P, Altinkaya SA (2016) Improvement of barrier and mechanical properties of whey protein isolate based food packaging films by incorporation of zein nanoparticles as a novel bionanocomposite. Food Hydrocoll 54:1–9. https://doi.org/10.1016/j.foodhyd.2015.08.030
6. Lara BRB, Araújo ACMA, Dias MV, et al (2019) Morphological, mechanical and physical properties of new whey protein isolate/ polyvinyl alcohol blends for food flexible packaging. Food Packag Shelf Life 19:. https://doi.org/10.1016/j.fpsl.2018.11.010
7. Chen X, Cui F, Zi H, et al (2019) Development and characterization of a hydroxypropyl starch / zein bilayer edible film. Int J Biol Macromol 141:1175–1182
8. Popelka A, Novák I, Al-Maadeed MASA, et al (2018) Effect of corona treatment on adhesion enhancement of LLDPE. Surf Coatings Technol 335:118–125. https://doi.org/10.1016/j.surfcoat.2017.12.018
9. Andrade T, Lina L, Pedro B, et al (2018) The effect of surface modifications with corona discharge in pinus and eucalyptus nanofibril films. Cellulose 3:5017–5033
10. Mahanwar PA, Gadekar PT (2019) Effect of glutaraldehyde on thermal and mechanical properties of starch and polyvinyl alcohol blends. Des Monomers Polym 22:164–170
11. Figueiredo KCS, Alves TLM, Borges CP (2009) Poly (vinyl alcohol) Films Crosslinked by

Glutaraldehyde Under Mild Conditions. J Appl Polym Sci 111:3074–3080. https://doi.org/10.1002/app

12. Albano KM, Cavallieri ÂLF, Nicoletti VR (2018) Electrostatic interaction between proteins and polysaccharides: Physicochemical aspects and applications in emulsion stabilization. Food Rev Int 35:54–89. https://doi.org/10.1080/87559129.2018.1467442

13. Andrade R, Castro C, Osorio F, et al (2014) Wettability of gelatin coating formulations containing cellulose nanofibers on banana and eggplant epicarps. LWT - Food Sci Technol 58:158–165. https://doi.org/https://doi.org/10.1016/j.lwt.2014.02.034

14. Farris S, Introzzi L, Biagioni P, et al (2011) Wetting of biopolymer coatings: Contact angle kinetics and image analysis investigation. 27:7563–7574. https://doi.org/https://doi.org/10.1021/la2017006

15. Karbowiak T, Debeaufort F, Voilley A (2006) Importance of surface tension characterization for food, pharmaceutical and packaging products: a review. Crit Rev Food Sci Nutr 46:391–407. https://doi.org/Importance of surface tension characterization for food, pharmaceutical and packaging products: a review

16. Kurek M, Galus S, Debeaufort F (2014) Surface, mechanical and barrier properties of bio-based composite films based on chitosan and whey protein. Food Packag Shelf Life 1:56–67. https://doi.org/https://doi.org/10.1016/j.fpsl.2014.01.001

17. Wiacek AE (2015) Effect of surface modification on starch biopolymer wettability. 48:228–237. https://doi.org/https://doi.org/10.1016/j.foodhyd.2015.02.005

18. Yin Y-C, Yin S-W, Yang X-Q, et al (2014) Surface modification of sodium caseinate films by zein coatings. Food Hydrocoll 36:1–8. https://doi.org/10.1016/j.foodhyd.2013.08.027

19. Ferreira AS, Nunes C, Castro A, et al (2014) Influence of grape pomace extract incorporation on chitosan films properties. Carbohydr Polym 113:490–49. https://doi.org/https://doi.org/10.1016/j.carbpol.2014.07.032

20. ASTM D7334-08 (2013) Standard Practice for Surface Wettability of Coatings , Substrates and Pigments by Advancing Contact Angle Measurement. Annu. B. ASTM Stand.

21. Sharma P (2001) Surface Studies Relevant to Microbial Adhesion and Bioflotation of Sulphide Minerals. Luleå University of Technology, Sweden

22. OWENS DK, WENDT RC (1969) Estimation of the Surface Free Energy of Polymers. J Appl Polym Sci 13:1741–1747. https://doi.org/https://doi.org/10.1002/app.1969.070130815

23. ASTM D882-02 (2002) Standard Test Method for Tensile Properties of Thin Plastic Sheeting

24. ASTM E96/E96M-10 (2010) Standard Test Methods for Water Vapor Transmission. 4:1–12

25. Crank J (1975) The Mathematics of Diffusion, 2nd ed. Clarendon Press

26. Robertson GL (2013) Food Packaging Principles and Practice, 3rd ed. CRC Press, Boca Raton

27. Janjarasskul T, Tananuwong K (2019) Role of Whey Proteins in Food Packaging. Ref. Modul. Food Sci. 30

28. Rocca-smith JR, Karbowiak T, Marcuzzo E, et al (2016) Impact of corona treatment on PLA fi lm properties. Polym Degrad Stab 132:109–116

29. Dai L, Xu D (2019) Polyethylene surface enhancement by corona and chemical co-treatment. https://doi.org/10.1016/j.tetlet.2019.03.013

30. Louzi VC, Sinézio J, Campos DC (2019) Corona treatment applied to synthetic polymeric mono fi laments (PP , PET , and PA-6). Surfaces and Interfaces 14:98–107

31. Martucci JF, Ruseckaite RA (2010) Biodegradable three-layer film derived from bovine gelatin. J Food E 99:377–383. https://doi.org/10.1016/j.jfoodeng.2010.02.023

32. Doak KW (1986) Ethylene polymers. In: Mark HM, Bilakes NM, Overberg CG, Mendes & G (eds) Encyclopedia of polymer science and engineering. John-Wiley, New York

33. Shebani A, Klash A, Elhabishi R, et al (2018) The Influence of LDPE Content on the Mechanical Properties of HDPE/LDPE Blends. Res Dev Mater Sci 7:791–797. https://doi.org/10.31031/RDMS.2018.07.000672

34. Jin-Hua T, Guo-Qin L, Huang C, Lin-Jian S (2012) Mechanical Properties and Thermal Behaviour of LLDPE/MWNTs Nanocomposites. https://doi.org/10.1590/S1516-14392012005000122

35. SpecialChem SA (2020) Young's Modulus: Tensile Elasticity Units, Factors & Material Table. https://omnexus.specialchem.com/polymer-properties/properties/young-modulus. Accessed 21 Jan 2020

36. Selke SE, Hernandez RJ (2001) Packaging: Polymers in Flexible Packaging. In: Encyclopedia of Materials: Science and Technology. Elsevier, pp 6652–6656

37. Lara BRB, Dias M V, Guimarães Junior M, et al (2020) Water Sorption Thermodynamic Behavior Of Whey Protein Isolate/ Polyvinyl Alcohol Blends For Food Packaging. Food Hydrocoll 103:9. https://doi.org/10.1016/j.foodhyd.2020.105710

CONCLUSÃO GERAL E SUGESTÕES PARA TRABALHOS FUTUROS

O estudo desenvolvido nesta tese provou ser possível o desenvolvimento do novo compósito de isolado proteico de soro de leite (IPS), poli (álcool vinílico) (PVOH) e nano-sílica (NS), sendo esse um material inovador tanto em termos de composição, quanto do que fiz respeito ao processamento por laminação com descarga corona. Além disso, a pesquisa mostrou que a adição de NS ao WPI/PVOH é justificada para aumentar resistência mecânica, melhorar barreira à umidade e melhorar a estabilidade da embalagem, a qual é indicada para atmosferas resfriadas e alimentos com atividade de água abaixo de 0.75, como o caso de frutas desidratadas, mel e geleias. Por fim, concluiu-se que a produção do compósito por laminação associada à descarga corona, com uma primeira camada de PVOH/NS e uma segunda de IPS/NS, é indicada a fim de aumentar a resistência mecânica, a flexibilidade e ductilidade de biofilmes de WPI/PVOH/NS.

A fim de aprofundar no estudo da aplicação do biocompósito desenvolvido, além de entender mais a fundo o material em si e compará-lo com as matérias primas comerciais comumente utilizadas na área de embalagens, sugere-se como trabalhos futuros: (i) a submissão das matérias-primas do filme de forma isolada aos mesmos testes que foram realizados nesta pesquisa (IPS e PVOH puros); (ii) submeter uma amostra de polietileno de baixa densidade ou outro plástico comercial aos mesmos testes realizados nesta pesquisa, sob as mesmas condições, para fins de comparação de propriedades; (iii) testar a possível atividade antibacteriana e acidulante conferida pelo ácido acético presente no filme; (iv) avaliar a possibilidade de aplicação do filme em papel como um novo compósito laminado; (v) testar a produção do filme laminado em maior escala utilizando a técnica de espalhamento de filme com barra de espatulagem; (vi) estudar como as formulações utilizadas nessa pesquisa em escala laboratorial poderiam ser aplicadas na indústria e avaliar o custo; e (vii) avaliar a influência da NS em maiores quantidades (acima de 4%) em blendas de IPS/PVOH.